DOI: 10.3969/j.issn.1000-9760.2020.01.002

蒲公英黄酮类成分超声辅助半仿生提取及含量测定*

李艳芝　刘树玲　刘文杰　李爱花
(济宁医学院药学院，日照 276826)

摘　要　目的　研究蒲公英黄酮类成分超声辅助半仿生提取工艺，并对不同采收时间蒲公英地上部分及根中所含黄酮类成分槲皮素、木犀草素和芦丁进行含量测定。**方法**　在单因素试验基础上，通过正交试验对提取工艺参数乙醇浓度、料液比、超声时间、超声温度进行优化。采用高效液相色谱法对蒲公英中槲皮素、木犀草素和芦丁进行含量测定。**结果**　4 种因素对蒲公英总黄酮提取率影响大小顺序为乙醇浓度 > 料液比 > 超声时间 > 超声温度，其中乙醇浓度和料液比为显著性影响因素；最佳提取工艺条件为乙醇浓度为 95%，料液比为 1∶20，超声时间 30min，超声温度为 40℃。建立了同时测定蒲公英中槲皮素、木犀草素和芦丁的 HPLC 方法。**结论**　不同时期蒲公英地上部分及根中槲皮素、木犀草素和芦丁的含量有明显差别，4 月份采收的样品含量高于其它采收时间。

关键词　蒲公英；黄酮；半仿生提取；含量测定
中图分类号：R284.1　　**文献标识码**：A　　**文章编号**：1000-9760(2020)02-005-05

Ultrasonic-assisted semi-bionic extraction and content determination of flavonoid constituent from *Taraxacum mongolicum* Hand.-Mazz.

LI Yanzhi, LIU Shuling, LIU Wenjie, LI Aihua
(*College of Pharmacy, Jining Medical University, Rizhao* 276826, *China*)

Abstract: ***Objective***　To optimize the Ultrasonic-assisted semi-bionic extraction process of the flavonoid constituent from *Taraxacum mongolicum* Hand.-Mazz. and determine the contents of quercetin, luteolin and rutin from acrial part and root of *T. mongolicum* Hand.-Mazz. in different periods. ***Methods***　We optimized the extraction parameter by orthogonal test on the basis of single factor test. The contents of flavonoid was determined by HPLC. ***Results***　Among the four factors, the ratio of liquid to solid and ethyl alcohol concentration were significant influencing factors and the order of the more influence factor of the yield was: ethyl alcohol concentration > ratio of liquid to solid > ultrasonic time > ultrasonic temperature. The best extraction condition was as followed: ethyl alcohol concentration (95%), ratio of liquid to solid (1∶20), ultrasonic time (30min), ultrasonic temperature (40℃). The contents of quercetin, luteolin and rutin from the acrial part and root of *T. mongolicum* Hand.-Mazz. were obviously different in different periods. ***Conclusion***　The contents of quercetin, luteolin and rutin from the acrial part and root of *T. mongolicum* were obviously different in different periods and the content in April is higher than others.

Keywords: *Taraxacum mongolicum* Hand.-Mazz.; Flavonoid; Semi-bionic extraction; Content determination

蒲公英(*Taraxacum mongolicum* Hand.-Mazz.)为菊科多年生草本植物，别名黄花地丁、婆婆丁、黄花三七等，其嫩苗是人们喜爱的野菜，食用历史悠久，始载于《唐本草》，另外《本草纲目》《本草新编》等本草著作中也有记载[1]。蒲公英含有多种人体所必需的氨基酸，Ca、P、Fe 等多种矿物质的含量也显著高于普通果蔬[2]。研究表明，蒲公英含多种化学成分，如黄酮类[3-4]、萜类[5-6]、香豆素类[7]等，有降血脂、降血糖[8]、抗氧化、抗炎[9]、抗

* [基金项目] 济宁医学院青年教师科研扶持基金重点项目(JY2016KJ010Z)

肿瘤等生物活性[10]。半仿生提取法是模仿人体胃肠道环境，在特定的酸碱环境下提取化学成分，从生物药剂学角度为口服给药制剂提供一种新技术[11-12]。本文对蒲公英所含有的黄酮类成分超声辅助半仿生提取工艺进行研究，并对不同采收时间蒲公英地上部分及根中所含黄酮类成分槲皮素、木犀草素和芦丁含量进行测定，为蒲公英合理采收和有效利用提供科学依据。

1 材料及仪器

1.1 材料试剂

蒲公英采自山东日照（采集时间 2017 年 3 月 3 日－6 月 1 日，期间每 10 天采集 1 次），洗净，50℃烘干，粉碎过 40 目筛备用。芦丁对照品（上海源叶生物科技有限公司，批号：Y05M6S1）；木犀草素对照品（上海源叶生物科技有限公司，批号：YA0408YA14）；槲皮素对照品（上海源叶生物科技有限公司，批号：Y26D5Y1）；甲醇（色谱纯）；其它试剂为分析纯。

1.2 仪器设备

SHIMADZU LC-20AT 双泵高效液相色谱仪（日本岛津公司）；超声波清洗机（深圳市深华泰超声洗净设备有限公司）；FA1004 电子分析秤（常州市幸运电子设备有限公司）；101-OS 电热鼓风干燥箱（天津宏诺仪器有限公司）；Q-250B 高速多功能粉碎机（上海冰都电器有限公司）。

2 方法与结果

2.1 蒲公英总黄酮半仿生提取

2.1.1 供试品溶液的制备 准确称量蒲公英（采于 2017 年 3 月 23 日）地上部分粉末 4.5g，加入一定量的提取溶剂，超声提取 3 次（3 次提取溶剂的 pH 分别为 2.0、7.5 和 8.3），超声提取一定时间，合并提取液，旋转蒸发回收溶剂，定容于 100ml 容量瓶中，作为待测液。

2.1.2 芦丁标准品溶液的制备 用分析天平精密称取 4.5mg 芦丁标准品，95% 乙醇定容至 25ml 容量瓶中，得浓度为 0.18mg/ml 的标准品溶液。

2.1.3 测定波长的确定

按照文献[13]显色方法分别对供试品溶液和标准品溶液显色，在 200～700nm 波长范围内进行波谱扫描，结果表明，在 502nm 波长处二者均出现了最大吸收峰，所以确定 502nm 为测定波长。见图 1。

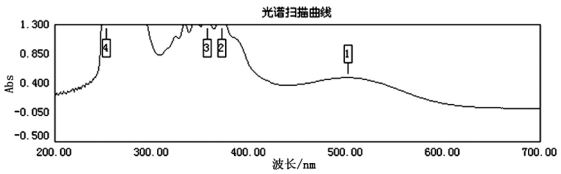

图 1 供试品溶液和标准品溶液紫外光谱扫描图

2.1.4 标准曲线的制备 用移液管分别量取 0.0、1.0、2.0、3.0、4.0、5.0ml 的芦丁标准品母液，置于 6 个 10ml 的容量瓶中，按文献[13]所示方法显色配制溶液，最终得 0.000、0.018、0.036、0.054、0.072、0.090mg/ml 不同浓度的标准品溶液，在 502nm 波长处分别测定其吸光度。以芦丁标准品溶液浓度 C（mg/ml）为横坐标，以吸光度 A 为纵坐标，得到标准曲线的回归方程：$A = 0.10565C + 0.00081$，$r^2 = 0.9995$.

2.1.5 总黄酮含量测定 精密量取“2.1.1”项下的蒲公英待测溶液 4ml 至 250ml 容量瓶中，按照文献[13]方法配制溶液，在 502nm 波长处测定其吸光度，代入“1.3.4”项下的回归方程计算，得出提取液中黄酮类化合物的浓度，最终得出蒲公英总黄酮提取率。

$$总黄酮提取率(\%) = C \times V \times n/1000m \times 100\%$$

此公式中，C：提取液中黄酮类化合物的浓度（mg/ml）；V：被测液体积（ml）；n：稀释倍数；m：蒲公英粉末的质量（g）。

2.1.6 单因素试验

1）乙醇浓度对提取率的影响。分别以 10 倍量的 45%、55%、75%、85%、95% 乙醇为提取溶剂，40℃，按照“2.1.1”项下方法超声提取 2 次，每次 20min，测定蒲公英总黄酮提取率。结果显示，随着乙醇浓度增大提取率不断提高，75% 时达到最高值，之后逐渐降低。

2）料液比对提取率的影响。以 75% 乙醇为提取溶剂，40℃，分别考察 8、10、20、25、30 倍量提取溶剂对提取率的影响。结果显示，随着料液比的增加提取率不断提高，20 倍量时达到最高值，之后提高不明显。

3）提取温度对提取率的影响。以 20 倍量的 75% 乙醇为提取溶剂，分别考察 30℃、40℃、50℃、

60℃、70℃不同温度对提取率的影响。结果显示，温度不断升高提取率随之提高，50℃达到最高，之后明显下降。

4）提取时间对提取率的影响。以 20 倍量的 75% 乙醇为提取溶剂，50℃，分别考察 10、15、20、30、40min 不同提取时间对提取率的影响。结果显示，随着提取时间的延长提取率随之提高，30min 时达到最高，之后有所下降。

2.1.7　正交试验　为系统考察提取条件参数，在单因素研究结果基础上，确定其因素水平（见表 1），选用 $L_9(3^4)$ 正交表进行正交设计，进一步优化半仿生超声提取蒲公英总黄酮的工艺条件。正交试验结果和直观分析见表 2，方差分析见表 3。

表 1　正交试验因素水平表

水平	A 乙醇浓度/%	B 超声时间/min	C 超声温度/℃	D 料液比
1	55	20	40	1∶10
2	75	30	50	1∶20
3	95	40	60	1∶30

表 2　正交试验结果和直观分析

序号	A	B	C	D	总黄酮提取率/%
1	1	1	1	1	4.63
2	2	2	2	2	5.28
3	1	3	3	3	4.00
4	2	1	2	3	3.75
5	2	2	3	1	4.13
6	2	3	1	2	4.50
7	3	1	3	2	5.65
8	3	2	1	3	5.13
9	3	3	2	1	4.75
K1	4.637	4.677	4.753	4.503	
K2	4.127	4.847	4.593	5.143	
K3	5.177	4.417	4.593	4.293	
R	1.050	0.430	0.160	0.850	

表 3　方差分析

因素	偏差平方和	自由度	*F* 比	*F* 临界值	*P*
乙醇浓度	1.654	2	32.431	19.000	<0.05
超声时间	0.281	2	5.510	19.000	
超声温度	0.051	2	1.000	19.000	
料液比	1.176	2	23.059	19.000	<0.05
误差	0.05	2			

按照“2.1.1”项下的供试品溶液制备方法分别制备表 2 所列各提取条件样品，分别计算其提取率。结果显示，各因素对蒲公英总黄酮提取率影响大小顺序为：A > D > B > C，即乙醇浓度 > 料液比 > 超声时间 > 超声温度，其中乙醇浓度和料液比为显著性影响因素；最佳提取工艺条件为 $A_3B_2C_1D_2$，即乙醇浓度为 95%，料液比为 1∶20，超声时间 30 min，超声温度为 40℃。

2.1.8　验证试验　准确称取 5 份蒲公英粉末各 50 g，按照最佳工艺条件 $A_3B_2C_1D_2$ 进行提取，计算总黄酮提取率，结果平均提取率为 5.75%，RSD 为 0.31%，表明此工艺条件稳定可行。

2.2　不同采收时间蒲公英中槲皮素、木犀草素、芦丁含量测定

2.2.1　色谱条件　色谱柱：Agilent HC-C18（250mm×4.6mm，5μm）；流动相：甲醇-0.2% 磷酸水溶液（52∶48）；流速：0.8ml/min；检测波长：360nm；柱温：室温；进样量：10μl。在该色谱条件下，槲皮素的保留时间为 7.5min，木犀草素保留时间 19.0min，芦丁保留时间 23.7min。见图 2。

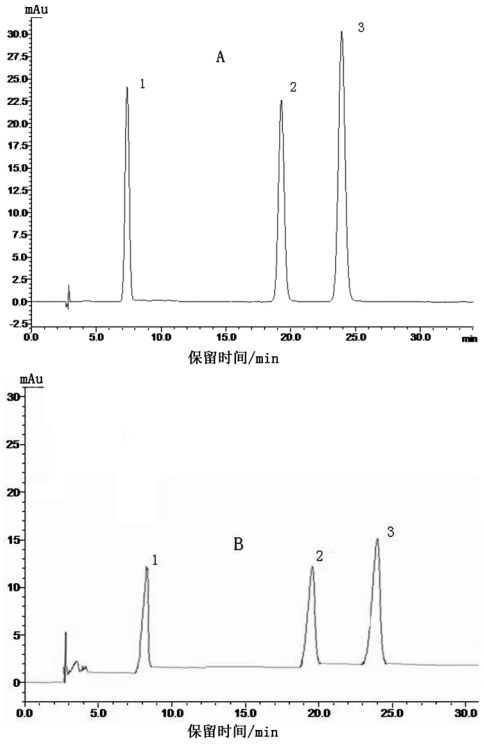

注：1. 槲皮素；2. 木犀草素；3. 芦丁

图 2　混合对照品（A）和蒲公英样品（B）的 HPLC 色谱图

2.2.2　对照品溶液的制备　分别精密称取干燥至恒重的槲皮素对照品 22.00mg，木犀草素对照品 14.00mg 和芦丁对照品 21.20mg，分别用甲醇定容至 100ml 容量瓶中，配制成 0.2200mg/ml 的槲皮素溶液，0.1400mg/ml 的木犀草素溶液和 0.2120mg/ml 的芦丁溶液。分别吸取槲皮素对照品溶液 5ml，木犀草素对照品溶液 10ml，芦丁对照品溶液 10ml，用甲醇定容于 100ml 容量瓶中，得三者混合对照品溶液。

2.2.3　供试品溶液的配制　分别称取不同采收时间的蒲公英地上部分和根部粉末 3g，按照所得的半仿生最佳提取工艺条件（乙醇浓度为 95%，超声时间 30min，超声温度为 40℃，料液比为 1∶20）进行提取，提取液浓缩成浸膏，用甲醇定容于 25ml 容量瓶中，得供试品溶液。

2.2.4　线性关系考察　精密吸取混合对照品溶液 1.0、2.0、4.0、6.0、8.0、10.0ml，用甲醇分别定容于 10ml 容量瓶中，得到一系列不同浓度的混合对照品溶液，在“2.2.1”项色谱条件下，测定不同浓度溶液中槲皮素、木犀草素、芦丁的峰面积，以浓度 X 为横坐标，峰面积 Y 为纵坐标分别绘制槲皮素、木犀草素、芦丁的标准曲线，得到槲皮素的回归方程为 $y=4000000x-840.73$（$r=0.9999$），木犀草素的回归方程为 $y=4000000x-3408.7$（$r=0.9999$），芦丁的回归方程为 $y=4000000x-5090.4$（$r=0.9999$）。结果表明，槲皮素、木犀草素、芦丁分别在 1.10～11.00μg/ml、1.14～14.00μg/ml 和 2.12～21.20μg/ml 范围内线性关系良好。

2.2.5　精密度试验　取“2.2.2”项下混合对照品溶液，连续进样 6 次，分别记录各成分峰面积，计算槲皮素的峰面积 RSD 为 0.36%，木犀草素的峰面积 RSD 为 0.46%，芦丁的峰面积 RSD 为 0.79%，表明仪器精密度良好。

2.2.6　稳定性试验　取 3 月 23 日采集的蒲公英地上部分，按“2.2.3”项下制备供试品溶液，在“2.2.1”项的色谱条件下分别于 0、2、4、6、8、10、12h 进样分析，计算槲皮素、木犀草素、芦丁峰面积的 RSD 分别为 0.42%、2.73% 和 1.12%，可见在 12h 内供试品溶液稳定性良好。

2.2.7　重复性试验　取 3 月 23 日采集的蒲公英地上部分，按“2.2.3”项下平行制备 6 份供试品溶液，在“2.2.1”项下色谱条件分别进样，记录峰面积，计算槲皮素、木犀草素、芦丁峰面积的 RSD 分别为 1.31%、2.31% 和 1.52%，说明所建立的方法重复性良好。

2.2.8　加样回收率试验　精密秤取已知含量的蒲公英地上部分（3 月 23 日）6 份，按“2.2.3”项下制备供试品溶液，按照文献[14]的方法进行加样回收率试验，结果为槲皮素的平均加样回收率是 91.1%，木犀草素为 93.0%，芦丁为 98.0%；槲皮素、木犀草素、芦丁的 RSD 分别为 1.21%、1.81% 和 1.42%。考察结果说明建立的方法准确性良好。

2.2.9　样品测定　制备各个时期采集的蒲公英地上部分和根部样品溶液，在“2.2.1”项的色谱条件下进行色谱分析，测定各个样品的槲皮素、木犀草素、芦丁的含量，色谱图见图 2，测定结果见表 4。

表 4　各个时期蒲公英地上部分和根部槲皮素、木犀草素、芦丁的含量（$mg \cdot g^{-1}$）

采收时间	槲皮素含量		木犀草素含量		芦丁含量	
	地上部分	根部	地上部分	根部	地上部分	根部
3 月 3 日	0.5310	0.1259	0.2177	0.0830	2.5038	0.5667
3 月 13 日	0.5440	0.1207	0.2123	0.0573	2.4436	0.5613
3 月 23 日	0.9250	0.1087	0.3700	0.0582	4.2550	0.4946
4 月 2 日	1.1430	0.3810	0.4572	0.1524	5.2578	1.7526
4 月 12 日	1.0673	0.3083	0.4392	0.1388	4.9309	1.5962
4 月 22 日	1.0410	0.3470	0.4164	0.1319	4.7886	1.4182
5 月 2 日	0.8701	0.2637	0.3625	0.1233	4.0111	1.2130
5 月 12 日	0.4951	0.2094	0.1526	0.0953	1.5539	0.9570
5 月 22 日	0.4609	0.1507	0.2009	0.0682	2.1165	0.7931
6 月 1 日	0.3350	0.1199	0.1943	0.0675	2.0537	0.6902

结果可见蒲公英中槲皮素、木犀草素、芦丁的含量高低顺序为芦丁＞槲皮素＞木犀草素；4 月份采收的蒲公英中三者的含量高于其他月份，同一时期采收的蒲公英地上部分三者的含量都明显较根部含量高。

3　讨论

随着生活水平的不断提高，人们对绿色保健品需求逐渐增加。绿色保健品特别是以中草药为原料提取加工生产的受到了人们的青睐。蒲公英在我国分布广泛，资源丰富，用经历史悠久。蒲公英营养丰富具有多方面的保健功能，激发了广大研究者的兴趣，世界各国均在积极研制蒲公英保健产品，目前已有蒲公英酒、蒲公英咖啡、蒲公英饮料、蒲公英粥、蒲公英花粉等商品上市[15]。黄酮类成

分具有降血脂、降胆固醇、抗氧化等活性,可用于治疗心血管疾病[16]。本研究通过正交试验优化了半仿生提取蒲公英总黄酮的工艺条件,最佳工艺条件为乙醇浓度为 95%,超声时间 30min,超声温度为 40℃,料液比为 1∶20,提取率为 5.75 %,高于董默等[17]的提取结果 4.33 %。该提取工艺可保障蒲公英中黄酮类成分的高效提取,确保蒲公英资源的充分利用。

中药材的质量好坏取决于所含有效成分高低,与众多因素有关,其中采收时间是重要影响因素之一。在不同时期,中药中的有效成分含量不同,通过探索其变化规律寻求最佳采收时间对保证中药材的质量起着至关重要的作用。我们按照所得最佳提取条件,对不同采收时间蒲公英地上部分和根部所含黄酮类成分槲皮素、木犀草素和芦丁进行了含量测定。通过研究,不但建立了同时测定蒲公英中三种黄酮类成分的 HPLC 方法,而且探究了蒲公英中所含三种成分在不同时期的含量变化规律,结果表明地上部分含量明显高于根部,4 月份采收的样品含量高于其它采收时间,三种成分含量高低顺序为芦丁 > 槲皮素 > 木犀草素。该研究结果为蒲公英的合理采收和质量控制提供了科学依据。

蒲公英作为药食两用的常用中药材,不但具有多方面的生物活性,如清热解毒、抗炎、健胃、利尿等功效,可治疗咽炎、急性扁桃腺炎及妇女乳痛等;而且具有多种保健功能,如抗氧化、免疫调节[18]等。随着人们对其广泛和深入研究,必将在医药、食品、保健等领域具有广阔的市场前景。

参考文献:

[1] 丁惠,张馨方,纪文华,等. 蒲公英药用研究进展[J]. 辽宁中医药大学学报,2018,20(9):156-159.

[2] 李伟民,王军宝,张苗苗,等. 蒲公英-苹果复合功能饮料的研制[J]. 许昌学院学报,2018,37(8):50-54.

[3] 施树云,周宏灏,张宇平,等. 管花蒲公英化学成分研究[J]. 中国中药杂志,2009,34(8):1002-1004.

[4] Yadava RN,Khan S. A new flavonoidal constituent from Taraxacum Officinale (L.) Weber[J]. Asian Journal of Chemistry,2013,25(7):4117-4118. DOI: 10.14233/ajchem.2013.14046.

[5] Daisuke S,Takeshi Y,Yasuko I,et al. Officinatrione: an unusual(17S)-17,18-seco-lupane skeleton,and four novel lupane-type triterpenoids from the roots of Taraxacum officinale[J]. Tetrahedron,2013,69: 1583-1589. DOI: 10.1016/j.tet.2012.12.001.

[6] Tsutomu W,Kaoru U,Toshio M. Constituents from the roots of Taraxacum platycarpum and their effect on proliferation of human skin fibroblasts[J]. Chem Pharm Bull,2012,60(2): 205-212. DOI: 10.1248/cpb.60.205.

[7] 许丹,侯凤飞,吴立军,等. 蒲公英的化学研究[J]. 中国中药杂志,2004,29(3):278-278.

[8] 王亚茹,李雅萌,杨娜,等. 蒲公英属植物的化学成分和药理作用研究进展[J]. 特产研究,2017,4:67-75.

[9] 赵惠茹,郭婷. 反相高效液相色谱法同时测定蒲公英中槲皮素和木犀草素的含量[J]. 中国药师,2014,17(7):1106-1108.

[10] 谢沈阳,杨晓源,丁章贵,等. 蒲公英的化学成份及其药理作用[J]. 天然产物研究与开发,2012,24(S1):141-151.

[11] 王京龙,郑丹丹,王 磊,等. 均匀设计法优化葛根半仿生提取工艺[J]. 中成药,2017,39(5):1084-1087.

[12] 薛璇玑,罗 俊,张新新,等. 半仿生酶法提取柿叶中总黄酮的工艺筛选及优化[J]. 中国药房,2017,28(13):1813-1816.

[13] 陈桂,刘跃进,肖翠. 超声辅助半仿生提取半枝莲总黄酮的实验研究[J]. 湘潭大学自然科学学报,2014,36(2):77-80.

[14] 刘爱朋,郭利霄,薛紫鲸,等. 基于指纹图谱和多组分含量测定的蒲公英药材质量控制研究[J]. 中国中药杂志,2018,43(18):3715-3721.

[15] 刘 萍. 蒲公英腌制菜的工艺研究[J]. 吉林农业科技学院学报,2017,26(4):7-10.

[16] 田梦南,周秀秀,周欣,等. 魔芋中黄酮类化合物的提取工艺及挥发油成分研究[J]. 食品研究与开发,2019,40(1):124-131.

[17] 董默,韩婷. 蒲公英黄酮类物质提取条件的优化与含量测定[J]. 氨基酸和生物资源,2014,36(3):72-74.

[18] 孙珊珊,张千,丁林,等. 蒲公英总黄酮含量测定及对小鼠体液免疫功能的影响[J]. 济宁医学院学报,2018,41(4):235-237. DOI: 10.3969/j.issn.1000-9760.2018.04.002.

(收稿日期 2020-01-09)

(本文编辑: 石俊强)

DOI: 10.3969/j.issn.1000-9760.2020.01.005

苹果多酚对蟾蜍心脏活动的影响及其机制*

孙　悦　李　晓　刘梅芳△
(济宁医学院药学院，日照 276826)

摘　要　目的　研究苹果多酚(apple polyphenols，AP)对蟾蜍心脏活动的影响及其机制。**方法**　采用在体心搏曲线记录法，观察 AP 对蟾蜍心肌收缩力和心率的影响；离体蛙心灌流法观测 AP 作用的剂量和时间曲线，并探讨其作用与 β 受体和钙内流之间的关系。**结果**　AP 在离体和在体两个水平均能显著抑制蟾蜍心肌收缩力，而对心率没有明显影响；AP 对心肌收缩力的抑制作用具有浓度和时间依赖性；AP 可以部分抑制肾上腺素引起的正性肌力作用；AP 对心肌收缩力的抑制作用具有钙离子依赖性。**结论**　AP 可以显著抑制蟾蜍心肌收缩力，其作用机制可能与抑制 β 受体和减少钙内流有关。

关键词　苹果多酚；离体蛙心；心率；心肌收缩力；机制
中图分类号：R258.5　　**文献标识码**：A　　**文章编号**：1000-9760(2020)02-019-05

Effects of apple polyphenols on cardiomotility of toads and the underlying mechanisms

SUN Yue, LI Xiao, LIU Meifang△
(*College of Pharmacy, Jining Medical University, Rizhao* 276826, *China*)

Abstract: ***Objective***　To investigate the direct effects of apple polyphenols (AP) on heart rates and myocardial contractility of toads. ***Methods***　In the experiment in vivo, heart beat curve of toad was recorded with the BL-420F data acquisition and analysis system. AP or normal ringer's solution were given by lymph gland injection. In the experimentin vitro, isolated toad heart perfusion method was used to observe the effect of AP on myocardial contractility. ***Results***　AP obviously depressed the myocardial contractility both in vivo and in vitro, but AP had little effects on heart rates. AP decreased the myocardial contractility in both time-and dose-dependent manner. AP significantly inhibited the enhanced myocardial contractility stimulated by β-adrenal agonist or elevated calcium ions in the perfusion solution. ***Conclusion***　AP reduced the cardiac contractility of the toad in both normal condition and adrenaline stimulated condition. The effect of AP on heart was calcium-dependent, and the mechanism was concerned with the inhibition of β-adrenal receptors and the influx of calcium ions.

Keywords: Apple polyphenols; Isolated heart of toad; Heart rate; Cardiac contractility; Mechanism

苹果多酚(apple polyphenols，AP)是苹果中所含多元酚类物质的总称，具有清除自由基、抗氧化、降血压等多种生物学功能[1]。AP 可通过抑制血管紧张素转换酶来降低血压[2]，缓解和减少高血压以及心肌缺血过程中的氧化应激和炎症[3]，改善血管内皮功能，降低血中胆固醇，具有抗动脉粥样硬化的作用[4-6]。经常吃苹果可使心脏病的发病率降低 13% ~ 22%[7]。本研究以蟾蜍为实验对象，在离体和在体两个水平观测 AP 对于心脏活动的影响，并探讨其作用机制。

1　材料和方法

1.1　材料

1.1.1　动物　健康蟾蜍，体重 80 ~ 100g，雌雄不限，由济宁医学院日照校区实验动物中心提供。在体研究中，蟾蜍分为对照组和实验组，每组 8 只；离

* [基金项目] 国家级大学生创新训练计划项目(201610443038)，济宁医学院大学生创新训练计划项目(cx2016038)
△ [通信作者] 刘梅芳，E-mail: lmf_bjmu@163.com

体水平研究中，每组 5 ~ 8 只，制备离体蛙心，用于灌流实验。

1.1.2 主要试剂 AP 干粉由东北林业大学王振宇教授惠赠，纯度约 70%[8]；盐酸肾上腺素注射液（上海禾丰制药有限公司）。所用其他试剂均为分析纯，包括 NaCl、KCl、无水 $CaCl_2$、$NaHCO_3$、NaH_2PO_4 和葡萄糖。蛙心灌流所用任氏液 6 种，无钙任氏液和 5 种不同钙离子浓度的任氏液（$CaCl_2$ 浓度分别为 0.06、0.12、0.18、0.24 和 0.30mg/ml）。其中含有 0.12mg/ml $CaCl_2$ 的任氏液为正常钙离子浓度任氏液（正常任氏液）。用正常任氏液将 AP 干粉配制成 100mg/ml 的原液，分装后置于 -20℃冻存，实验前将 AP 原液配稀释成不同浓度的灌流液。

1.1.3 仪器 FT-100 生物张力换能器、蛙心插管、BL-420F 生物机能实验系统购自成都泰盟科技有限公司。其他实验用品均由济宁医学院药学院综合实验室提供。

1.2 方法

1.2.1 在体心搏曲线记录法 记录蟾蜍在体心搏曲线[9]，待曲线稳定后，采用大腿淋巴囊注射给药的方式研究 AP 对心脏活动的影响。对照组注射正常任氏液 100μl；实验组注射 100mg/ml AP 液 100μl。比较两组给药后 3min 和 6min 的心率以及心肌收缩力变化。

1.2.2 离体蛙心灌流法 采用斯氏法制备离体蛙心标本[9]。为保证曲线的稳定性，我们对传统蛙心灌流法进行改进[10]。蛙心离体后每 3min 更换 1 次正常任氏液，待收缩曲线稳定后进行药物灌流实验，为观察 AP 对肾上腺素作用的影响，采用以下灌流方案。对照灌流组，首先更换新鲜正常任氏液，观察正常曲线 1min，然后换入含 0.1μg/ml 肾上腺素的灌流液，观察效应 2min；实验灌流组采用药物预孵育的方式，先用含 AP（0.5mg/ml 或 1mg/ml）的灌流液预孵育 1min，再换入含有 0.1μg/ml 肾上腺素和 AP 的灌流液，观察 2min。为观察灌流液中钙离子浓度对 AP 作用的影响，采用以下灌流方案：首先，用正常任氏液进行灌流。曲线稳定后，加入含有特定浓度 $CaCl_2$ 的任氏液，待曲线稳定后（约 1min），再加入 1mg/ml AP 灌流液，观察 2min。观察效应完毕后，均更换 3 ~ 4 次正常任氏液，每次间隔 1min，待曲线恢复到正常水平进行下一组灌流观察[10-11]。

1.3 统计学方法

实验数据属于正态分布，以 $\bar{x} \pm s$ 表示。采用 PRISM 8.0 软件进行统计学分析。两组多个时间点的比较，首先采用重复测量资料的方差分析进行比较，然后选用 Sidak's multiple comparisons test 对两组同一时间点进行两两比较。多组之间比较采用单因素方差分析，然后选用 Tukey's multiple comparisons test 进行两两比较。

2 结果

2.1 在体条件下 AP 对心脏活动的影响

淋巴囊注射给药后，实验组蟾蜍心肌收缩力下降幅度大于对照组，差异具有统计学意义（$F = 10.11$，$P = 0.0067$）；不同时间点的心肌收缩力差异有统计学意义（$F = 59.39$，$P < 0.001$）；AP 对心肌收缩力的抑制作用随时间发生改变（$F = 50.34$，$P < 0.001$）。与对照组相比，实验组蟾蜍的心肌收缩力在 AP 注射后第 3min 和第 6min 均显著降低，而心率没有显著性变化。见图 1、表 1。

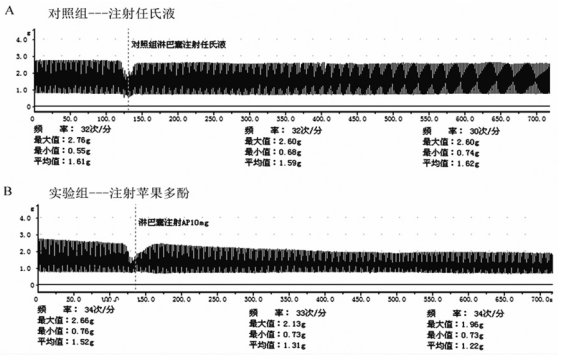

注：图为蟾蜍在体心搏曲线，曲线分两段，给药前和给药后。组别如图所示，A 对照组，注射正常任氏液 100μl；B 实验组，注射 100mg/ml AP 100μl。

图 1 在体条件下 AP 对蟾蜍心率和心肌收缩力的影响

表 1 在体条件下 AP 对蟾蜍心率和心肌收缩力的影响（n = 8）

	心肌收缩力/g			心率/次·min^{-1}		
	给药前	给药后 3min	给药后 6min	给药前	给药后 3min	给药后 6min
对照组	2.35 ± 0.07	2.36 ± 0.08	2.32 ± 0.06	43.38 ± 2.17	42.50 ± 1.69	41.62 ± 2.44
实验组	2.40 ± 0.08	1.96 ± 0.06*	1.72 ± 0.09**	42.81 ± 2.53	42.25 ± 1.97	40.75 ± 2.06

注：与对照组同一时间点相比，* $P < 0.01$，** $P < 0.001$。

3.2　不同浓度 AP 对心肌收缩力的影响

AP 在离体水平也可以显著降低心肌收缩力（见图 2）。0.125mg/ml AP 对心肌收缩力没有明显影响；0.25mg/ml、0.5mg/ml 和 1mg/ml AP 均使心肌收缩力显著降低（见表 2）。计算给药前后的差值，对不同浓度 AP 的负性肌力作用进行比较，结果显示不同浓度 AP 对心肌收缩力的抑制作用不同（$F=63.41$，$P<0.001$），其作用随浓度增加而增强（见表 2）。此外，实验中发现 2 mg/ml AP 可以引起心脏收缩骤停（图 2E）。值得注意的是 AP 的抑制作用可以通过换洗消除，三次换洗后心肌收缩力可以恢复到正常水平，甚至高于正常水平。这说明，AP 对心肌收缩力的抑制作用不是由于急性损伤导致的。

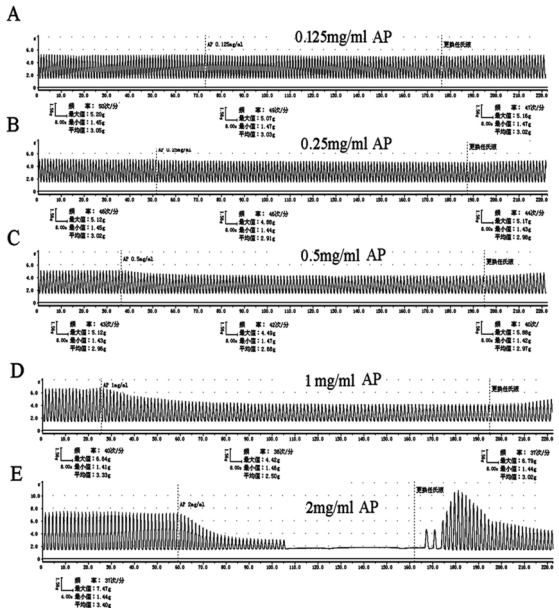

注：图为蛙心灌流心搏曲线，A-E 来自同一只蟾蜍，灌流液中 AP 浓度如图所示。每组灌流曲线分为 3 段，给药前、给药后以及换洗恢复阶段。

图 2　不同浓度 AP 对蟾蜍心肌收缩力的影响

表 2　不同浓度 AP 对蟾蜍心肌收缩力的影响（n = 8）

心肌收缩力/g	AP 浓度/mg·ml^{-1}			
	0.125	0.25	0.5	1
给药前	5.03 ± 0.05	5.02 ± 0.07	4.95 ± 0.08	5.33 ± 0.17
给药后	4.92 ± 0.05	4.67 ± 0.08*	4.19 ± 0.09*	3.47 ± 0.12*
差值	0.12 ± 0.02	0.36 ± 0.07	0.76 ± 0.08**	1.86 ± 0.10***

注：与给药前相比，* $P<0.001$；与 0.25mg/ml AP 组的差值相比，** $P<0.001$；与 0.5mg/ml AP 组的差值相比，*** $P<0.001$。

3.3　不同孵育时间对 AP 负性肌力作用的影响

1mg/ml AP 可以降低蟾蜍心肌收缩力（$F=26.22$，$P=0.0005$）；孵育时间不同，AP 对心肌收缩力的抑制作用也有差异（$F=210.20$，$P<0.001$）；AP 的负性肌力作用随孵育时间的延长发生改变（$F=464.90$，$P<0.001$）。与对照组相比，1mg/ml AP 在第 1min 已经使心肌收缩力略有下降，无统计学差异；在第 3、5、7min AP 均表现出显著的负性肌力作用；不同时间点，AP 对心肌收缩力的抑制作用不同（$F=55.18$，$P<0.001$），且其抑制作随时间延长而增加。见图 3、表 3。

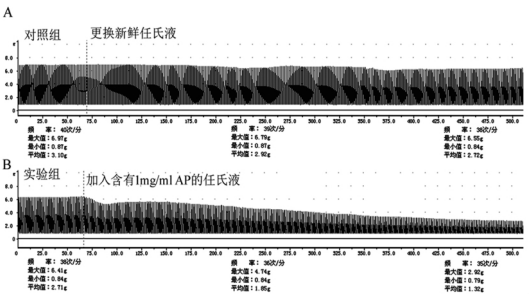

注：图为蛙心灌流心搏曲线，A，B 来自同一只蟾蜍，组别如图所示；每组灌流曲线分为两段，给药前和给药后。

图 3　AP 对心肌收缩力的抑制作用与时间的关系

表 3　1mg/ml AP 在不同孵育时间对心肌收缩力的抑制作用（n = 6）

分组	心肌收缩力/g				
	给药前	给药后			
		1min	3min	5min	7min
对照组	5.45 ± 0.27	5.4 ± 0.25	5.34 ± 0.23	5.13 ± 0.52	4.75 ± 0.21
实验组	5.36 ± 0.22	4.68 ± 0.20	3.70 ± 0.19*#	2.74 ± 0.14*△	2.27 ± 0.10*△

注：与同一时间点的对照组相比，* $P<0.01$；与 AP 处理后 1min 组相比，# $P<0.01$；与 AP 处理后 3min 组相比，△ $P<0.01$。

3.4　AP 对肾上腺素（AD）正性肌力作用的影响

与给药前相比，0.1μg/ml AD、0.1μg/ml AD + 0.5mg/ml AP 和 0.1μg/ml AD + 1mg/ml AP 3 个组均可以使心肌收缩力明显增强，但是在 0.5mg/ml 和 1mg/ml AP 存在的条件下，AD 的正性肌力作用显著降低。见图 4、表 4。

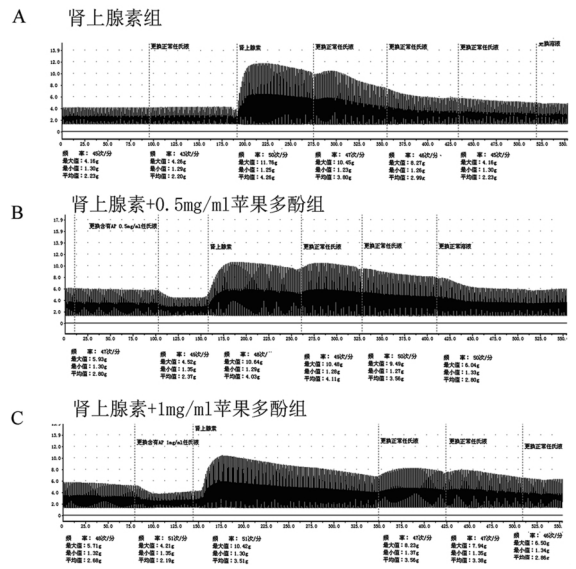

注: 图为蛙心灌流心搏曲线,A、B、C 来自同一只蟾蜍,灌流组别如图所示。每组灌流曲线分为 4 段,给药前、预孵育、给药后以及换洗恢复阶段。

图 4 AP 对肾上腺素刺激条件下心肌收缩力的影响

表 4 AP 抑制肾上腺素刺激引起的心肌收缩力增强(n = 6)

组别	心肌收缩力/g		
	给药前	给药后	差值
0.1μg/ml AD	5.51 ± 0.22	13.68 ± 0.40*	8.17 ± 0.36
0.5mg/ml AP + 0.1μg/ml AD	5.49 ± 0.28	10.69 ± 0.88*	5.19 ± 1.78#
1mg/ml AP + 0.1μg/ml AD	5.53 ± 0.37	9.09 ± 0.50*	3.55 ± 0.19#

注: 与给药前相比,* $P < 0.001$; 与 0.1μg/ml AD 组差值相比,#$P < 0.001$。

3.5 灌流液中钙浓度对 AP 抑制作用的影响

我们进一步观察灌流液中钙离子浓度对 AP 负性肌力作用的影响。将正常灌流液更换为无钙任氏液后,心肌收缩幅度很小,此时 AP 对心肌收缩力抑制作用微弱; 灌流液中 $CaCl_2$ 浓度范围在 0.06 ~ 0.30mg/ml 时,1mg/ml AP 均能降低心肌收缩力(见图 5) 。AP 给药前后心肌收缩力变化显著($F = 965.78$, $P < 0.001$) ,不同钙离子灌流液条件下心肌收缩力有差异($F = 236.27$, $P < 0.001$) ,AP 对心肌收缩力的抑制作用随灌流液中钙离子浓度的变化而改变($F = 48.99$, $P < 0.001$) 。计算不同钙离子浓度灌流条件下给药前后的差值后进行比较,结果显示 AP 对心肌收缩力的抑制作用随着钙离子浓度的增加而增强(见表 5) 。

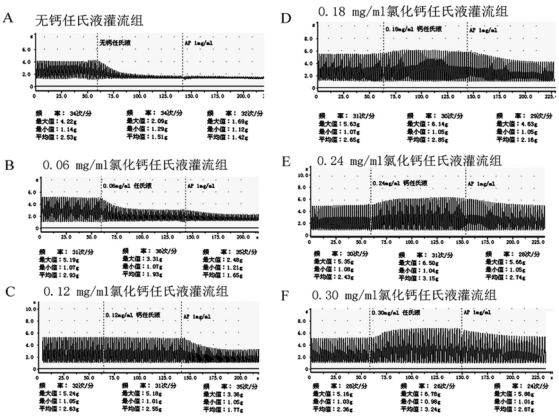

注: 图为蛙心灌流心搏曲线,A-F 来自同一只蟾蜍,灌流液中 $CaCl_2$ 浓度如图所示,AP 均为 1mg/ml; 每组灌流曲线分为 3 段,正常灌流,特定钙离子浓度任氏液灌流,特定钙离子浓度任氏液 + AP 灌流阶段。

图 5 灌流液中钙离子浓度对 AP 抑制作用的影响

表 5 灌流液中钙离子浓度对 AP 抑制心肌收缩力的影响(n = 5)

心肌收缩力/g	灌流液中氯化钙的浓度/mg · ml^{-1}					
	0	0.06	0.12	0.18	0.24	0.3
给药前	1.53 ± 0.13	3.35 ± 0.19	5.27 ± 0.11	6.91 ± 0.12	8.16 ± 0.22	8.62 ± 0.22
给药后	1.33 ± 0.15	2.43 ± 0.21*	3.47 ± 0.07*	5.12 ± 0.11*	5.85 ± 0.17*	6.21 ± 0.21*
差值	0.17 ± 0.03	0.92 ± 0.06	1.81 ± 0.14#	1.79 ± 0.13#	2.31 ± 0.21#	2.40 ± 0.09#△

注: 与给药前相比,* $P < 0.001$; 与 0.06mg/ml 钙离子浓度组相比,#$P < 0.001$; 与 0.12mg/ml 钙离子浓度组相比,△$P < 0.001$。

4 讨论

AP 是一种非常安全的功能性食品[12],具有良好的抗氧化性和抗炎作用[3-4,7],其对于心脏的保护作用受到国内外广泛关注。苹果提取物可以降低小鼠血清中胆固醇、低密度脂蛋白和甘油三酯的含量,增加高密度脂蛋白,增强血液的抗氧化活性,从而减少心血管疾病的发生[5]。苹果类黄酮可以扩张血管,降低血压,具有预防心血管疾病的作用[6]。国内文献报道,AP 可以通过抗氧化和减少性粒细胞浸润发挥对缺血-再灌注后心肌的保护作用[13]。这些研究表明,AP 可以通过扩张血管、降血压、抗氧化、抑制炎症等作用对心脏发挥保护作用。但是 AP 对心脏的直接影响却鲜有报道。

本文以蟾蜍为实验对象,在离体和在体两个水平研究 AP 对于心脏的直接作用。在体的研究结果表明,AP 可以显著抑制蟾蜍心肌收缩力,但对心率无明显影响;离体水平的研究结果显示,AP 可呈剂量和时间依赖性抑制正常条件下的心肌收缩力,并可显著拮抗肾上腺素的正性肌力作用。这提示 AP 抑制心肌收缩力的作用可能与抑制 β 受体有关。交感神经系统兴奋时,血中肾上腺素和去甲肾上腺素增加,作用于心脏 β1 受体引起心肌收缩力增强,升高血压。本文结果显示 AP 可以抑制肾上腺素刺激引起的心肌收缩力增强,这提示 AP 可能通过抑制心肌收缩力发挥降低血压的作用。此外,心脏 β1 受体过度激动会诱发心肌缺血和损伤,AP 可能通过抑制心肌收缩力避免心肌过度劳累,从而发挥对心脏的保护作用。

钙离子是心肌细胞电活动和机械活动的关键离子,本文结果显示,AP 对心肌收缩力的抑制效果随灌流液中钙离子浓度增加而增强。这提示 AP 对心肌收缩力的抑制作用具有钙离子依赖性。研究还发现,AP 可以抵消或者部分抵消高钙引起的心肌收缩力增强,这说明 AP 对心肌收缩力的抑制作用与抑制钙离子内流有关。钙超载是引起心肌缺血—再灌注损害的重要机制之一。心肌细胞内大量 Ca^{2+} 累积,会影响线粒体氧化磷酸化过程,导致细胞能量代谢障碍[12]。本文结果提示,AP 可能通过抑制钙离子内流,防止心肌细胞钙超载,发挥心脏保护作用。

综上所述,本文首次发现 AP 可以显著降低正常以及肾上腺素刺激条件蟾蜍心肌收缩力,其作用具有钙离子依赖性,可能与抑制 β 受体和钙离子内流有关。

参考文献:

[1] 杨薇,张晓旭,李景明. 苹果多酚功能及其作用机理的研究进展[J]. 食品研究与开发,2012,33(1):193-196. DOI:10.3969/j.issn.1005-6521.2012.01.054.

[2] 王艺璇,王世平,马丽艳. 苹果多酚提取物对血管紧张素转化酶活性的抑制[J]. 中国农学通报,2012,28(6):257-261. DOI:10.3969/j.issn.1000-6850.2012.06.048.

[3] Denis MC,Furtos A,Dudonne S,et al. Apple peel polyphenols and their beneficial actions on oxidative stress and inflammation[J]. PLoS One,2013,8(1):e53725. DOI:10.1371/journal.pone.0053725.

[4] Auclair S,Silberberg M,Gueux E,et al. Apple polyphenols and fibers attenuate atherosclerosis in apolipoprotein E-deficient mice[J]. J Agric Food Chem,2008,56(14):5558-63. DOI:10.1021/jf800419s.

[5] Ogino Y,Osada K,Nakamura S,et al. Absorption of dietary cholesterol oxidation products and their downstream metabolic effects are reduced by dietary apple polyphenols[J]. Lipids,2007,42(2):151-161. DOI:10.1007/s11745-006-3008-2.

[6] Bondonno CP,Yang X,Croft KD,et al. Flavonoid-rich apples and nitrate-rich spinach augment nitric oxide status and improve endothelial function in healthy men and women:a randomized controlled trial[J]. Free Radic Biol Med,2012,52(1):95-102. DOI:10.1016/j.freeradbiomed.2011.09.028.

[7] 谭飚,秦晓晓,苏卿,等. 苹果生物活性物质研究与利用现状[J]. 食品工业科技,2013,34(1):58-361,367.

[8] 王振宇,刘春平. 大孔树脂 AB-8 对苹果多酚的分离纯化[J]. 食品研究与开发,2009,30(4):21-24. DOI:10.3969/j.issn.1005-6521.2009.04.007.

[9] 张艳霞. 生理学实验指导[M]. 北京:人民卫生出版社,2005:63-65.

[10] 刘梅芳,刘世东. 蛙心灌流实验中心肌收缩力不稳定的原因分析与对策[J]. 生物学通报,2015,50(7):45-47.

[11] 刘峰,马庆坤,李艳芝,等. 枸骨叶水提物对蟾蜍心肌收缩力的影响及其机制初探[J]. 济宁医学院学报,2016,39(4):275-279. DOI:10.3969/j.issn.1000-9760.2016.04.014.

[12] Akazome Y,Kametani N,Kanda T,et al. Evaluation of safety of excessive intake and efficacy of long-term intake of beverages containing apple polyphenols[J]. J Oleo Sci,2010,59(6):321-338. DOI:10.5650/jos.59.321.

[13] 生守喜. 苹果多酚的提取及对心脏保护作用的研究[D]. 济南:山东师范大学,2015.

(收稿日期　2016-03-28)
(本文编辑:石俊强)

[文章编号] 1000-4718(2020)05-0899-07

枸骨叶水提物对小鼠肥胖的预防作用及对脂肪分化的影响*

刘梅芳△, 孙 悦, 李 丽
(济宁医学院药学院, 山东 日照 276826)

[摘 要] **目的**：研究枸骨叶水提物(ICAE)对高脂饮食(HFD)小鼠肥胖的预防作用及对脂肪分化的影响. **方法**：本研究采用HFD诱导小鼠肥胖,同时灌胃给予ICAE,以奥利司他(orlistat)为阳性对照药。39只昆明雄性小鼠分成4组,包括对照组(n=10)、肥胖模型组(n=9)、orlistat治疗组(n=10)和ICAE治疗组(n=10)。以体重、腹内和皮下脂肪含量、肝重以及血清甘油三酯(TG)和总胆固醇(TC)水平为指标,观察ICAE对肥胖的预防作用;在实验第5周,连续5 d监测ICAE对小鼠24 h平均摄食量的影响; HE染色观察ICAE对脂肪组织的影响。分离和培养大鼠附睾来源的前脂肪细胞,尼罗红染色观察ICAE对分化脂肪细胞内脂滴形态的影响,Western blot法检测ICAE对细胞内过氧化物酶体增殖物激活受体γ(PPARγ)、脂滴包被蛋白1(Plin1)及激素敏感性脂肪酶(HSL)蛋白表达的影响。**结果**：ICAE可以显著抑制HFD引起的小鼠体重、腹内和皮下脂肪含量以及肝重的增加(P<0.01),并且显著降低血清TC和TG水平(P<0.01),但是对摄食量无显著影响; HE染色显示, ICAE能够显著减少HFD引起的白色脂肪细胞肥大。此外,在原代培养的大鼠分化脂肪细胞中, ICAE可以显著抑制细胞内脂滴的积累,并且显著下调脂肪分化关键转录因子PPARγ以及脂肪分化标志物Plin1和HSL的蛋白水平(P<0.01)。**结论**：ICAE对HFD诱导的小鼠肥胖具有预防作用,但对摄食量无明显影响; ICAE可以显著抑制脂肪分化过程,此作用可能与下调PPARγ的蛋白表达有关。

[关键词] 枸骨叶水提物; 肥胖; 脂肪分化; 过氧化物酶体增殖物激活受体γ; 脂滴包被蛋白1; 激素敏感性脂肪酶
[中图分类号] R965; R589.2 [文献标志码] A doi: 10.3969/j.issn.1000-4718.2020.05.019

Preventive effect of *Ilex cornuta* aqueous extract on obese mice and its effects on adipose differentiation

LIU Mei-fang, SUN Yue, LI Li
(*College of Pharmacy*, *Jining Medical University*, *Rizhao* 276826, *China*. *E-mail*: *lmf_bjmu*@163.*com*)

[**ABSTRACT**] **AIM**: To investigate the preventive effect of *Ilex cornuta* aqueous extract (ICAE) on high-fat diet (HFD)-induced obesity in mice and its effects on adipose differentiation. **METHODS**: Male Kunming mice were fed with HFD to induce obesity, ICAE were intragastrically administered at the same time, and orlistat was used as a positive control drug. The mice (n=39) were divided into 4 groups, including control group (n=10), obesity model group (n=9), orlistat treatment group (n=10), and ICAE treatment group (n=10). The body weight, the weight of intra-abdominal and subcutaneous adipose tissue, the liver weight, and the serum levels of triglyceride (TG) and total cholesterol (TC) were determined to evaluate the preventive effect of ICAE on obesity. Average 24-h food consumption of the mice were recorded for 5 times in the fifth week of the experiment to investigate the effect of ICAE on food intake. HE staining was used to observe the influence of ICAE on adipose tissue. The preadipocytes derived from rat epididymal fat pads were adopted to study the effect of ICAE on adipose differentiation. The morphological changes of lipid droplets were observed by Nile red staining, and the protein levels of peroxisome proliferator-activated receptor γ (PPARγ), perilipin 1 (Plin1) and hormone-sensitive lipase (HSL) were examined by Western blot. **RESULTS**: ICAE significantly prevented the increases in the body

[收稿日期] 2019-09-17 [修回日期] 2020-01-08
*[基金项目] 国家级大学生创新训练计划项目(No. 201610443038); 济宁医学院大学生创新训练计划项目(No. cx2016038)
△通讯作者 Tel: 0633-2983678; E-mail: lmf_bjmu@163.com

weight, intra-abdominal and subcutaneous fat tissue weight, and the liver weight induced by HFD ($P<0.01$). ICAE also reduced the serum levels of TC and TG ($P<0.01$), but no effect on food intake was observed. Furthermore, HE staining showed that ICAE obviously prevented the enlargement of adipocytes induced by HFD. In addition, ICAE effectively inhibited the lipid droplet accumulation during differentiation, and significantly decreased the protein levels of PPARγ, a key adipogenic transcription factor, as well as the adipose differentiation markers Plin1 and HSL in primary rat differentiated adipocytes ($P<0.01$). **CONCLUSION**: ICAE has preventive effect on HFD-induced obesity, and has no effect on food intake in mice. ICAE reduces adipose differentiation significantly, and the mechanism might be concerned with the down-regulation of PPARγ protein expression.

[**KEY WORDS**] *Ilex cornuta* aqueous extract; Obesity; Adipose differentiation; Peroxisome proliferator-activated receptor γ; Perilipin 1; Hormone-sensitive lipase

肥胖是一种以体内脂肪含量过多为重要特征的慢性疾病，是脂肪肝、糖尿病、高血压和心脏病的高危因素[1]。预防和治疗肥胖对于维护机体健康具有重要意义。枸骨叶是冬青科冬青属植物枸骨的干燥叶片，又称“角刺茶”和“功劳叶”。枸骨叶与同科属的大叶冬青和苦丁茶冬青一起作为苦丁茶的主要来源[2]。基于中国传统药食同源的理论，苦丁茶的药用价值已经受到广泛关注，很多学者对苦丁茶冬青及大叶冬青的化学成分与药理作用做了深入研究，而对枸骨叶的研究相对较少。现代药理学研究表明，枸骨叶提取物具有抑菌、抗氧化、免疫抑制、降血压、抑制心肌收缩力和降血脂等多种作用[3-7]。枸骨叶水提物(*Ilex cornuta* aqueous extract, ICAE)可以剂量依赖性降低高脂饮食诱导的高脂血症[6]，能够抑制胆固醇合成酶，具有降血脂和抗脂肪肝的作用[7]。但是枸骨叶水提物是否具有减肥作用，是否影响脂肪分化过程尚未见报道。本研究采用高脂饮食(high-fat diet, HFD)诱导小鼠肥胖模型，以目前常用的减肥药奥利司他(orlistat)作为阳性对照药，观察ICAE对肥胖的预防作用，并进一步采用大鼠附睾来源的分化脂肪细胞进行细胞实验，研究ICAE对脂肪分化的影响。

材 料 和 方 法

1 实验动物和分组

实验动物购自济南朋悦实验动物繁育有限公司，许可证号为SCXK(鲁)2014-0007。6周龄清洁级雄性SD大鼠6只，体重150~160 g，用于前脂肪细胞的原代培养。7~8周龄清洁级雄性昆明小鼠50只，体重25~30 g，普通饲料适应性喂养1周，分选出体质量相似的小鼠39只，分成4组，采用HFD诱导小鼠肥胖，orlistat作为阳性对照药[8]，观察ICAE对肥胖的预防作用。动物分为对照(control)组、肥胖模型(obesity model)组、orlistat治疗组和ICAE治疗组，除对照组外，其余3组小鼠均给予HFD。ICAE治疗组给予ICAE 100 mg·kg^{-1}·d^{-1}(相当于生药浓度3 g·kg^{-1}·d^{-1})[6-7]，orlistat治疗组给予orlistat混悬液60 mg·kg^{-1}·d^{-1}[9]于每天上午9:00~10:00灌胃给药，连续5周，对照组则灌胃等体积生理盐水；在实验的第5周，连续5 d监测各组小鼠24 h平均摄食量；末次给药当晚禁食，次日对动物进行称重和取材。每组随机选取3只小鼠，麻醉后经心脏灌流4%多聚甲醛进行组织固定，然后取材，用于后续切片染色。其余小鼠摘眼球取血，分离血清，-80℃冰箱冻存，用于血糖、血清总胆固醇(total cholesterol, TC)和甘油三酯(triglyceride, TG)的测定；取血后的小鼠脱颈椎处死后打开腹腔，取出附睾周围脂肪、肾周脂肪、腹股沟皮下脂肪及肝脏，准确称量其湿重。

2 主要试剂和仪器

ICAE干粉和高脂饲料由本实验室自制；orlistat胶囊(舒尔佳)购自山东新时代药业有限公司；细胞培养所需低糖DMEM培养液和DMEM/F12培养液，前脂肪细胞分离和分化所需Ⅰ型胶原酶、三碘甲状腺原氨酸(T3)、胰岛素和生物素均购自Sigma；四季青胎牛血清购自浙江天杭科技有限公司；胆固醇、HE染色试剂盒、血糖、血清TG和TC测定试剂盒均购自北京索莱宝科技有限公司；兔抗脂滴包被蛋白1(perilipin 1, Plin1)抗体和兔抗激素敏感性脂肪酶(hormone-sensitive lipase, HSL)抗体由美国国立卫生研究院Constantine Londos教授惠赠；兔抗过氧化物酶体增殖物激活受体γ(peroxisome proliferator activated receptor 8, PPARγ)抗体购自Abcam；辣根过氧化物酶标记山羊抗兔II抗购自Sigma；尼罗红染液购自北京普利莱基因技术有限公司。

3 主要方法

3.1 ICAE的制备 枸骨叶采于济宁医学院日照校区本草园，洗净晾干后放入烘箱烘干备用。采用煎煮法制备ICAE[5]。将干燥枸骨叶粉碎，过筛，得到细

粉；称取粉末30 g，加500 mL蒸馏水浸泡30 min后煎煮1 h，然后用纱布分离药渣，再加500 mL蒸馏水，重复煮2次，每次1 h；合并3次煎液进行抽滤，得到澄清水煎液，此澄清水煎液经初步浓缩后放入旋转蒸发仪内，最终形成棕黄色浸膏；将浸膏转入坩埚内，放入干燥箱干燥成ICAE干粉。制备2次ICAE，共得到干粉1.984g，-20 ℃冻存，临前用配制。

3.2 高脂饲料的制备 诱导小鼠肥胖所用高脂饲料系本实验室手工制作而成。参考常用的高脂饲料配方[8-9]，为提高肥胖诱导效果并缩短造模周期我们对配方进行了改良，提高了饲料中猪油的含量。配方如下：基础饲料66%、胆固醇1%、猪油20%、蛋黄粉10%、淀粉3%。材料准备：基础饲料粉碎后过筛，得到细粉；鸡蛋煮熟，取蛋黄，烘干后，碾碎过筛，得到蛋黄粉；用新鲜肥肉炼制猪油；用木薯淀粉做淀粉糊。制作过程：首先在容器内将基础饲料细粉和蛋黄粉混匀，将胆固醇加入猪油中溶解；然后将猪油分次加入到粉末中抓匀，最后加入淀粉糊，和成面团，用去掉前端的5 mL注射器将面团拓成短圆柱形，再放入烘箱50℃烘干。为防止饲料变质，待烘干和烘干后的饲料均放在-20℃冰箱保存。

3.3 HE染色 经灌注取材后的附睾周围脂肪组织，放入4%多聚甲醛中继续固定12 h，然后浸入20%蔗糖溶液中过夜，经过脱水，透明，浸蜡，包埋成蜡块。切片厚度设定为8 μm，染色步骤遵循试剂盒说明书进行，染色结束后进行梯度乙醇脱水，二甲苯透明以及中性树胶封片，晾干后拍照。

3.4 大鼠附睾周围脂肪组织来源前脂肪细胞的分离和培养 采用酶消化法分离大鼠附睾周围脂肪来源的前脂肪细胞[10]。首先将SD大鼠断头处死，取附睾周围脂肪垫，快速剪碎后加入胶原酶Ⅰ工作液（含0.8 g/L胶原酶Ⅰ和1%牛血清白蛋白的KRB溶液），37℃水浴摇床内消化40~50 min使脂肪细胞完全离散。消化结束后加入DMEM培养液20 mL进行稀释，然后用100目滤网过滤，静置10 min，使脂肪细胞自然上浮，吸取下层液体，此液体内含有前脂肪细胞。用含10%血清的DMEM/F12培养液将前脂肪细胞接种于24孔板内。培养24 h后，换入无血清分化液（含有胰岛素5 mg/L、T3 200 pmol/L和生物素33 μmol/L的DMEM/F12培养液）启动分化3 d，然后更换为无血清DMEM/F12培养液，ICAE组加入过滤除菌后的ICAE贮备液，使终浓度为100 mg/L[5]；对照组给予同等体积的生理盐水。给药处理3 d后，用倒置相差显微镜进行活细胞摄相。

3.5 Western blot 给药处理3 d后的分化脂肪细胞，加入细胞裂解液提取蛋白，用于Western blot检测[10]。蛋白分离采用10% SDS-PAGE，用湿转法将蛋白转移至PVDF膜，室温封闭后加入Ⅰ抗，4℃孵育过夜，漂洗3次，孵育辣根过氧化酶标记的Ⅱ抗，洗涤同前。用ECL化学发光检测试剂盒发光、显影和定影。发光后的膜用膜再生液洗去结合的抗体，重新孵育抗体检测其它蛋白。

3.6 脂滴的尼罗红染色 尼罗红染色观察分化脂肪细胞内脂滴的变化[10]。前脂肪细胞接种于细胞爬片，在加入分化液诱导后的第1~6天，每日取出部分细胞爬片，经PBS洗涤后，加入4%多聚甲醛PBS溶液室温固定20 min，然后加入尼罗红染液避光染色10 min分钟，PBS洗涤2次后用75%甘油封片，荧光显微镜下观察和拍照。

4 统计学处理

实验数据以均数±标准误（mean±SEM）表示，采用Prism 8.02软件进行统计学分析，多组之间比较采用单因素方差分析（one-way ANOVA），组间两两比较采用最小显著性差异法（LSD）法，以$P<0.05$为差异有统计学意义。

结 果

1 ICAE对HFD小鼠体重、脂肪重量、肝重和摄食量的影响

与对照组相比，肥胖模型组小鼠体重，附睾、肾脏和腹股沟周围脂肪及肝脏重量均显著增加（$P<0.01$）；ICAE治疗组和orlistat治疗组与肥胖模型组相比，此5项指标均显著下降（$P<0.01$）。从摄食量看，ICAE治疗组和肥胖模型组小鼠的摄食量显著低于对照组（$P<0.01$）；ICAE治疗组小鼠摄食量与肥胖模型组相比略有降低，但是无显著性差异，而orlistat治疗组小鼠摄食量显著高于肥胖模型组和ICAE治疗组（$P<0.01$），与对照组相比无显著差异，见图1。

2 ICAE对HFD小鼠血脂的影响

肥胖模型组小鼠血清TG和TC水平显著高于对照组（$P<0.01$），但是血糖无显著变化；与肥胖模型组相比，orlistat治疗组血清TG和TC水平显著下降（$P<0.01$），ICAE治疗组血清TC和TG也降低（$P<0.05$），但降低幅度较小，与orlistat治疗组相比有显著差异（$P<0.05$），见图2。

3 ICAE对HFD小鼠脂肪组织形态的影响

附睾周围脂肪组织HE染色结果显示，对照组脂肪细胞直径小，有较多胞浆；肥胖模型组脂肪细胞显著增大，与对照组相比直径增加约1倍；ICAE治疗组

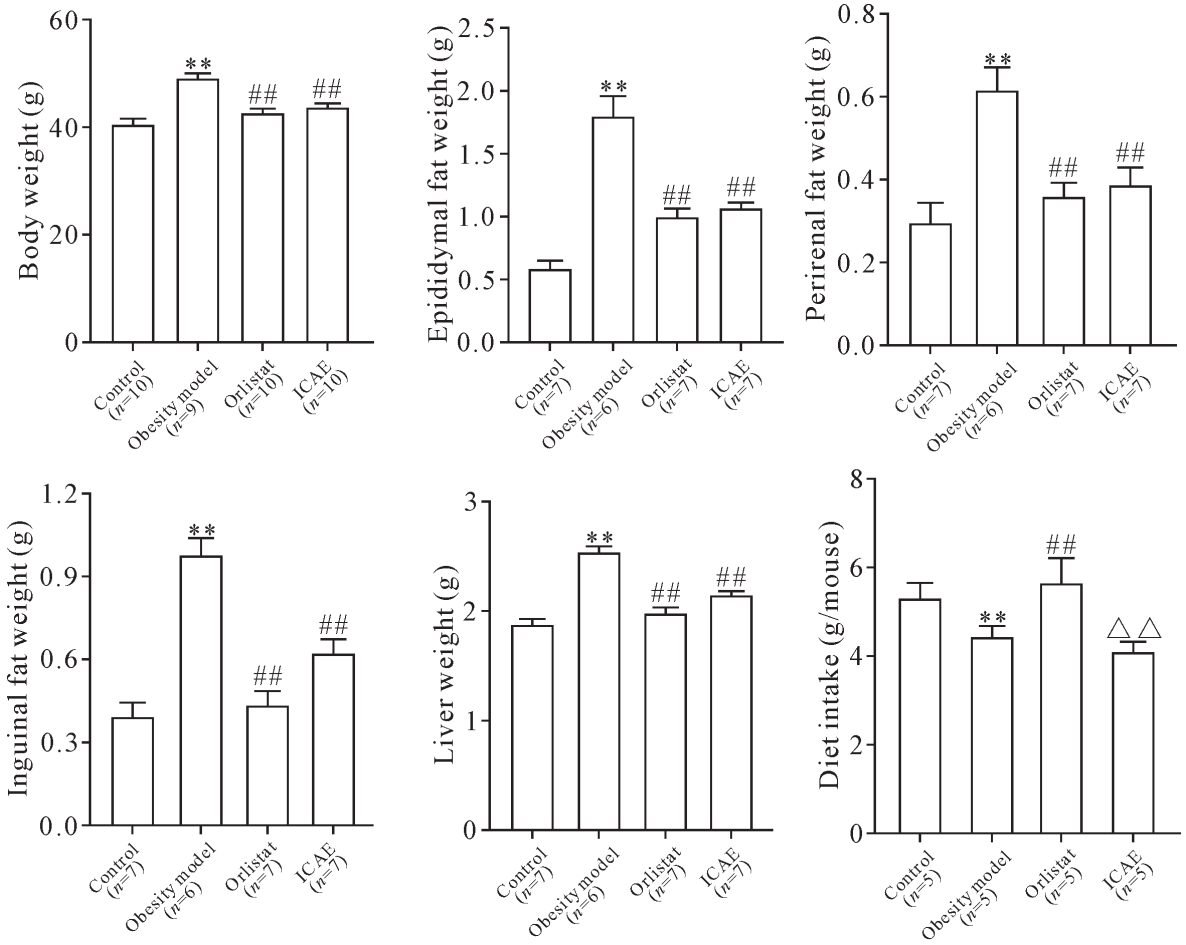

Figure 1. Effects of ICAE on body weight, epididymal fat weight, perirenal fat weight, inguinal fat weight, liver weight, and food intake of HFD-induced mice. Mean±SEM. $^{**}P<0.01$ *vs* control group; $^{\#\#}P<0.01$ *vs* obesity model group; $^{\triangle\triangle}P<0.01$ *vs* orlistat group.

图1　ICAE对HFD小鼠体重、附睾周围脂肪、肾周脂肪、腹股沟脂肪、肝脏重量及摄食量的影响

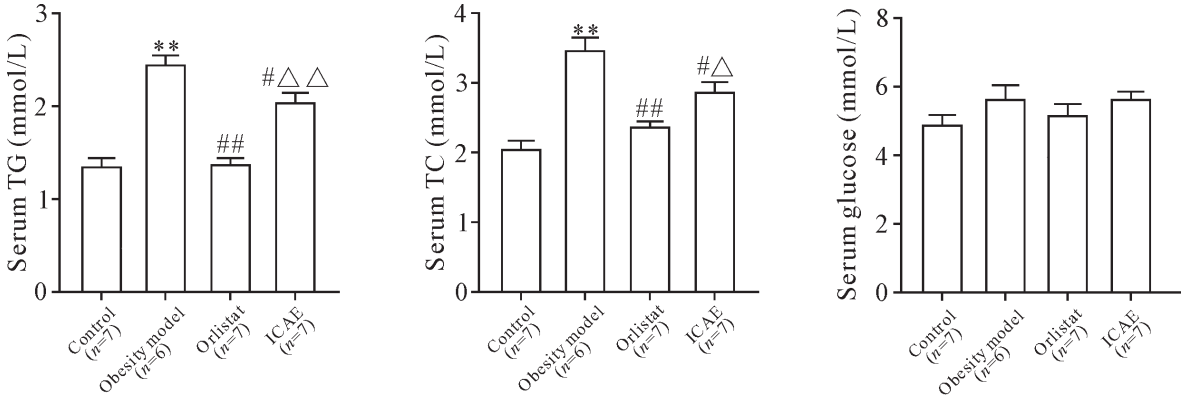

Figure 2. Effects of ICAE on serum triglyceride (TG), total cholesterol (TC) and glucose levels in HDF-induced mice. Mean±SEM. $^{**}P<0.01$ *vs* control group; $^{\#}P<0.05$, $^{\#\#}P<0.01$ *vs* obesity model group; $^{\triangle}P<0.05$, $^{\triangle\triangle}P<0.01$ *vs* orlistat group.

图2　ICAE对HFD小鼠血清甘油三酯、总胆固醇和葡萄糖水平的影响

和orlistat治疗组与肥胖模型组相比，脂肪细胞直径均显著减小，见图3。

4　ICAE对分化脂肪细胞内脂滴的影响

正常情况下，在分化液的诱导下大鼠前脂肪细胞可以分化成为多房脂肪细胞，分化各天细胞内脂滴的特点如图4A所示。加入分化液诱导1 d，细胞由原来的梭形变成多角形，胞浆内有非常微小的脂滴；诱导分化2 d，细胞内出现簇状分布的小脂滴；诱导分化3 d，脂滴直径显著增加，分布在胞浆内。诱导分化3 d后，将分化液更换为无血清DMEM/F12培

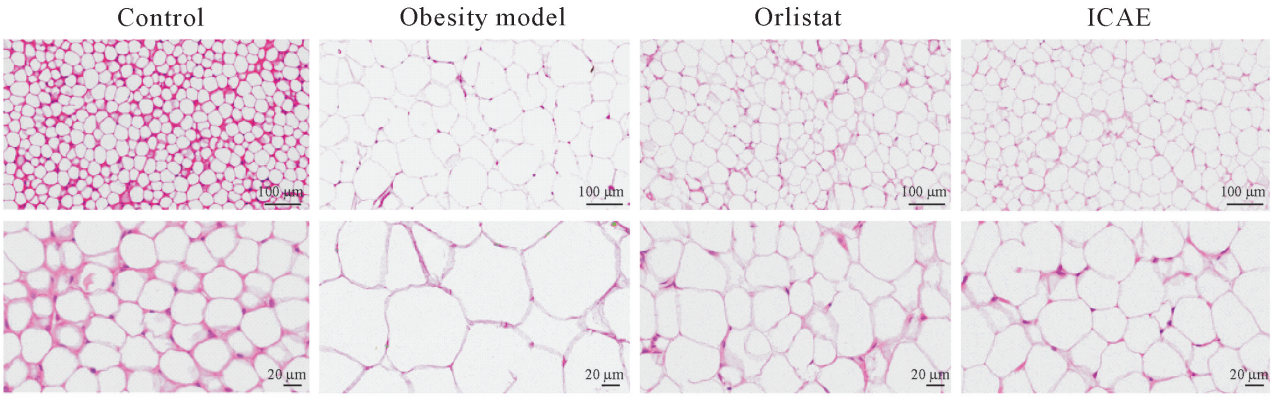

Figure 3. Influences of ICAE on epididymal adipose tissue of HFD-induced mice. Photomicrographs of epididymal adipose tissue of different groups with HE staining.

图3 ICAE对HFD小鼠附睾周围白色脂肪组织形态的影响

养液，细胞内脂滴继续增大，较大的脂滴位于细胞中央。为观察ICAE对脂肪细胞分化的影响，本研究在为细胞更换为无血清DMEM/F12培养液后，给予ICAE（终浓度为100 mg/L）处理3 d。结果显示，对照组脂肪细胞分化程度较为一致，大部分细胞已经出现较大脂滴，符合第6天分化脂肪细胞的特点；而ICAE处理组大部分细胞内脂滴较小，符合第3~4天分化脂肪细胞的特点，见图4B。

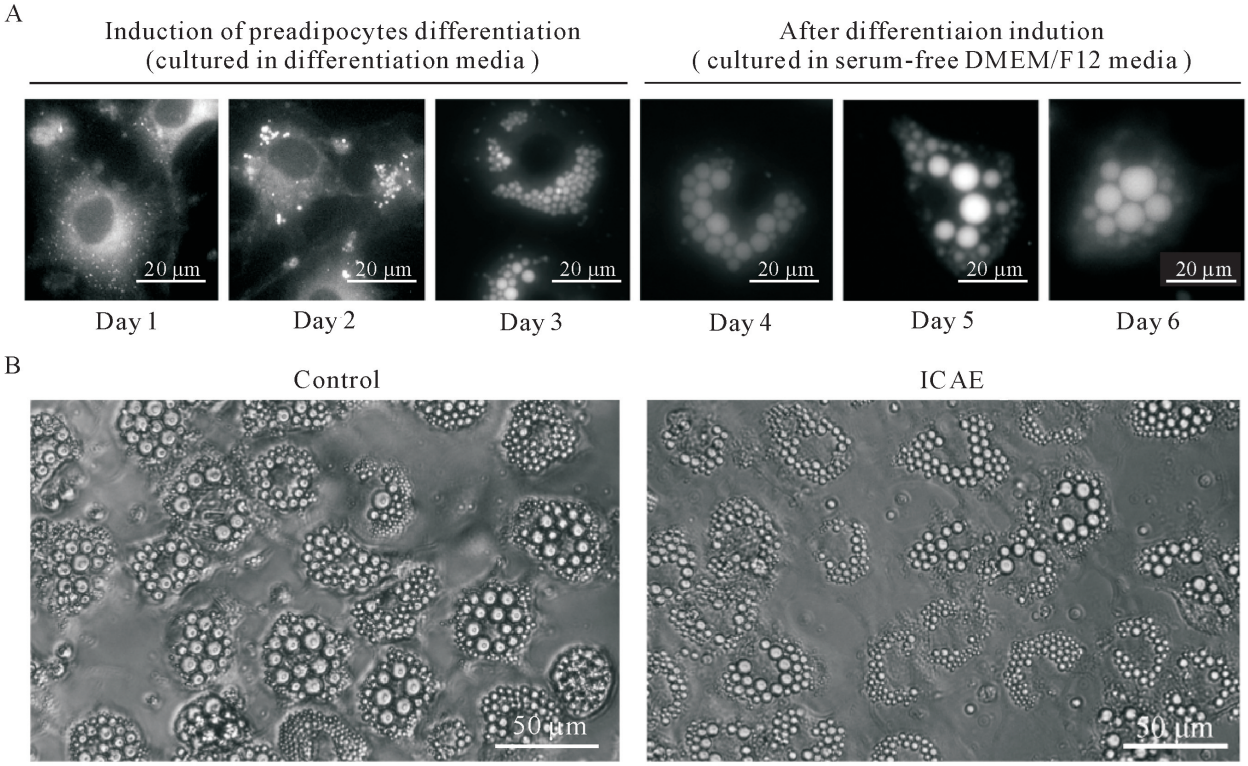

Figure 4. Effects of ICAE on lipid droplet accumulation in rat differentiated adipocytes. A: the morphological changes of lipid droplets in rat differentiated adipocytes form day 1 to day 6 after induction. Preadipocytes were initiated with differentiation media for 72 h, and then the differentiated media were replaced by serum-free DMEM/F12 media. Cells were fixed and stained with Nile red and visualized with fluorescence microscopy on various days. B: effects of ICAE on the lipid accumulation of differentiated adipocytes. On day 3 of differentiation, rat differentiated adipocytes were treated with or without 100 mg/L ICAE after medium replacement. On day 6 of differentiation, living cells were visualized by microscopy

图4 枸骨叶水提物对大鼠分化脂肪细胞内脂滴积累的影响

5 ICAE对脂肪细胞分化关键蛋白表达的影响

利用Western blot观察ICAE对脂肪细胞分化关键蛋白表达的影响。结果显示，100 mg/L ICAE孵育3 d，可以显著抑制分化脂肪细胞PPARγ的蛋白表达（$P<0.01$），并且使脂肪细胞分化标志物Plin1和HSL的蛋白表达显著下降（$P<0.01$），见图5。

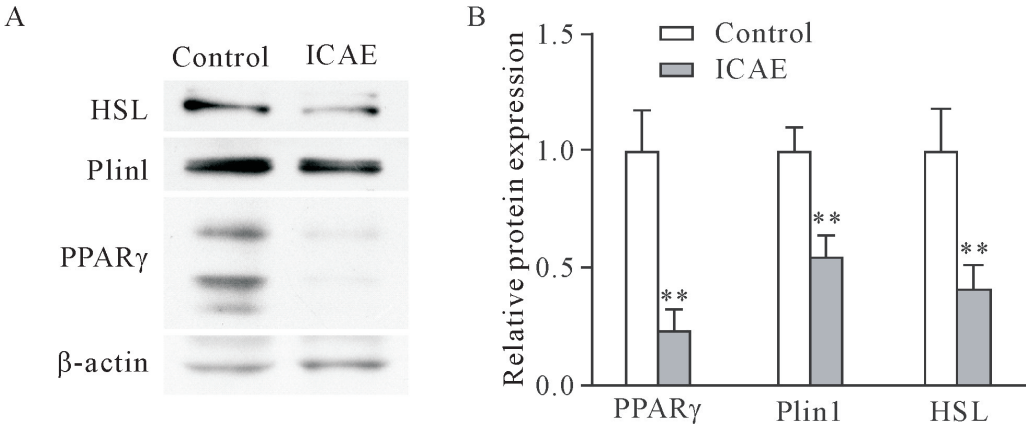

Figure 5. Effects of ICAE on the protein expression of PPARγ, Plin1 and HSL in rat differentiation adipocytes. On day 3 of differentiation, rat differentiated adipocytes were treated with or without ICAE (100 mg/L). On day 6 of differentiation, the protein levels of PPARγ, Plin1 and HSL were detected by Western blot. Mean±SEM. $n=3$. $^{**}P<0.01$ *vs* control group.

图5 ICAE对大鼠分化脂肪细胞PPARγ、Plin1和HSL蛋白表达的影响

讨 论

1 ICAE可抑制HFD诱导的小鼠肥胖

肥胖已被世界卫生组织认定为影响健康的五大危险因素之一。治疗肥胖的常用方法是药物治疗，但是很多减肥药具有严重副作用，目前orlistat是国家食品药品监督管理总局批准的唯一一种减肥药。近些年来，大量研究致力于从植物来源的天然产物中寻找新型安全有效的减肥药物[9,12]。枸骨叶是我国传统中药，有文献报道ICAE具有降血脂的功效[6-7]，但其是否具有减肥作用，尚未见报道。HFD诱导小鼠肥胖是较为理想的肥胖动物模型，可以模拟人类肥胖的发病过程和机制[8]。本实验采用改良的高脂饲料，选用成年雄性昆明小鼠进行造模[8]，成功建立小鼠肥胖模型。HFD喂养5周后，肥胖模型组小鼠的体重、腹内和皮下脂肪组织重量以及肝重均显著高于正常对照组，这说明本研究所用高脂饲料的配方、制作和保存方法合理可行。ICAE处理组小鼠体重、附睾、肾脏、腹股沟周围脂肪组织以及肝重，与肥胖模型组相比均显著降低，且ICAE对上述指标的降低作用与orlistat相比无显著性差异。这说明ICAE作用效果与orlistat相当。血脂测定结果显示，ICAE可以显著降低血清TG和TC水平，这与前人报道一致[6-7]。曾庆峰等[6]研究结果显示ICAE可以剂量依赖性降低HFD诱导的大鼠高脂血症，6 g/kg ICAE的降血脂效果与1.33 mg/kg辛伐他汀相当。本研究观察到ICAE降血脂的效果较弱，这可能与所用剂量较低有关。

2 ICAE对摄食量无显著影响

摄食量是影响体重变化的重要因素。研究结果显示，ICAE治疗组小鼠的摄食量与肥胖模型组相比略有降低，但无显著性差异，这说明ICAE对摄食量无显著影响。肥胖模型组和ICAE治疗组小鼠摄食量显著低于对照组，这可能是由于富含脂肪、胆固醇和蛋白的饲料容易使小鼠产生饱腹感，并延缓胃排空。出乎意料的是，orlistat治疗组小鼠摄食量显著高于肥胖模型组和ICAE治疗组。实验中还观察到，orlistat治疗组小鼠与其它组小鼠相比，排出的粪便量较多，质地较软且具有油性光泽。冯孔龙等[11]在HFD诱导的大鼠肥胖模型中也观察到orlistat治疗组摄食量高于肥胖模型组。这可能是由于orlistat抑制脂类食物的消化吸收，降低了食物的转化率，导致动物摄食量代偿性增加。从摄食量的变化分析，ICAE的减肥机制可能与orlistat有所不同。

3 ICAE抑制脂肪细胞肥大和脂肪细胞分化

脂肪组织是机体主要的能量贮库，长期能量摄入过多，会使脂肪细胞体积和数目持续增加，最终导致肥胖。附睾周围组织HE染色结果显示，ICAE可以显著减小附睾周围脂肪组织脂肪细胞的直径，其作用效果与orlistat相当。这提示ICAE可能具有抑制脂肪细胞肥大的作用。本研究采用了大鼠附睾周围脂肪组织来源的分化脂肪细胞进行了进一步研究。结果表明，ICAE可以显著抑制分化脂肪细胞内

脂滴的积累，并且降低Plin1和HSL的蛋白表达。分化脂肪细胞内脂滴的大小在一定程度上可以反映脂肪细胞的成熟度[12-13]；Plin1和HSL是成熟脂肪细胞表达的功能蛋白，在脂滴TG的贮存和分解中发挥重要作用，被认为是脂肪细胞分化成熟的标志物[12]。所以，此结果提示ICAE具有抑制脂肪细胞分化成熟的作用。PPARγ是脂肪细胞分化过程所必需的转录因子，能与视黄醛X受体α形成异源二聚体，促进大多数与脂肪发育相关基因的表达[13]。有文献报道*PPARγ*基因的表达水平与脂肪细胞的大小及脂肪细胞的分化程度呈正相关[14]，PPARγ拮抗剂能阻止前脂肪细胞分化，并抵抗HFD引起的脂肪细胞过度肥大[15]。本研究显示，ICAE可以显著抑制分化脂肪细胞PPARγ的蛋白表达。因此ICAE抑制脂肪细胞肥大和分化的作用可能与下调PPARγ的蛋白表达有关。

综上所述，本研究证实了ICAE对HFD诱导的小鼠肥胖具有预防作用，但对其摄食量无明显影响；ICAE可以显著抑制脂肪细胞分化，此作用可能与抑制PPARγ的蛋白表达有关。本研究将为ICAE在预防和治疗肥胖方面的应用提供实验证据。

［参　考　文　献］

［1］ 贺媛，曾强，赵小兰. 中国成人肥胖、中心性肥胖与高血压和糖尿病的相关性研究[J]. 解放军医学杂志，2015，40(10)：803-808.

［2］ 李维林，郭荣麟，傅晖，等. 苦丁茶、功劳叶和枸骨的本草考证[J]. 中药材，2003，26(8)：595-598.

［3］ 张晶，林晨，岑颖洲，等. 枸骨叶抗真菌作用初探[J]. 中国病理生理杂志，2003，19(11)：1562.

［4］ 王存琴，何丹. 枸骨的化学成分及药理活性研究进展[J]. 包头医学院学报，2016，32(8)：160-162.

［5］ 刘峰，马庆坤，李艳芝，等. 枸骨叶水提物对蟾蜍心肌收缩力的影响及其机制初探[J]. 济宁医学院学报，2016，39(4)：275-279.

［6］ 曾庆锋，谭军. 枸骨叶提取物对高脂血症模型大鼠脂代谢及血液流变学的影响[J]. 中国药师，2016，19(4)：631-633.

［7］ 王宏婷，何丹，王存琴，等. 枸骨叶水提物对高脂小鼠胆固醇合成代谢的影响[J]. 中国现代医学杂志，2016，26(23)：1-5.

［8］ 陈秋平. 油茶蒲减肥降脂功能因子研究[D]. 杭州：浙江大学，2011.

［9］ 和兴萍，罗燕，李雪，等. 几种降脂减肥实验动物模型的建立与比较[J]. 中华中医药学刊，2017，35(7)：1747-1751.

［10］ 刘梅芳，杜从阔，苏雪莹. Forskolin引起大鼠脂肪细胞内脂滴重塑[J]. 生理学报，2019，71(3)：379-387.

［11］ 冯孔龙，朱晓艾，陈彤，等. 川陈皮素对高脂膳食诱导大鼠的降脂减肥及预防脂肪肝形成作用[J]. 食品科学，2018，39(1)：213-220.

［12］ Sztalryd C，Kimmel AR. Perilipins：lipid droplet coat proteins adapted for tissue-specific energy storage and utilization，and lipid cytoprotection[J]. Biochimie，2014，96：96-101.

［13］ 杨谷良，潘敏雄，向福，等. PPARγ调控脂肪细胞增殖和分化机理研究进展[J]. 食品科学，2017，38(3)：272-278.

［14］ Guo L，Sun B，Shang Z，et al. Comparison of adipose tissue cellularity in chicken lines divergently selected for fatness[J]. Poultry Science，2011，90(9)：2024-2034.

［15］ Nakano R，Kurosaki E，Yoshida S，et al. Antagonism of peroxisome proliferator activated receptor gamma prevents high-fat diet-induced obesity *in vivo*. Biochem Pharmacol，2006，72(1)：42-52

（**责任编辑**：林白霜，余小慧）

Hindawi
Evidence-Based Complementary and Alternative Medicine
Volume 2020, Article ID 8899762, 13 pages
https://doi.org/10.1155/2020/8899762

Research Article

Polysaccharides of *Scrophularia ningpoensis* Hemsl.: Extraction, Antioxidant, and Anti-Inflammatory Evaluation

Jian'an Wang,[1] **Lufen Huang**,[1] **Qiang Ren**,[1] **Yanjun Wang**,[1,2] **Lirun Zhou**,[1] **Yingjie Fu**,[1] **Chunmei Sai**,[1] **Shafii Shaibu Pella**,[1] **Yingying Guo**,[1] **and Li-Na Gao**[1,3]

[1]*School of Pharmacy, Jining Medical University, Rizhao, Shandong 276826, China*
[2]*Maternal and Child Health Care Family Planning Service Center, Ju Xian, Shandong 276500, China*
[3]*Townsend Family Laboratories, Department of Psychiatry, The University of British Columbia, 2255 Wesbrook Mall, Vancouver BC V6T 1Z3, Canada*

Correspondence should be addressed to Li-Na Gao; linagao228@126.com

Received 30 August 2020; Revised 23 October 2020; Accepted 5 December 2020; Published 15 December 2020

Academic Editor: Jianping Chen

The roots of *Scrophularia ningpoensis* Hemsl. are a famous traditional Chinese medicinal herb and are also used as health food. However, information about polysaccharides from *S. ningpoensis* (SNPS) is very limited. We applied the ultrasonic-assisted extraction (UAE) process to extract SNPS. The UAE conditions were optimized using single-factor experiments and response surface analysis. Under the optimized conditions of ultrasonic power of 550 W, extraction time of 26 min, and extraction temperature at 50°C, the highest yield of 13.47% ± 1.63% was obtained, which was in accordance with the predicted value of 13.71%. In comparison with traditional hot water extraction, the optimized UAE method significantly increased the extraction yield with lower extraction temperature and shorter extraction time. Furthermore, the *in vitro* antioxidant evaluation showed that EC_{50} values of SNPS were 2.43 ± 0.21, 4.40 ± 0.35, and 0.56 ± 0.062 mg/mL for 2,2-diphenyl-1-picrylhydrazyl radical (DPPH) radical, hydroxyl free radical, and 2,2'-azinobis (3-ethylbenzothiazoline-6-sulfonic acid) (ABTS) radical scavenging assay, respectively. The anti-inflammatory potential of SNPS was detected in lipopolysaccharide (LPS) induced ICR mice. Real-time reverse transcription-polymerase chain reaction and enzyme-linked immunosorbent assay showed that SNPS significantly improved LPS-stimulated inflammatory response by decreasing mRNA and protein expression of interleukin (IL)-6 and tumour necrosis factor (TNF)-α in a dose-dependent manner. In conclusion, the extraction process of SNPS established in this study is reliable, and SNPS possesses potential antioxidant and anti-inflammatory activities, which will provide a theoretical basis for guiding the clinical application of *S. ningpoensis*.

1. Introduction

The roots of *Scrophularia ningpoensis* Hemsl. (*Radix Scrophulariae ningpoensis*) are a perennial plant which belongs to the Scrophulariaceae family. Its dried roots are known in China as Xuanshen, a traditional medicine that has been used as an antipyretic and for the treatment of sore throat and prurigo for over 1000 years [1, 2]. It has also been used as a health food. The main chemical substances of the roots of *S. ningpoensis* include iridoids, alkaloids, flavonoids, essential oils, and carbohydrates, which have been reported to possess anti-inflammatory actions [3–5]. Moreover, these plant-derived bioactive components are characterized by potential antioxidant activities [6, 7]. However, few studies focused on the activity of polysaccharides from *S. ningpoensis* (SNPS). Polysaccharides are among the most active substances found in nature, with a variety of biological activities, such as antitumour, antioxidation, anti-inflammation, and immune regulation, with relatively low toxicity and side effects [8–10].

The development of efficient extraction methods for polysaccharides is important. The main polysaccharides

extraction methods include hot water extraction (HWE), ultrasonic-assisted extraction (UAE), enzyme-assisted extraction (EAE), and microwave-assisted extraction (MAE) [11–14]. The UAE method utilizes the mechanical and thermal action generated by the high-frequency oscillation of ultrasonic waves, which results in a sharp increase in the frequency and rate of movement of the molecules inside the materials, thereby causing the rupture of the tissues and cells and the release of the active ingredients. This method is widely used, simple to operate, and associated with high extraction efficiency [15, 16]. More importantly, UAE has potential advantages of protecting the structure and biological activity of active components [17–19].

In this study, the water-soluble polysaccharides from *S. ningpoensis* were extracted using the UAE method, and the extraction process was optimized by single-factor experiments and response surface method (RSM). After the deproteinization of the crude polysaccharides obtained from *S. ningpoensis*, the structure and monosaccharide compositions of SNPS were determined using Fourier transform infrared spectroscopy (FT-IR) and high-performance liquid chromatography (HPLC), respectively. To further investigated the antioxidant potential of SNPS, 2,2-diphenyl-1-picrylhydrazyl (DPPH) radical, hydroxyl free radical, and 2,2'-azinobis (3-ethylbenzothiazoline-6-sulfonic acid) (ABTS) radical scavenging tests were performed. Simultaneously, lipopolysaccharide (LPS) induced *in vivo* inflammatory mice model was used to detect the anti-inflammatory activities of SNPS. These results will provide a theoretical basis for the further development and utilization of polysaccharides from *S. ningpoensis*.

2. Materials and Methods

2.1. Chemicals and Reagents. The roots of *S. ningpoensis* were collected from the experimental field of Jining Medical University (Rizhao, Shandong, China) and identified by Jian'an Wang (Medical Botanist, Jining Medical University). Monosaccharide standards D-glucose (D-Glc), D-galactose (D-Gal), D-arabinose (D-Ara), L-fucose (L-Fuc), D-mannose (D-Man), L-rhamnose (L-Rha), D-fructose (D-Fru), D-xylose (D-Xyl), D-GlcA, and D-GalA were purchased from Sigma-Aldrich (St. Louis, MO, USA). 2,2-Diphenyl-1-picrylhydrazyl (DPPH) free radical was purchased from Sigma-Aldrich (St. Louis, MO, USA). 2,2'-azinobis (3-ethylbenzothiazoline-6-sulfonic acid) (ABTS) free radical was purchased from the Shanghai Yuanye Biotechnology Co. Ltd. (Shanghai, China). ImProm-II Reverse Transcription System was obtained from Promega Corporation (Madison, WI, USA). IL-6 Mouse ELISA Kit was purchased from Invitrogen (Carlsbad, CA, USA). TNF-α Mouse ELISA Kit was obtained from PeproTech (Rocky Hill, NJ, USA). UNIQ-10 column Trizol total RNA extraction kit was obtained from Sangon Biological Engineering Technology and Services Co., Ltd. (Shanghai, China). FastStart Universal SYBR Green Master (ROX) kit was purchased from Roche (Mannheim, Germany). All chemical reagents were of analytical grade, and the deionized water was used in the whole experiment.

2.2. Pretreatment of the Roots of S. Ningpoensis. After washing the roots of *S. ningpo*ensis, they were drained and then dried under vacuum at 65°C. Root powder was obtained after pulverizing and sifting the dried roots with a 40-mesh sieve. Subsequently, the dried powder was mixed with acetone (at a ratio of 1 : 5) to remove fat-soluble substances by uniformly stirring for 24 h. The precipitate was concentrated and lyophilized (40°C, 12 h) to obtain the pretreated root sample.

2.3. Ultrasonic-Assisted Extraction Process. UAE was performed according to the described procedure of Jian-Hua Xie with slight modifications [20]. In detail, a total of 5.0 g of the pretreated *S. ningpoensis* powder was extracted by adding 150 mL deionized water. The reaction system was placed in an ultrasonic cell pulverizer (Xinyi 1200E, Ningbo Xinyi Ultrasonic Equipment Co., Ltd., Ningbo, China) with a low constant temperature tank (DC-8006, Ningbo Xinyi Ultrasonic Equipment Co., Ltd., Ningbo, China). The ultrasonic power was set to 285, 380, 475, 570, and 665 W, respectively. The extraction temperature was set to 30, 40, 50, 60, and 70°C, respectively. The extraction time was set to 5, 15, 25, 35, and 45 min, respectively. The solutions obtained after the reactions were diluted with a quadruple volume of absolute ethanol to a final alcohol content of 80%, and the mixtures were stored at 4°C overnight and then centrifuged at 3500 rpm for 15 min. The precipitates were freeze-dried to obtain the crude polysaccharides. The resulting crude SNPS were redissolved in deionized water, deproteinized according to the method reported by Sevag et al. [20], and lyophilized to obtain purified SNPS for subsequent analysis.

The extract yield of SNPS was determined by the phenol sulfuric acid method with minor modification [21] and calculated according to the following formula:

$$\text{Extraction yield (\%)} = \frac{C \times V}{W} \times 100\%, \quad (1)$$

where C (mg/mL) is the concentration of the SNPS solution, V is the dilution factor, and W is the dry weight of the pretreated powder.

2.4. Optimization of Extraction Process. Based on the results of monofactor tests, RSM was further used to optimize the extraction parameters. BBD was applied to determine the effect of extract temperature (X_1, °C), ultrasonic power (X_2, W), and extract ultrasonic time (X_3, min) at three levels on the extraction yield of SNPS. As shown in Table 1, the above 3 factors were designed at three levels respectively, and −1, 0, and 1 represented the low, medium, and high levels of the independent variables, respectively.

Based on experiment results from BBD, a second-order polynomial model was performed as follows:

$$Y = A_o + \sum_{i=1}^{3} A_i X_i + \sum_{i=1}^{3} A_{ii} X_i^2 + \sum_{i=1}^{2} \sum_{i=j+1}^{3} A_{ij} X_i X_j, \quad (2)$$

where Y is the response variable (extraction yield of SNPS); A_0 is a constant, Ai is the linear coefficient, Aii is the

Table 1: Coded and uncoded levels of independent variables used for BBD.

Independent variable	Coded levels		
	−1	0	1
Ultrasonic temperature (X_1) (°C)	30	50	70
Ultrasonic power (X_2) (W)	285	475	665
Ultrasonic time (X_3) (min)	15	25	35

quadratic coefficient, and Aij is the interaction coefficient. Xi and Xj are independent variables ($i \neq j$).

2.5. Monosaccharide Component Analysis. The monosaccharide component was determined by HPLC (Waters1525, Waters Co., USA). A total of 2.0 mg SNPS sample was mixed with 1 mL trifluoroacetic acid (TFA, 2 mol/L) and then hydrolyzed in an oven at 121°C for 2 h. Subsequently, the volume was adjusted to 50 mL with water, and the mixture was filtered with a 0.45 μm microporous membrane for HPLC analysis. All standard sugars were prepared according to the same method. The sample and standards were analyzed by ion chromatography using ICS-5000 ion chromatograph (Dean Inc., USA) with a pulsed amperometric detector (PAD) as previously reported [22], with some modifications. An UltrahydrogelTM Linear column (300 mm × 7.8 mm) was used with a flow rate of 0.5 mL/min. The detailed liquid phase was shown in Table 2.

2.6. FT-IR Analysis of SNPS. A total of 1.0 mg of SNPS was mixed with potassium bromide for tableting, and the dried polysaccharides were subjected to 4000-400 cm^{-1} scanning using FT-IR (IR Tracer-21, Shimadzu Corporation, Tokyo, Japan).

2.7. DPPH Radical Scavenging Activity of SNPS. The DPPH radical scavenging activity of SNPS was evaluated as previously reported [23], with slight modifications. Briefly, SNPS solutions were diluted with DPPH-ethanol solution and incubated at room temperature in the dark for 30 min. The DPPH solution was replaced with anhydrous ethanol in the control tube, and the polysaccharides solution was replaced with distilled water in the blank tube. The absorbance of each solution was measured at a wavelength of 517 nm and ascorbic acid (Vitamin *c*, Vc) was used as a positive control. The scavenging rate was calculated according to the following formula:

$$\text{Scavenging activity } (\%) = \left(1 - \frac{A_S - A_C}{A_b}\right) \times 100, \quad (3)$$

where A_s was the absorbance of DPPH-ethanol solution, deionized water and SNPS samples, A_c was the absorbance of SNPS solution with equivolumetric anhydrous ethanol instead of DPPH, A_b was the absorbance of DPPH solution with equivolumetric deionized water (without SNPS).

2.8. Hydroxyl Free Radical Scavenging Rate of SNPS. The hydroxyl radicals scavenging activity of SNPS was determined according to the method reported by Li with a slight modification [24]. In short, SNPS was added sequentially with 2.0 mL ferrous sulfate solution (9 mmol/L, $FeSO_4$), 2.0 mL salicylic acid in ethanol (9 mmol/L, $C_7H_6O_3$), and 2.0 mL hydrogen peroxide solution (9 mmol/L, H_2O_2). The mixtures were shaken well and incubated at 37°C for 30 min. Deionized water was used as a reference and the absorbance was measured at a wavelength of 510 nm. Vc of the same mass concentration was used as a positive control. The scavenging rate was calculated according to equation (3), where As was the absorbance of the samples in the $FeSO_4$–$C_7H_6O_3$ reaction system, Ac was the absorbance of the samples in deionized water, and Ab was the absorbance of the $FeSO_4$–$C_7H_6O_3$ reaction system with deionized water.

Table 2: Mobile phase and gradient for monosaccharide composition analysis.

Time (min)	Water (%)	NaOH (250 mM, %)	NaAc (1 M, %)
0	97.4	2.6	0
21	97.4	2.6	0
21.1	92.4	2.6	5
30	77.4	2.6	20
30.1	20	80	0
50	20	80	0

2.9. ABTS Free Radical Scavenging Rate of SNPS. The ABTS radical scavenging activity of SNPS was determined using a modified method, according to Re et al. [25]. Equivalent amounts of 7 mmol/L ABTS solution and 2.45 mmol/L potassium persulfate solution were mixed and incubated at room temperature in the dark for 12–16 h to prepare the $ABTS^+$ stock solution. Then the $ABTS^+$ assay solution was obtained by diluting the stock solution with distilled water. Different concentrations of SNPS samples were mixed with $ABTS^+$ assay solution followed by incubation at room temperature in the dark for 60 min. The absorbance was measured immediately at 734 nm. Vc was used as a positive control. The ABTS radical scavenging activity was calculated using equation (3), with ABTS solution instead of DPPH.

2.10. In Vivo Anti-Inflammatory Evaluation of SNPS. Male-specific pathogen-free (SPF) grade imprinting control region (ICR) mice (18–22 g) were purchased from Qingdao Daren Fortune Animal Technology Co., Ltd (Qingdao, China). All mice were housed under controlled environmental conditions (temperature, 22 ± 1°C; relative humidity, 50 ± 5%; light/dark cycle, 12 h). The animal experiments were conducted according to the NIH Guide for the Care and Use of Laboratory Animals and the protocol was approved by the Ethics Committee of Jining Medical University.

After adaptation for 7 days, a total of 48 mice were randomly assigned into 6 groups ($n = 8$): (1) Normal control group; (2) Model group; (3) Positive group (aspirin 10 mg/kg); (4–6) SNPS (100, 200 or 400 mg/kg, respectively). SNPS was dissolved in sterile pyrogen-free saline solution. The mice in the normal control group and model group were

gastrointestinally treated with 0.9% saline for 4 days (once per day). Mice in the positive group and the SNPS group were treated with aspirin and corresponding dosages of SNPS, respectively, for 4 days, once per day. Thirty minutes after the final administration, the mice (in addition to the control group) were intraperitoneally injected with LPS (1 mg/kg). The mice in the control group were treated with equal volumes of saline. After 90 min, all mice were sacrificed by diethyl ether asphyxiation. The blood was collected, and serum was prepared and stored at −20°C for the detection of protein levels of TNF-α and IL-6. Simultaneously, the liver tissues were harvested and weighed; the liver tissues were used for the determination of the mRNA expression.

2.11. Real-Time RT-PCR Assay. The mRNA expressions of IL-6 and TNF-α in the mouse liver were detected by real-time RT-PCR. In brief, the liver tissues (approximately 50 mg) were homogenized in 500 μL Trizol, and the total RNA was isolated using a Sangon UNIQ-10 column Trizol total extraction kit. Then, reverse transcriptions were performed using the ImProm-II Reverse Transcription System cDNA synthesis kit according to the manufacturer's instructions. The real-time RT-PCR oligonucleotide primers used for the mouse IL-6, TNF-α, and β-actin (an internal control) are listed in Table 3. The reaction processes were performed as previously described [26].

2.12. Analysis for Serum IL-6 and TNF-α Expression. The serum concentrations of TNF-α and IL-6 were detected according to the commercial ELISA kits. The serum samples for TNF-α and IL-6 were assayed at a 100-fold and 50-fold dilution in the assay buffer, respectively.

2.13. Statistical Analyses. Statistical analysis was performed using the Origin 8.0 software (Northampton, MA, USA). In vitro, data were expressed as the means ± S.D. from three independent experiments. In vivo, data were expressed as the means ± S.E. Differences between groups were analyzed by one-way analysis of variance (ANOVA). A P-value less than 0.05 was considered statistically significant.

3. Results and Discussion

3.1. Effect of Ultrasonic Power on the Yield of SNPS. In this study, the UAE method was applied to extract SNPS from the roots of *S. ningpoensis*. The extraction power, temperature, and time were evaluated, and the results are shown in Figure 1. To examine the effect of the ultrasonic power on the extraction efficiency, the ratio of material to liquid, extraction temperature, and extraction time was set as 1 : 30 g/mL, 50 °C and 25 min, respectively. As shown in Figure 1(a), with an ultrasonic power of 475 W, the extraction efficiency reached its maximum of 12.45% ± 0.16%. Subsequently, however, the extraction yield decreased with a further increase of ultrasonic power. The ultrasonic power, therefore, had a significant influence on the extraction yield. We speculated that higher ultrasonic power would induce the degradation of polysaccharides [27]. Therefore, 475 W was chosen as the optimal extraction power for subsequent optimization experiments.

3.2. Effect of Ultrasonic Temperature on the Yield of SNPS. A total of 5.0 g of acetone-extracted *S. ningpoensis* powder was weighed accurately. The ratio of material to liquid, ultrasonic power, and extraction time was set as 1 : 30 g/mL, 475 W, and 25 min, respectively, in order to detect the effect of temperature on the extraction efficiency. When the temperature increased, the vapor pressure made more solvent vapors enter the bubble cavity and induce the collapse of the cell wall. Thus, it made the solvent penetrate deeply into the sample matrix, resulting in higher extraction efficiency. As shown in Figure 1(b), a maximum yield of 13.21% ± 0.087% was observed at 50°C. The extraction efficiency decreased at higher temperatures, likely due to the increased dissolution of impurities [28, 29].

3.3. Effect of Extraction Time on the Yield of SNPS. The effect of the ultrasonic time on the yield of SNPS was investigated from 5 to 45 min, with other extraction conditions fixed as follows: the ratio of material to liquid, 1 : 30 g/mL; ultrasonic power, 475 W; and temperature, 50°C. As shown in Figure 1(c), the yield of SNPS increased from 10.90% ± 0.073% to 13.35% ± 0.10% from 5 to 25 min, respectively. The yield then decreased with increasing extraction time, likely due to the ultrasonic cavitation energy, which generated many cavities on the external surface of the plant's cell wall, thus accelerating the release of the bioactive constituents into the liquid [30]. A previous study showed that excessive ultrasonication durations cause polysaccharide degradation [31]. According to the results from the single-factor studies, extraction power, temperature, and time significantly affected the yield of SNPS. Therefore, we further optimized these three parameters.

3.4. Optimization of SNPS Extraction by BBD

3.4.1. Fitting the Model. The effect of the extraction temperature (X_1), ultrasonic power (X_2), and ultrasonic time (X_3) on the extraction yield of SNPS was evaluated at three levels using BBD. The results are shown in Table 4. The yield of SNPS ranged from 10.56% ± 0.69% to 13.71% ± 1.63%. Experiment 14 (extraction temperature, 50°C; extraction power, 475 W; extraction time, 25 min) produced the highest yield, while experiment 5 (extraction temperature, 30°C; extraction power, 475 W; extraction time, 15 min) produced the lowest yield. The following second-order polynomial was obtained by multiple regression analysis:

$$\begin{aligned}\text{Yield\%} = {} & 13.38 + 0.071X_1 + 0.43X_2 + 0.27X_3 \\ & + 0.20X_1X_2 - 0.38 \times 1 \times 3 + 0.077X_2X_3 \\ & - 0.82(X_1)^2 - 0.57(X_2)^2 - 1.10(X_3)^2.\end{aligned} \quad (4)$$

According to the ANOVA of the quadratic regression model (Table 5), the values of determination coefficient R^2 was 0.954, indicating that 95.4% of the variables can be

Table 3: The real-time RT-PCR oligonucleotide primers.

Gene	Primer	Sequence (5'-3')	PCR product (bp)
β-actin	Forward	TGTTACCAACTGGGACGACA	165
(NM_007393.3)	Reverse	GGGGTGTTGAAGGTCTCAAA	—
IL-6	Forward	TCCAGTTGCCTTCTTGGGAC	140
(NM_031168.1)	Reverse	GTGTAATTAAGCCTCCGACTTG	—
TNF-α	Forward	TAGCCAGGAGGGAGAACAGA	127
(NM_013693.2)	Reverse	TTTTCTGGAGGGAGATGTGG	—

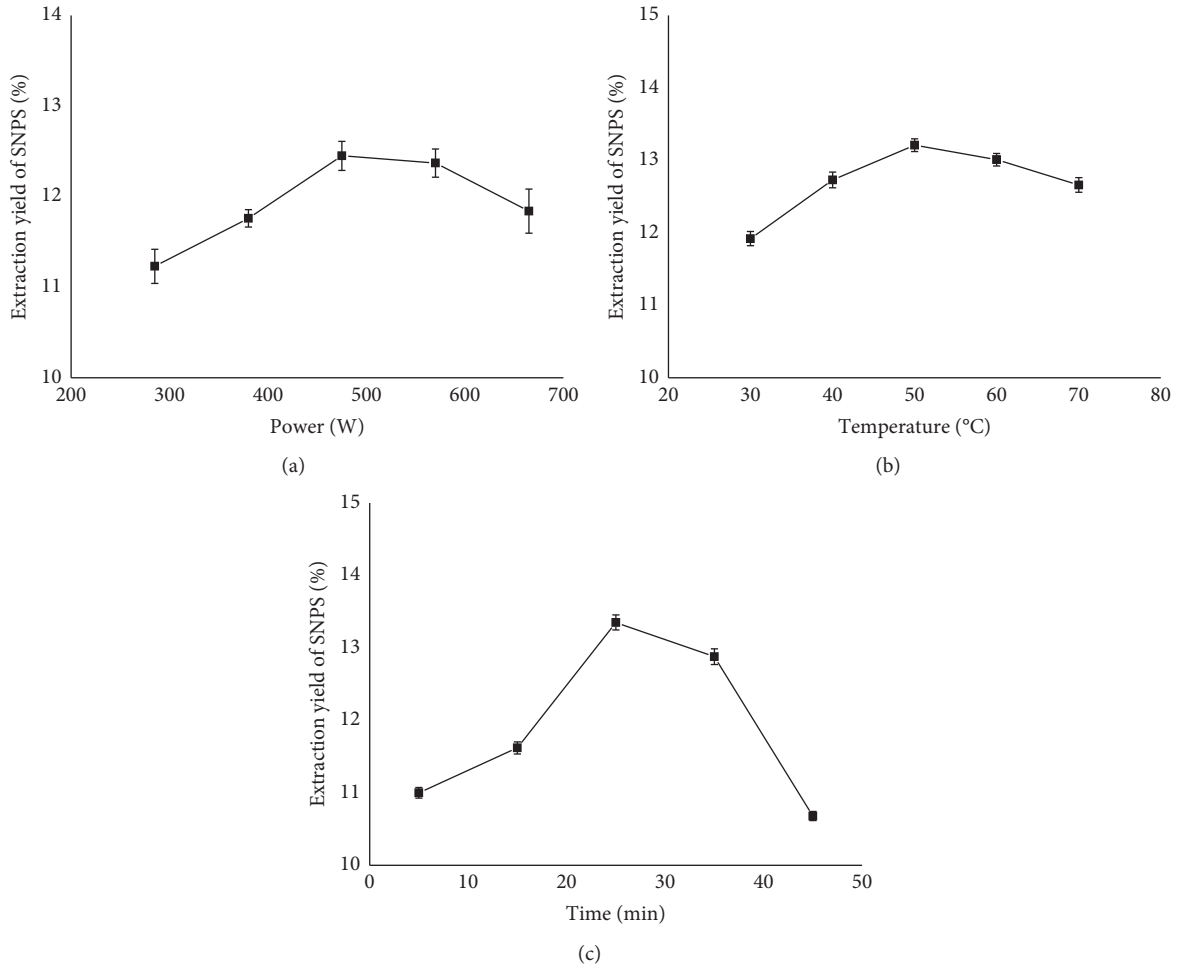

Figure 1: Effect of different extraction parameters on the yield of SNPS. (a) Ultrasonic power (W). (b) Extraction temperature (°C). (c) Extraction time (min).

explained by the fitting model. The adjusted determination coefficient R^2 (R^2_{adj}, 0.895) indicated a relatively high degree of correlation between the experimental and predicted values. The coefficient of variation (C.V.%) was 2.47, indicating the reliability of the experimental values. The F-value (2.26) and P-value (0.224) of the lack-of-fit factor test represented there was no lack-of-fit factor in this model.

Furthermore, the linear coefficients (X_2 and X_3), the quadratic term coefficients (X_1^2, X_2^2, and X_3^2), and the interaction coefficient (X_1X_3) affected the yield of SNPS highly significantly ($P < 0.05$ or $P < 0.01$), while the other coefficients were not significant ($P > 0.05$). The F-value showed that the extraction yield was influenced by the three ultrasonic extraction parameters, in the following order: power > time > temperature; the interaction effects were in the following order: $X1X3 > X1X2 > X2X3$. Therefore, the regression equation can be applied to demonstrate the real relationship between the extraction yield of SNPS and variables.

3.4.2. Diagnosis of Model Adequacy. Model adequacy is very vital for checking whether the established model would give a sufficient approximation to the actual values. Figure 2(a) shows the internally studentized residuals versus actual runs; all data points lay within the acceptable limits (±2). As

Table 4: Box-Behnken design with independent variables and response values.

Run	Independent variables			Response	
	X_1 (°C)	X_2 (W)	X_3 (min)	Experimental yield (%)	Predicted yield (%)
1	−1 (30)	−1 (285)	0 (25)	11.55 ± 0.99	11.68
2	1 (70)	−1 (285)	0 (25)	11.36 ± 1.01	11.43
3	−1 (30)	1 (665)	0 (25)	12.23 ± 1.11	12.16
4	1 (70)	1 (665)	0 (25)	12.82 ± 0.87	12.69
5	−1 (30)	0 (745)	−1 (15)	10.56 ± 0.69	10.73
6	1 (70)	0 (745)	−1 (15)	11.41 ± 0.88	11.64
7	−1 (30)	0 (745)	1 (35)	12.27 ± 1.00	12.04
8	1 (70)	0 (745)	1 (35)	11.59 ± 0.93	11.42
9	0 (50)	−1 (285)	−1 (15)	11.37 ± 1.12	11.07
10	0 (50)	1 (665)	−1 (15)	11.88 ± 0.77	11.78
11	0 (50)	−1 (285)	1 (35)	11.37 ± 0.83	11.47
12	0 (50)	1 (665)	1 (35)	12.19 ± 1.03	12.49
13	0 (50)	0 (745)	0 (25)	13.22 ± 1.10	13.38
14	0 (50)	0 (745)	0 (25)	13.71 ± 1.63	13.38
15	0 (50)	0 (745)	0 (25)	13.39 ± 0.92	13.38
16	0 (50)	0 (745)	0 (25)	13.49 ± 0.88	13.38
17	0 (50)	0 (745)	0 (25)	13.08 ± 1.12	13.378

Data show mean ± SD ($n = 3$).

Table 5: Analysis of variance (ANOVA) of the quadratic model and lack-of-fit.

Source	Sum of squares	Df	Mean square	F-value	P Value	Significance
Model	13.22	9	1.47	16.13	0.00007	***<0.0001
X_1	0.041	1	0.041	0.45	0.5256	—
X_2	1.51	1	1.51	16.53	0.0048	**<0.01
X_3	0.60	1	0.60	6.64	0.0366	*<0.05
X_1X_2	0.15	1	0.15	1.67	0.2372	—
X_1X_3	0.59	1	0.59	6.43	0.0389	*<0.05
X_2X_3	0.024	1	0.024	0.26	0.6233	—
X_1^2	2.81	1	2.81	30.83	0.0009	***<0.0001
X_2^2	1.38	1	1.38	15.10	0.0060	**<0.01
X_3^2	5.13	1	5.13	56.36	0.0001	***<0.0001
Residual	0.64	7	0.091	—	—	—
Lack-of-fit	0.40	3	0.13	2.26	0.224	—
Pure error	0.24	4	0.059	—	—	—
Cor total	13.86	16	—	—	—	—
R^2	0.954	—	—	—	—	—
Adj. R^2	0.895	—	—	—	—	—
Adeq. Precision	11.447	—	—	—	—	—

C.V.% = 2.47, *significant at 0.05 level; **significant at 0.01 level; *** significant at 0.001 level.

shown in Figure 2(b), the data points lay almost close to the straight line, indicating that the normality assumption was satisfied. Meanwhile, the plot of internally studentized residuals versus predicted response values (Figure 2(c)) showed that the residuals randomly scattered within the range of −3 and + 3 in the y-axis, suggesting that the predicted response was within the acceptable limits. Therefore, these data implied that the present model was reliable.

3.4.3. Response Surface Analysis. A response surface analysis was performed, including the extraction yield, extraction conditions, and level of each extraction condition; this map highlights the influence of each extraction condition on the response value [32]. The values of the extraction conditions, and the interactions between the extraction conditions under optimal conditions, can be revealed by a contour map [33]. In the present study, the 3D response surface and 2D contour plots showed the relationship between the extraction temperature (X_1), extraction power (X_2), extraction time (X_3), and extraction yield of SNPS (Figure 3). Figures 3(a) and 3(b) illustrate the effect of extraction temperature and extraction power on the yield when the extraction time was set as 25 min. The extract yield of SNPS initially increased when the extraction temperature and power increased in the range of 30–51.24°C and 285–550.63 W, respectively. However, with the above extract temperature of 51.24°C and ultrasonic power 550.63 W, a decreased extract yield was observed. Thus, the highest yield was obtained with ultrasonic power of 550.63 W and extract temperature of 51.24°C. In addition, the curved surface of the extraction power was steeper than that of the extraction temperature, suggesting that extraction power influenced

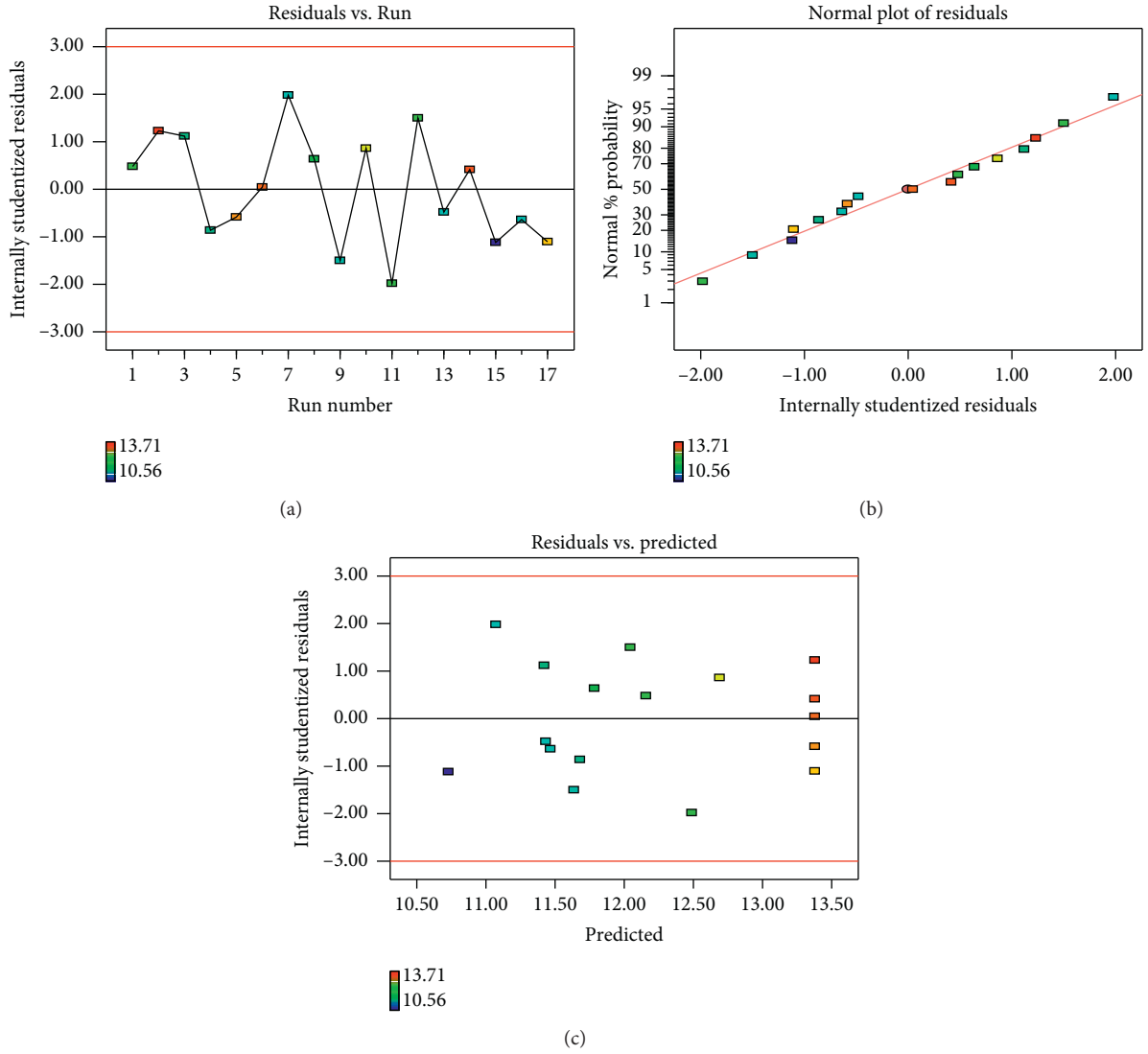

FIGURE 2: Diagnostic plots for the model adequacy. (a) The plot of internally studentized residuals vs. the actual run. (b) Normal probability plot of the studentized residuals. (c) Residuals vs. predicted plot graph.

the yield more significantly than that of the extraction temperature.

Figures 3(c) and 3(d) exhibit the effects of the extraction temperature and extraction time on the yield of SNPS. When fixing the extraction power at 475 (W), an obvious increase in the yield was observed with the extraction temperature increasing from 30°C to 51.24°C, and the extraction time increasing from 5 min to 26.28 min. However, the extraction yield decreased, followed by prolonging the ultrasonic time and temperature in the range of 26.28–45 min and 51.24–70°C, respectively. The extraction yield of SNPS was the highest when the ultrasonic time was 26.28 min, and the temperature was 51.24°C. Statistically, the interaction effect between extraction temperature and time was significant ($P = 0.0389$, as shown in Table 5).

Figures 3(e) and 3(f) illustrate the interactions between the extraction power and extraction time on the yield of SNPS when fixing the temperature at 50°C. When the ultrasonic power and time varied within the range of 285–550.63 (W) and 5–26.28 min, respectively, the extract yield gradually increased. However, the yield then decreased with increasing extraction time from 26.28 min to 45 min or ultrasonic power from 550.63 W to 665 (W). It indicated that SNPS was more likely to be degraded at a high extraction power. The yield of SNPS reached the maximum with ultrasonic power of 550.63 W and ultrasonic time of 26.28 min.

3.4.4. Experimental Verification of the Regression Model. The optimal extraction conditions calculated from the model are as follows: ultrasonic time of 26.28 min, the ultrasonic temperature at 51.24°C, and ultrasonic power of 550.63 W. Under this condition, the yield of SNPS reached to 13.48%. To easy control the extraction parameters during actual operation, the optimal extraction conditions were corrected

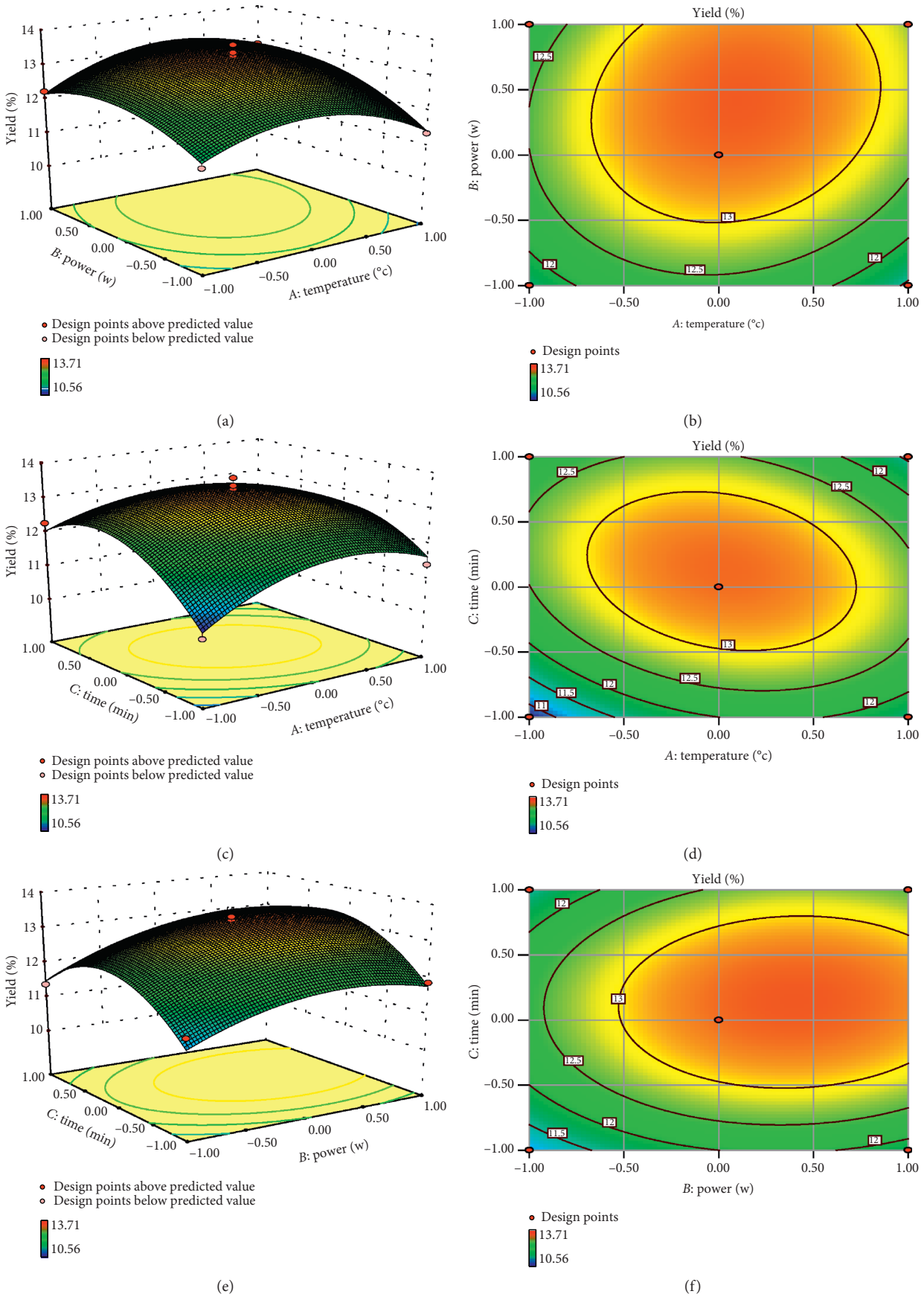

Figure 3: Interactive effects of ultrasonic power, ultrasonic temperature, and ultrasonic time on the yield of SNPS. (a and b) Response surface and contour plots of the effect of ultrasonic power and temperature on the extraction rate of SNPS; (c and d) Response surface and contour plots of the effect of ultrasonic time and temperature on the extraction rate of SNPS; (e and f) Response surface and contour plots of the effect of ultrasonic power and time on the extraction rate of SNPS.

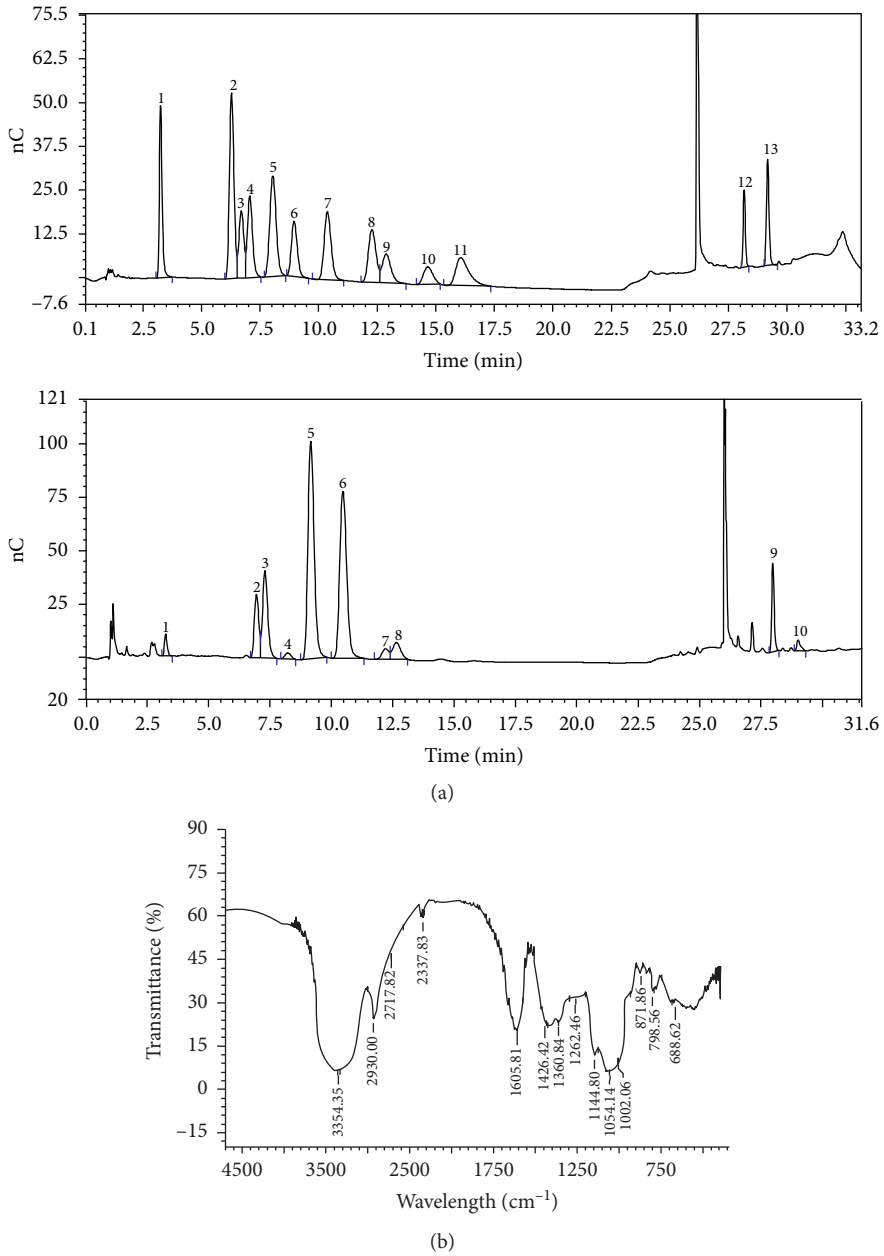

Figure 4: Characterization of SNPS. (a) HPLC analysis of monosaccharide components of SNPS (1. Fucose; 2. Rhamnose; 3. Arabinose; 4. Galactosamine; 5. Galactose; 6. Glucose; 7. Xylose; 8. Mannose; 9. Galacturonic acid; 10. Glucuronic acid). (b) FT-IR analysis of SNPS.

with a slight modification of ultrasonic time of 26 min, ultrasonic power of 550 W, and temperature at 50°C. Under these conditions, the actual extraction yield of SNPS was 13.47% ± 1.63% ($n = 3$), and the yield rate of purified polysaccharides extract 2.15% ± 0.12% ($n = 3$), suggesting that the parameters of the ultrasonic extraction condition optimized by the RSM are accurate and reliable.

3.5. Monosaccharide Composition and FT-IR Characterization of SNPS. The total carbohydrate content of SNPS was 91.53% as determined by the phenol sulfuric acid method. Total protein content of 1.086% was determined by the Coomassie Brilliant Blue method. The monosaccharide composition determined by HPLC is shown in Figure 4(a). SNPS consisted of 1.30% fucose, 6.34% rhamnose, 9.95% arabinose, 0.82% aminogalactose, 29.98% galactose, 25.99% glucose, 1.56% xylose, 2.97% mannose, 4.86% galacturonic acid, and 0.90% glucuronic acid.

As shown in Figure 4(b), SNPS presents the typical absorption peaks of polysaccharides in the range of 4500-500 cm^{-1}. The strong and broad signal at 3354 cm^{-1} corresponds to the O–H stretching vibration in the constituent sugar residues [34]. The absorption peak at 2930 cm^{-1} represents a stretching vibration of the C–H of the sugar ring. The absorption peaks at 1426 cm^{-1} and 1360 cm^{-1} were

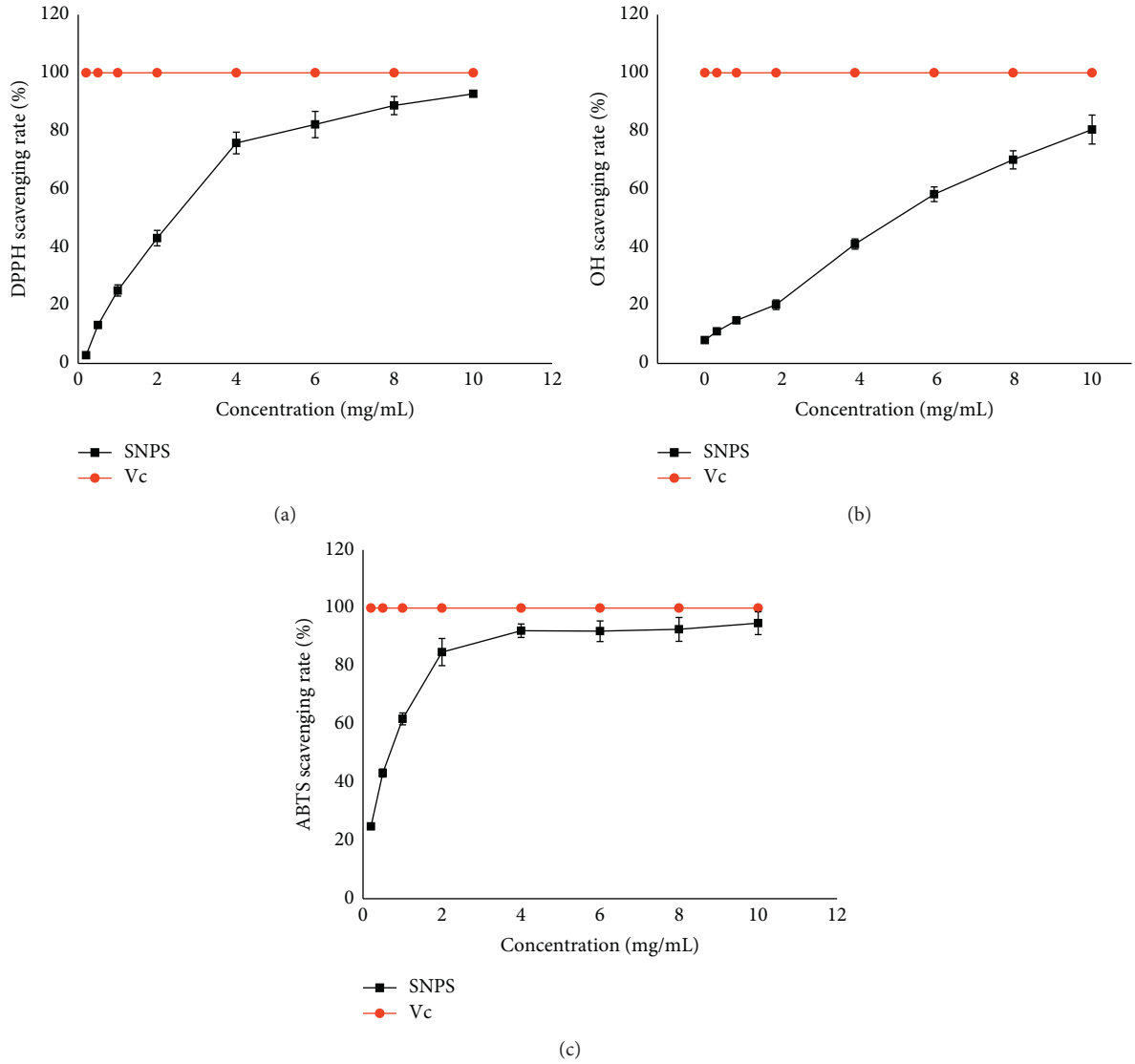

Figure 5: Antioxidant activities of SNPS. (a) Scavenging of DPPH radical. (b) Scavenging of OH free radical. (c) Scavenging of ABTS radical. Data are presented as the mean means ± S.D., $n = 4$. Vc was used as a positive control.

assigned to C–O stretching vibrations. The strong absorptions at 1140 cm^{-1}, 1064 cm^{-1}, and 1002 cm^{-1} indicate the vibrations of C–O–C and C–O–H bond [35].

3.6. Antioxidant Activities of SNPS. DPPH is a stable free radical that can accept an electron or hydrogen radical, forming a stable diamagnetic molecule with decreased absorbance at 517 nm. DPPH has been widely used to investigate the radical scavenging activity of natural polysaccharides [36]. As shown in Figures 5(a) and 5(b), SNPS and the positive control (Vc) exhibited obvious and concentration-dependent radical scavenging activity using DPPH radical and hydroxyl radical assay. The EC_{50} value of SNPS on DPPH and OH was 2.43 ± 0.21 mg/mL and 4.40 ± 0.35 mg/mL, respectively.

The ABTS assay is a decolorization assay applicable for both lipophilic and hydrophilic antioxidants at different $_{p}$H levels [37]. The ABTS radical scavenging activities of SNPS and Vc are shown in Figure 5(c). Significant and dose-dependent ABTS scavenging activity was observed, even at SNPS concentrations <1.0 mg/mL. The maximum scavenging rate reached as high as 94.79% and the EC_{50} value was 0.56 ± 0.062 mg/mL. These data indicated that SNPS has a strong antioxidant activity.

3.7. Anti-Inflammatory Activities of SNPS. LPS is a prototypical bacterial endotoxin that can initiate a variety of inflammatory responses, resulting in the production of various proinflammatory cytokines, which causes liver damage *in vitro* [38]. In the early inflammatory response, IL-6 and TNF-α play a vital role in evoking inflammation. In the present study, we measured the mRNA expression of IL-6 and TNF-α to investigate the anti-inflammatory action of SNPS to further confirm the

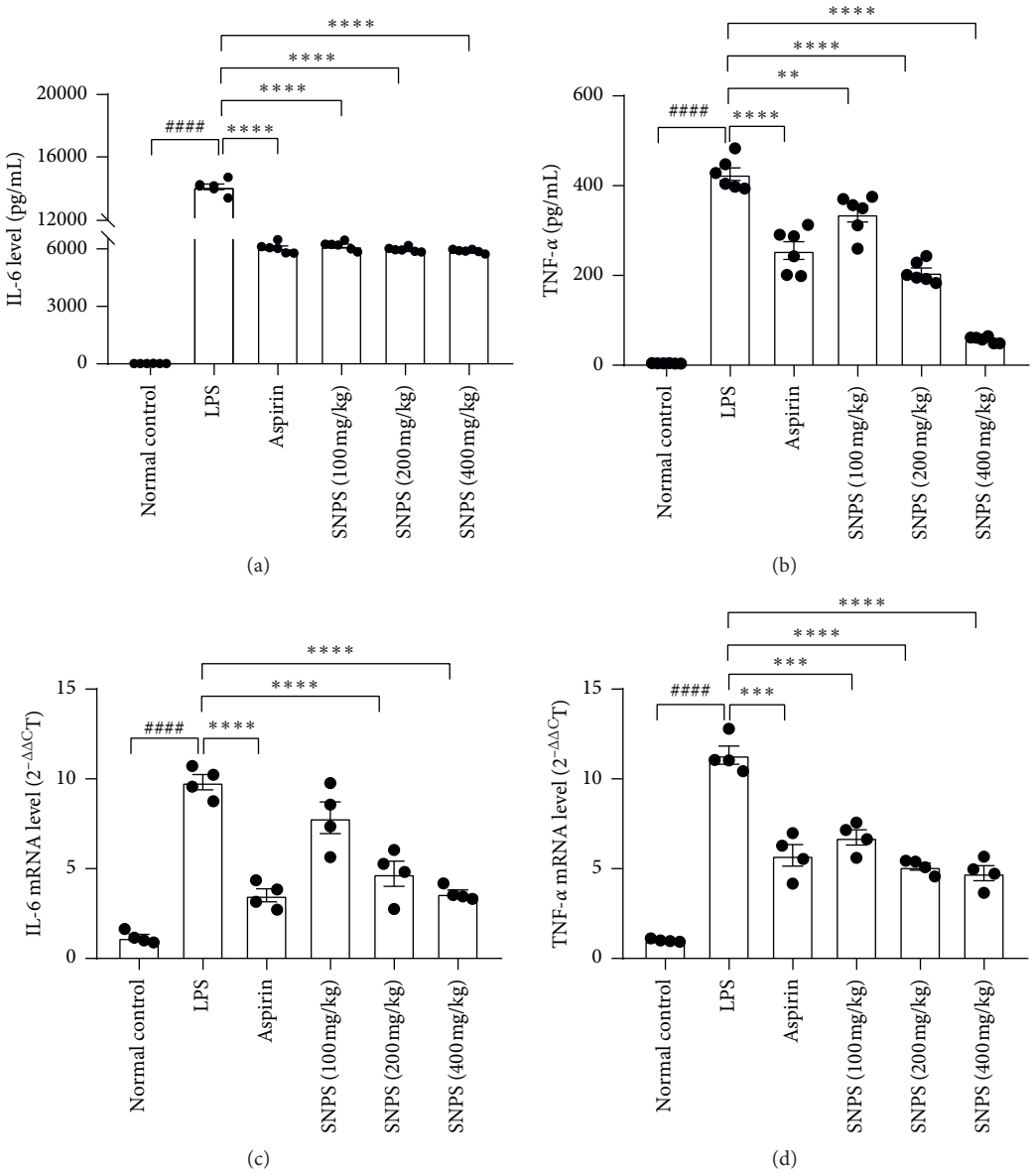

Figure 6: Anti-inflammatory activities of SNPS on LPS-induced mice. Mice were treated with SNPS (100, 200, and 400 mg/kg), aspirin (10 mg/kg), or saline for 4 days (once per day) and stimulated with LPS (1 mg/kg) for 90 min. The protein expression of (a) IL-6 and (b) in serum were determined by ELISA. Values are means ± S.E. (n = 6). The mRNA expression of IL-6 (c) and TNF-α (d) in the liver was measured using real-time RT-PCR. Values are means ± S.E. ($(n) = 4$). The β-actin was used as an internal control for real-time RT-PCR. Aspirin was used as a positive control. The significant difference compared with the normal control group, $^{\#\#\#\#}P < 0.0001$. The significant difference compared with LPS-treated alone, $^{**}P < 0.01$, $^{***}P < 0.001$, $^{****}P < 0.0001$.

effectiveness of SNPS extraction. As displayed in Figures 6(a) and 6(b), LPS injection induced a burst of IL-6 and TNF-α secretion in the serum ($P < 0.01$) in comparison with the normal control group. However, the treatment of SNPS or aspirin significantly suppressed the overproduction of IL-6 and TNF-α ($P < 0.01$). Additionally, the anti-inflammatory effect was more pronounced in the expression of TNF-α, indicating that SNPS may be effective for early inflammation treatment. The effect of SNPS on the expression of IL-6 and TNF-α mRNA in the liver was also investigated. As displayed in Figure 6(c) and 6(d), aspirin or SNPS treatment could effectively alleviate LPS-induced IL-6 and TNF-α mRNA increment ($P < 0.01$).

4. Conclusion

In the present study, an optimized UAE method was designed to extract polysaccharides from the roots of *S. ningpoensis*. Single-factor studies and RSM were employed to optimize the extraction conditions. At an optimal condition that ultrasonic power of 550 W, extraction temperature of 50°C, and extraction time of 26 min, the highest yield of SNPS (13.47% ± 1.63%) was obtained. Compared with the traditional hot water extraction method (the yield was 11.5%), the UAE method we applied significantly decreased extraction temperature and time and increased the extraction yield. The monosaccharide composition of SNPS analyzed by HPLC showed that SNPS was mainly composed of galactose and glucose, with lower levels of other monosaccharides. The FT-IR results illustrated that SNPS consisted primarily of carbohydrate substances, with no observed impurities. Furthermore, antioxidant and anti-inflammatory evaluations revealed that SNPS exhibited good antioxidant and anti-inflammatory activities in a dose-dependent manner. In conclusion, we proposed a reliable extraction process of polysaccharides and the resulting SNPS possesses potential biological activities, which will provide a theoretical basis for guiding the clinical application of *S. ningpoensis*.

Data Availability

The datasets used in and/or analyzed during the current study available from the corresponding author on reasonable request.

Conflicts of Interest

The authors declare that they have no competing interests.

Authors' Contributions

Jian'an Wang and Lufen Huang contributed equally.

Acknowledgments

This work was supported by the National Natural Science Foundation of China (81903824), Special Subsidy for Public Health Service of Traditional Chinese Medicine in 2019 "National Survey of Traditional Chinese Medicine Resources" ([2019] no.39), and Supporting Fund for Teachers' research of Jining Medical University (Grant Nos. JY2017KJ047 and JYFC2019KJ015).

References

[1] P.-Y. Gong, Y.-W. He, J. Qi, C.-Z. Chai, and B.-Y. Yu, "Synergistic nourishing 'Yin' effect of iridoid and phenylpropanoid glycosides from Radix Scrophulariae in vivo and in vitro," *Journal of Ethnopharmacology*, vol. 246, Article ID 112209, 2020.

[2] S. Y. Sheu, Y. W. Hong, J. S. Sun, M. H. Liu, C. Y. Chen, and C. J. Ke, "Radix Scrophulariae extracts (harpagoside) suppresses hypoxia-induced microglial activation and neurotoxicity," *BMC Complementary and Alternative Medicine*, vol. 15, p. 324, 2015.

[3] Y.-F. Huo, H.-L. Wang, E.-H. Wei et al., "Two new compounds from the roots of Scrophularia ningpoensis and their anti-inflammatory activities," *Journal of Asian Natural Products Research*, vol. 21, no. 11, pp. 1083–1089, 2019.

[4] G. Zengin, A. Stefanucci, M. J. Rodrigues et al., "Scrophularia lucida L. as a valuable source of bioactive compounds for pharmaceutical applications: in vitro antioxidant, anti-inflammatory, enzyme inhibitory properties, in silico studies, and HPLC profiles," *Journal of Pharmaceutical and Biomedical Analysis*, vol. 162, pp. 225–233, 2019.

[5] A. Pasdaran and A. Hamedi, "The genus Scrophularia: a source of iridoids and terpenoids with a diverse biological activity," *Pharmaceutical Biology*, vol. 55, no. 1, pp. 2211–2233, 2017.

[6] C. Placines, V. Castañeda-Loaiza, M. João Rodrigues et al., "Phenolic profile, toxicity, enzyme inhibition, in silico studies, and antioxidant properties of Cakile maritima scop. (Brassicaceae) from southern Portugal," *Plants*, vol. 9, no. 2, p. 142, 2020.

[7] A. Della Valle, M. P. Dimmito, G. Zengin et al., "Exploring the nutraceutical potential of dried pepper capsicum annuum L. On market from altino in abruzzo region," *Antioxidants*, vol. 9, no. 5, p. 400, 2020.

[8] J.-K. Yan, L.-X. Wu, Z.-R. Qiao, W.-D. Cai, and H. Ma, "Effect of different drying methods on the product quality and bioactive polysaccharides of bitter gourd (*Momordica charantia L.*) slices," *Food Chemistry*, vol. 271, pp. 588–596, 2019.

[9] J. Liu, S. Willför, and C. Xu, "A review of bioactive plant polysaccharides: biological activities, functionalization, and biomedical applications," *Bioactive Carbohydrates and Dietary Fibre*, vol. 5, no. 1, pp. 31–61, 2015.

[10] J.-H. Xie, W. Tang, M.-L. Jin, J.-E. Li, and M.-Y. Xie, "Recent advances in bioactive polysaccharides from Lycium barbarum L., Zizyphus jujuba Mill, Plantago spp., and Morus spp.: structures and functionalities," *Food Hydrocolloids*, vol. 60, pp. 148–160, 2016.

[11] Y. Zhao, Y. Shi, H. Yang, and L. Mao, "Extraction of Angelica sinensis polysaccharides using ultrasound-assisted way and its bioactivity," *International Journal of Biological Macromolecules*, vol. 88, pp. 44–50, 2016.

[12] K. Feng, W. Chen, L. Sun et al., "Optimization extraction, preliminary characterization and antioxidant activity in vitro of polysaccharides from Stachys sieboldii Miq. tubers," *Carbohydrate Polymers*, vol. 125, pp. 45–52, 2015.

[13] D. U. Bhotmange, J. H. Wallenius, R. S. Singhal, and S. S. Shamekh, "Enzymatic extraction and characterization of polysaccharide from Tuber aestivum," *Bioactive Carbohydrates and Dietary Fibre*, vol. 10, pp. 1–9, 2017.

[14] Y. Yuan and D. Macquarrie, "Microwave assisted extraction of sulfated polysaccharides (fucoidan) from Ascophyllum nodosum and its antioxidant activity," *Carbohydrate Polymers*, vol. 129, pp. 101–107, 2015.

[15] D. C. Murador, A. R. C. Braga, P. L. G. Martins, A. Z. Mercadante, and V. V. de Rosso, "Ionic liquid associated with ultrasonic-assisted extraction: a new approach to obtain carotenoids from orange peel," *Food Research International*, vol. 126, Article ID 108653, 2019.

[16] F. Chemat, N. Rombaut, A.-G. Sicaire, A. Meullemiestre, A.-S. Fabiano-Tixier, and M. Abert-Vian, "Ultrasound assisted extraction of food and natural products. Mechanisms, techniques, combinations, protocols and applications. A review," *Ultrasonics Sonochemistry*, vol. 34, pp. 540–560, 2017.

[17] T. Lin, Y. Liu, C. Lai, T. Yang, J. Xie, and Y. Zhang, "The effect of ultrasound assisted extraction on structural composition, antioxidant activity and immunoregulation of polysaccharides from Ziziphus jujuba Mill var. spinosa seeds," *Industrial Crops and Products*, vol. 125, pp. 150–159, 2018.

[18] X. Wang, Y. Wu, J. Li et al., "Ultrasound-assisted deep eutectic solvent extraction of echinacoside and oleuropein from Syringa pubescens Turcz," *Industrial Crops and Products*, vol. 151, Article ID 112442, 2020.

[19] A. Stefanucci, G. Zengin, E. J. Llorent-Martinez et al., "Viscum album L. homogenizer-assisted and ultrasound-assisted extracts as potential sources of bioactive compounds," *Journal of Food Biochemistry*, vol. 44, no. 9, Article ID e13377, 2020.

[20] Z. Song, Y. Hu, L. Qi et al., "An effective and recyclable deproteinization method for polysaccharide from oyster by magnetic chitosan microspheres," *Carbohydrate Polymers*, vol. 195, pp. 558–565, 2018.

[21] W.-M. Chan and C.-Y. Ma, "Acid modification of proteins from soymilk residue (okara)," *Food Research International*, vol. 32, no. 2, pp. 119–127, 1999.

[22] D. Zeng and S. Zhu, "Purification, characterization, antioxidant and anticancer activities of novel polysaccharides extracted from Bachu mushroom," *International Journal of Biological Macromolecules*, vol. 107, pp. 1086–1092, 2018.

[23] K. H. Musa, A. Abdullah, and A. Al-Haiqi, "Determination of DPPH free radical scavenging activity: application of artificial neural networks," *Food Chemistry*, vol. 194, pp. 705–711, 2016.

[24] R. Leung, C. Venus, T. Zeng, and A. Tsopmo, "Structure-function relationships of hydroxyl radical scavenging and chromium-VI reducing cysteine-tripeptides derived from rye secalin," *Food Chemistry*, vol. 254, pp. 165–169, 2018.

[25] R. Re, N. Pellegrini, A. Proteggente, A. Pannala, M. Yang, and C. Rice-Evans, "Antioxidant activity applying an improved ABTS radical cation decolorization assay," *Free Radical Biology and Medicine*, vol. 26, no. 9-10, pp. 1231–1237, 1999.

[26] L.-N. Gao, Y.-L. Cui, Q.-S. Wang, and S.-X. Wang, "Amelioration of Danhong injection on the lipopolysaccharide-stimulated systemic acute inflammatory reaction via multi-target strategy," *Journal of Ethnopharmacology*, vol. 149, no. 3, pp. 772–782, 2013.

[27] M. Zhang, L. Sun, W. Zhao et al., "Cholesteryl-modification of a glucomannan from Bletilla striata and its hydrogel properties," *Molecules*, vol. 19, no. 7, pp. 9089–9100, 2014.

[28] B. K. Tiwari, "Ultrasound: a clean, green extraction technology," *TrAC Trends in Analytical Chemistry*, vol. 71, pp. 100–109, 2015.

[29] W. Chen, W.-P. Wang, H.-S. Zhang, and Q. Huang, "Optimization of ultrasonic-assisted extraction of water-soluble polysaccharides from Boletus edulis mycelia using response surface methodology," *Carbohydrate Polymers*, vol. 87, no. 1, pp. 614–619, 2012.

[30] M. Hadidi, A. Ibarz, and J. Pagan, "Optimisation and kinetic study of the ultrasonic-assisted extraction of total saponins from alfalfa (Medicago sativa) and its bioaccessibility using the response surface methodology," *Food Chemistry*, vol. 309, Article ID 125786, 2019.

[31] A. Raza, F. Li, X. Xu, and J. Tang, "Optimization of ultrasonic-assisted extraction of antioxidant polysaccharides from the stem of Trapa quadrispinosa using response surface methodology," *International Journal of Biological Macromolecules*, vol. 94, pp. 335–344, 2017.

[32] S. Shen, D. Chen, X. Li et al., "Optimization of extraction process and antioxidant activity of polysaccharides from leaves of Paris polyphylla," *Carbohydrate Polymers*, vol. 104, pp. 80–86, 2014.

[33] Z.-F. Zhang, G.-Y. Lv, X. Jiang, J.-H. Cheng, and L.-f. Fan, "Extraction optimization and biological properties of a polysaccharide isolated from Gleoestereum incarnatum," *Carbohydrate Polymers*, vol. 117, pp. 185–191, 2015.

[34] L. Wang, B. Zhang, J. Xiao, Q. Huang, C. Li, and X. Fu, "Physicochemical, functional, and biological properties of water-soluble polysaccharides from Rosa roxburghii Tratt fruit," *Food Chemistry*, vol. 249, pp. 127–135, 2018.

[35] X.-H. Yu, Y. Liu, X.-L. Wu, L.-Z. Liu, W. Fu, and D.-D. Song, "Isolation, purification, characterization and immunostimulatory activity of polysaccharides derived from American ginseng," *Carbohydrate Polymers*, vol. 156, pp. 9–18, 2017.

[36] J.-H. Xie, Z.-J. Wang, M.-Y. Shen et al., "Sulfated modification, characterization and antioxidant activities of polysaccharide from Cyclocarya paliurus," *Food Hydrocolloids*, vol. 53, pp. 7–15, 2016.

[37] K. M. Schaich, X. Tian, and J. Xie, "Reprint of "Hurdles and pitfalls in measuring antioxidant efficacy: a critical evaluation of ABTS, DPPH, and ORAC assays,"" *Journal of Functional Foods*, vol. 18, pp. 782–796, 2015.

[38] C. J. Kearney, S. P. Cullen, G. A. Tynan et al., "Necroptosis suppresses inflammation via termination of TNF- or LPS-induced cytokine and chemokine production," *Cell Death & Differentiation*, vol. 22, no. 8, pp. 1313–1327, 2015.

[文章编号] 1000-4718(2021)03-0543-08

高脂饮食联合慢性不可预知性温和应激诱导抑郁症模型的研究进展*

孙珊珊，刘 阳，高丽娜△
（济宁医学院药学院，山东 日照 276826）

Progress in high-fat diet/chronic unpredictable mild stress-induced depressive model

SUN Shan-shan, LIU Yang, GAO Li-na
(*School of Pharmacy*, *Jining Medical University*, *Rizhao* 276800, *China*. *E-mail*: *linagao*228@126.*com*)

[**ABSTRACT**] Effective animal model is the basis for investigating the pathological mechanism of depression and developing novel antidepressants. Based on the inflammatory injury and lipid metabolism disorders in clinical depression patients, we focuses a depression model induced by high-fat diet (HFD) combined with chronic unpredictable mild stress (CUMS), and summarizes the method of establishing the model, pathophysiological characteristics, application value, potential pathological mechanisms and drug targets. We point out that the biological basis of long-term HFD/CUMS-induced depression-like behaviors involves lipid metabolism, changes in microbial compositions and abundance, neuroinflammation, neurological dysfunction, etc. Toll-like receptor 4 participates in the occurrence and development of depression by regulating peripheral and central nervous system inflammatory responses-tryptophan metabolism-phospholipid metabolism, and can be used as a new target for novel antidepressant development. In this review, we aimed to provide new reference for exploring the pathogenesis of depression and the pathopharmacological evaluation of new antidepressants.

[关键词] 高脂饮食；慢性不可预知性温和应激；抑郁症；Toll样受体4；炎症；磷脂
[**KEY WORDS**] High-fat diet; Chronic unpredictable mild stress; Depression; Toll-like receptor 4; Inflammation; Phospholipid
[中图分类号] R749.4; R363 [文献标志码] A doi: 10.3969/j.issn.1000-4718.2021.03.022

抑郁症又称抑郁障碍，临床表现为心境低落、意志活动衰退、认知功能损害、躯体症状等。当今世界抑郁症患者高达4.3亿，数量仍持续上升且出现低龄趋势，同时，因患抑郁症引发的自杀事件频频发生。生物、心理、社会环境等诸多因素共同参与了抑郁症的发病过程[1]，而具体病因和发病机制仍不清楚。目前临床应用的抗抑郁药物为单一机制抗抑郁靶点药物，仅能减轻部分患者的抑郁症状且易产生副作用[2]。新型抗抑郁药物的研发需要通过多水平、多维度的药理学实验来评价其疗效及作用机制，因此构建合理的抑郁症动物模型是临床前研究的关键。

1 抑郁症研究假说

目前，学术界普遍认为抑郁症发病与中枢单胺类神经递质或其相应受体功能低下、炎症因子增加、下丘脑-垂体-肾上腺（hypothalamo-pituitary-adrenal，HPA）轴功能亢进、内分泌紊乱等有关[3]。抑郁症的“单胺类神经递质假说”指出，突触间隙中多巴胺（dopamine，DA）、去甲肾上腺素（norepinephrine，NE）和血清素（5-羟色胺，5-hydroxytryptamine，5-HT）缺乏可导致神经传递减少和认知功能受损[4-5]。此外，单胺功能缺陷可由蛋白质转运功能下降和神经递质受体功能异常引起[6]。大脑中的转运蛋白可促进突触前神经递质的再摄取，减少突触间隙神经

[收稿日期] 2020-09-18 [修回日期] 2021-01-05
*[基金项目] 国家自然科学基金资助项目（No. 81903824）；济宁医学院教师科研扶持基金资助项目（No. JYFC2018KJ047）
△通讯作者 Tel：0633-2983695；E-mail：linagao228@126.com

递质的可利用性，降低单胺氧化酶对神经递质的降解[6-7]。重度抑郁症患者接受药物治疗后，NE转运蛋白/受体的占有率显著增加[8]。神经递质-受体偶联受损、下游信号转导级联反应异常等也可导致神经递质功能障碍[7,9]。抑郁症患者在接受选择性5-HT再摄取抑制剂治疗后，其血清白细胞介素1β（interleukin-1β，IL-1β）、IL-2、IL-6和肿瘤坏死因子α（tumor necrosis factor-α，TNF-α）浓度均下降，说明炎症因子和抑郁症的发生有密切联系[10]。炎症因子可以通过体液和神经2种途径进入中枢，影响神经递质代谢和神经内分泌功能，造成中枢神经递质紊乱和神经传导环路失调。

HPA轴是神经内分泌系统的重要组成部分。抑郁症患者血浆中促肾上腺皮质激素释放激素（corticotropin-releasing hormone，CRH）、促肾上腺皮质激素（adrenocorticotropic hormone，ACTH）和糖皮质激素（glucocorticoid，GC）水平均高于健康对照组。患者体内过多的GC与海马组织糖皮质激素受体（glucocorticoid receptor，GR）结合后对海马体及蓝斑造成损伤，导致患者认知障碍和心境低落[11]，而海马体功能受损导致GR敏感性受损，抑制GC对HPA轴的负反馈调节过程，这一恶性循环导致患者HPA轴功能亢进和抑郁症病情加重[12]。炎症细胞因子可通过激活P38丝裂原活化蛋白激酶来降低GR的功能，说明抑郁症发生中HPA轴功能亢进和GC抵抗与炎症增加密切联系[13]。此外，患者脑脊液中CRH持续升高与其早期复发率呈正相关[14]。CRH受体1（CRH receptor 1，*CRHR1*）基因已被确定为重度抑郁症易感性的可能修饰因素，且与男性抑郁症患者自杀密切相关[15]。针对HPA轴成分的治疗选择有GR拮抗剂、CRHR1拮抗剂、色氨酸2,3-二加氧酶（tryptophan 2,3-dioxygenase，TDO）抑制剂和FK506结合蛋白5受体拮抗剂。但遗憾的是，目前并无新药获批。

迄今为止，基于单胺类神经递质传递、免疫炎症、神经可塑性和神经内分泌功能提出的抑郁症生物标记物大多是以蛋白质功能障碍为核心。脂质通过调节运输、锚定和结构支持在决定蛋白质的细胞功能中发挥重要作用[16]。脂质是神经元发挥功能的基础，参与调节膜流动性和渗透性、囊泡的形成和运输、神经递质的释放、细胞完整性和可塑性。代谢组学技术已被广泛用于研究抑郁症患者和健康受试者尿液和血浆代谢产物差异，并揭示抑郁症的发病机制与脂质代谢、氨基酸代谢、能量代谢等有关[17-18]。重度抑郁症患者血浆中溶血磷脂酰胆碱（lysophosphatidylcholine，LPC）、溶血磷脂酰乙醇胺（lysophosphatidylethanolamine，LPE）、磷脂酰胆碱（phosphatidylcholine，PC）、磷脂酰乙醇胺（phosphatidylethanolamine，PE）、磷脂酰肌醇（phosphatidylinositol，PI）、1-*O*-烷基-2-酰基-PE（1-*O*-alkyl-2-acyl-PE，PE O）、1-*O*-烷基-2-酰基-PC（1-*O*-alkyl-2-acyl-PC，PC O）、鞘磷脂（sphingomyelin，SM）、二酰基甘油（diacylglycerol，DG）和甘油三酯（triglyceride，TG）为显著性差异代谢产物，其中LPC、LPE、PC、PE、PI、TG等与抑郁症严重程度呈正相关，而PE O和SM则与抑郁症严重程度呈负相关；而且LPE 20∶4、PC 34∶1、PI 40∶4、SM 39∶1,2和TG 44∶2的组合脂质组被定义为潜在的诊断生物标志物，具有区分重度抑郁症患者和健康受试者的良好敏感性和特异性[19]。

常用的抑郁症动物模型主要有药物诱导模型（如利血平诱导的神经递质耗竭模型）、束缚应激模型、慢性应激（慢性不可预知性温和应激，chronic unpredictable mild stress，CUMS）模型、大鼠嗅球切除模型、电刺激小鼠角膜模型、转基因模型等[20]。因单一诱导因素只能模拟某一种或部分抑郁症发病机制，近年来多个模型联合使用的研究较为常见。CUMS作为诱导抑郁样行为的常用方法，合理地模拟了当代社会人们处于长期精神压力的生活状态；高脂饮食（high-fat diet，HFD）则模拟了现代社会生活中普遍存在的不良饮食习惯。二者联合应用构建的抑郁症动物模型可从精神状况和膳食摄取两方面模拟抑郁症的发病和发展过程。

2 动物模型的构建及病理生理学特点

2.1 HFD/CUMS诱导抑郁症模型的构建与评价

高脂饲料主要由基础饲料、胆固醇、猪油和蛋黄粉等组成，其中脂肪含量会影响造模周期长短。一般而言，喂养周期是由动物状态、血脂相关指标和代谢炎症改变程度等因素综合决定的[21]。如表1所示，除正常对照组和CUMS组大鼠给予正常饲料外，其余各组大鼠给予高脂饲料喂养。

CUMS主要包括光刺激、冰水游泳、震荡、禁食、昼夜颠倒（白天遮光12 h，晚上照亮12 h）、禁水和夹尾等[22]。除正常对照组和HFD组大鼠正常进食外，其余各组大鼠接受至少连续4周的CUMS刺激，建立抑郁症模型。每组动物每天随机给予一种刺激，每种刺激应用不超过5次。

HFD/CUMS诱导抑郁症模型通常选取大鼠作为研究对象。所有实验大鼠要进行1%糖水训练和1%糖水偏好测试，并记录大鼠体重。在末次给药的第2天开展行为学测试，记录大鼠在开放场中4 min内的行为学参数（如直立次数、活动总距等）。

表1　实验分组和给药

Table 1.　Experimental grouping and drug administration

Group	Normal feed	High-fat feed	CUMS	Experminal drugs or positive drugs
Normal control	+	−	−	−
HFD	−	+	−	−
CUMS	+	−	+	−
HFD+CUMS	−	+	+	−
Drug	−	+	+	+

HFD: high-fat diet; CUMS: chronic unpredictable mild stress.

2.2　HFD/CUMS影响糖类、脂质代谢　CUMS与HFD协同作用可导致模型动物体内脂质代谢异常与内分泌紊乱。长期HFD能增加大鼠的体重、血浆总胆固醇和低密度脂蛋白水平，降低高密度脂蛋白水平，诱发大鼠高脂血症，扰乱丘脑、纹状体局部的葡萄糖代谢，导致边缘系统-纹状体-丘脑环路功能异常，这一过程被认为参与了抑郁症的发生和发展[23]。CUMS通过提高大鼠血脂水平、激活Toll样受体4（Toll-like receptor 4, TLR4)/核因子κB（nuclear factor-κB, NF-κB)信号通路诱导抑郁症和高脂血症发生[24]。对肝脏的脂质代谢研究结果显示，CUMS与HFD联合作用才能对肝脏脂质代谢产生显著影响，如上调大鼠肝脏组织中B类清道夫受体1（scavenger receptor class B type 1, SRB1)和卵磷脂胆固醇脂酰转移酶（lecithin cholesterol acyltransferase, LCAT)的mRNA表达[25]，且联合刺激较CUMS单独作用效果更为明显，同时与HFD单独作用的结果相反。HFD联合CUMS可增加大鼠血清丙氨酸氨基转移酶（alanine aminotransferase, ALT)和天冬氨酸氨基转移酶（aspartate aminotransferase, AST)的活性，提高血清TG、胆固醇和高密度脂蛋白胆固醇及肝脏TG水平，引起大鼠血脂异常；降低血液中超氧化物歧化酶的活性，增加丙二醛浓度，诱导氧化应激[26]。此外，HFD和CUMS共同作用能促进大鼠下丘脑交感神经肽Y（sympathetic neuropeptide Y, NPY)释放并激活其在脂肪组织内的受体NPY-Y2[27]。代谢异常同样能引起心血管功能障碍，有研究表明HFD和CUMS在诱导大鼠抑郁症的同时可增加主动脉内膜和纤维层的厚度，引起大鼠动脉收缩压和血浆中皮质酮水平升高，加重大鼠动脉粥样硬化的发生[28-29]。HFD和CUMS也能通过兴奋大鼠心脏交感神经，提高大鼠的心率和收缩压，并增加高敏C反应蛋白水平[30-31]。然而，临床常用的抗抑郁症药物只能缓解大鼠抑郁样症状，无法应对抑郁症和心血管疾病之间的潜在联系问题。

2.3　HFD/CUMS诱导外周和中枢神经炎症损伤　抑郁症的“炎症因子假说”认为，长期不良事件可诱导神经炎症的发生，进而增加抑郁障碍的易感性[32]。长期HFD和CUMS可诱导大鼠脑内炎症因子升高，其中TNF-α可激活吲哚胺2,3-双加氧酶（indoleamine 2,3-dioxygenase, IDO)，引起色氨酸的犬尿氨酸通路代谢增加，抑制5-HT的合成[10]。同时，炎症因子通过抑制HPA轴负反馈机制，导致HPA轴功能亢进，皮质醇释放水平增加。大鼠海马中TNF-α水平上升也与其转化酶金属肽酶域17的mRNA表达增加有关[33]。通过静脉插管向大鼠快速灌注脂肪酸能使大鼠下丘脑内TNF-α升高，说明大鼠血脂水平升高可以引发下丘脑急性炎症反应[34]。长期HFD通过损伤肠道组织紧密连接蛋白1（zonula occludens-1, ZO-1)引起外周炎症，增加血清中单核细胞趋化蛋白1（monocyte chemoattractant protein-1, MCP-1)、IL-6和TNF-α的蛋白表达[35-36]。给予抗炎药物米诺环素可显著改善CUMS诱导的抑郁症状，降低外周TNF-α、IL-1β和IL-18蛋白水平，提示抗炎药物可作为抑郁症的辅助治疗方法之一[10]。长期HFD和CUMS在调控免疫因子方面存在复杂的相互作用，CUMS可以上调大鼠海马中IL-4和IL-5的mRNA表达，而这一反应能被HFD消除[37]。因此，CUMS和HFD对机体内细胞因子的复杂调控作用，是构建抑郁症模型的关键，也是阐明抑郁症发病机制的难点之一。

2.4　HFD/CUMS调控神经功能　CUMS诱导产生的抑郁行为与多个脑区[如中缝背核脑区5-HT神经元、海马CA1、CA3和齿状回（dentate gyrus, DG)区及前额叶皮层（prefrontal cortex, PFC)]脑源性神经营养因子（brain-derived neurotropic factor, BDNF)水平降低有关[38]。CUMS对小鼠空间记忆能力的损伤与脑内PFC区Wingless/Integrated 3a（Wnt3a)蛋白的表达减少有关[39]。CUMS还能下调大鼠海马和PFC区磷酸化细胞外信号调节激酶（phosphorylated extracellular signal-regulated kinase, p-ERK)蛋白水平及海马CA1和CA3区肾上腺素能α1受体表达，同时减少海马γ-氨基丁酸（gamma-aminobutyric acid, GABA)的

释放量，增加谷氨酸释放量[39]。CUMS诱导的抑郁样模型大鼠海马神经元及树突棘数量减少与海马组织中的死亡相关蛋白激酶1（death-associated protein kinase 1，DAPK1）表达升高有关[40]。

HFD和CUMS主要引起边缘系统中海马和杏仁核的损伤。首先，在HFD和CUMS刺激下，大鼠海马主导的空间记忆力出现明显衰退[41]；二者协同作用可导致大鼠海马CA3区神经元树突结构发生萎缩[42]，海马内突触标志物如βⅢ-tubulin、突触后致密蛋白95（postsynaptic density protein 95，PSD-95）和突触小体相关蛋白25（synaptosomal-associated protein-25，SNAP-25）减少，*N*-甲基-D-天冬氨酸（*N*-methyl-D-aspartate，NMDA）的受体NR2A表达增加，其作用机制与抑制BDNF-酪氨酸激酶受体B（tyrosine kinase receptor B，TrkB）通路有关[43]。其次，HFD和早期社会压力同时作用引起的大鼠皮质酮水平增加和胰岛素抵抗与杏仁核中TrkB和突触结合蛋白4的表达增加有关[44]。因此，长期HFD和CUMS可直接作用于中枢神经系统神经元结构和功能，进而引起学习记忆和行为学的改变。

2.5 HFD/CUMS改变肠道微生物组成　微生物-肠-脑轴是整合大脑和胃肠道功能的双向神经-体液交流系统，已成为研究抑郁症-炎症-代谢功能相互关系的重要基础。正常小鼠接种HFD诱导的肥胖小鼠的肠道菌群后出现抑郁样行为[45]。在HFD作用下，小鼠肠道中辅助吸收食物热量的厚壁菌门（*Firmicutes*）和蓝细菌门（*Cyanobacteria*）细菌相对丰度增加，而具有抗炎作用的拟杆菌门（*Bacteroidetes*）细菌相对丰度减少，结肠中的髓过氧化物酶水平降低[46]。CUMS可降低肠道中螺旋体（*Spirochaeta*）的丰度，增加具有助消化、排便功能的乳杆菌属（*Lactobacillus* Beijerinck，1901）的丰度，这可能是CUMS诱导大鼠体重下降的原因之一[47]。微生物群落多样性测序分析结果显示，HFD和CUMS联合作用下雄性小鼠肠道微生物群的操作分类单元（operational taxonomic unit，OTU）较雌性小鼠变化更加敏感[48]。抑郁症患者肠道厚壁菌门、能产生内毒素的拟杆菌门及变形菌门（*Proteobacteria*）丰度相对健康人群更高，厚壁菌/拟杆菌的丰度比值也明显高于健康人群，β多样性分析则显示其肠道中的有益菌如产丁酸盐菌（butyric-acid bacteria）丰度明显低于健康人群[49]。此外，抑郁症患者肠道中具有生物屏障、营养、改善肠道功能的菌类如双歧杆菌属（*Bifidobacterium*）、大肠杆菌属（*Escherichiacoli*）和乳杆菌属细菌丰度显著低于健康组人群[43]。患者肠道抗炎功能细菌拟杆菌门和栖粪杆菌属（*Coprothermobacter* Rainey and Stackebrandt）丰度与抑郁症病情严重程度呈负相关[50]。因此，肠道内的微生物群是压力（应激）、抑郁症和饮食习惯三者之间产生关联的重要纽带。

3　基于TLR4信号转导通路的研究进展

3.1 HFD和CUMS通过活化TLR4加强外周和中枢神经系统炎症反应的联系　近年来，对HFD和CUMS诱发抑郁症发病机制的研究显示，TLR4是联系肠-炎症-神经递质的重要桥梁。CUMS通过激活TLR4、糖原合成酶激酶3（glycogen synthase kinase-3，GSK3）、磷脂酰肌醇3-激酶（phosphatidylinositol 3-kinase，PI3K）/蛋白激酶B（protein kinase B，PKB/AKT）及其下游的炎症因子诱导抑郁样行为表型，而*TLR4*敲除可减少模型小鼠海马组织中细胞因子的增加[51]。此外，CUMS可诱导肠壁渗透性增加，并通过激活TLR4介导的炎症反应，加剧脂质过氧化损伤和蛋白质亚硝化损伤[52-53]。TLR4是调控膳食营养、肠道菌群和代谢炎症的关键分子[54]。如图1所示，长期HFD可导致肠壁渗透性增加，引起肠道中毒素成分如脂多糖（lipopolysaccharide，LPS）含量增加；LPS通过与CD14-TLR4复合物结合活化免疫细胞，并激活细胞内NF-κB转录，生成大量TNF-α、IL-6、环氧合酶2（cyclooxygenase-2，COX-2）等，诱发炎症反应[55]。细胞因子通过迷走神经、血脑屏障上的细胞因子转运蛋白等与中枢神经系统联系，引起神经炎症反应的发生，进而影响神经元活力及神经细胞间的相互交流[56]。在炎症发生过程中，细胞因子如TNF-α表达升高，可激活IDO，使色氨酸代谢趋向于犬尿氨酸和喹啉酸，诱导神经毒性，并抑制5-HT合成。这与抑郁症发病机制的“单胺能假说”中5-HT缺乏相吻合，是更直接的发病机制。

IDO是5-HT合成的关键酶，也是抑郁症中调控免疫反应和单胺能系统的关键靶点[57]。生理条件下，色氨酸主要通过肝脏TDO代谢生成烟酰胺；在炎性损伤状态下，IDO酶活性提高，加速色氨酸趋向犬尿氨酸途径代谢，3-羟基犬尿氨酸可以产生游离态自由基，引起机体氧化应激反应[58]。喹啉酸是NMDA受体激动剂，具有神经毒性作用，而犬尿喹啉酸是NMDA受体拮抗剂，具有神经保护作用。HFD和CUMS诱导肠道和中枢神经系统TLR4活化，使外周和中枢神经系统细胞因子含量升高，增加了外周和神经系统炎症反应的联系。因此，TLR4介导的炎症反应是联系外周和神经免疫反应的桥梁，是HFD和CUMS诱导抑郁症的疾病分子网络的重要节点，也是潜在的治疗靶点。

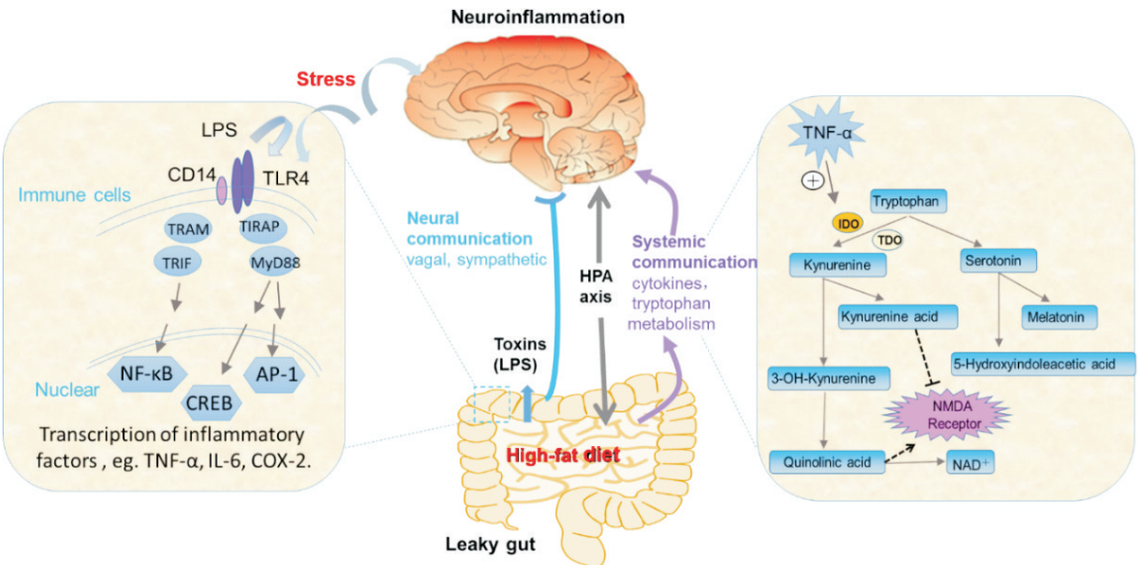

Figure 1. Immune signal transmission and tryptophan metabolism in the peripheral and central nervous systems after activation of TLR4 by high-fat diet/chronic unpredictable mild stress (CUMS).

图1 HFD/CUMS活化TLR4后外周与中枢神经系统的免疫信号传递和色氨酸代谢

3.2 HFD和CUMS通过活化TLR4介导炎症性磷脂代谢紊乱 长期HFD导致低密度脂蛋白和胆固醇在动脉壁中沉积，引起内皮细胞损伤并激活巨噬细胞[59]。巨噬细胞表面的膜受体TLR4可介导其摄取脂质并转换为泡沫细胞，与血管平滑肌细胞共同促进动脉粥样硬化斑块的形成[60]。在HFD诱导的兔动脉粥样硬化模型中，褪黑素通过抑制TLR4/NF-κB信号转导通路，改善脂质代谢，缓解血管内皮损伤和炎性损伤[59]，提示炎症反应-色氨酸代谢-脂质代谢途径有交汇点，以此作为药物干预靶点，可有效缓解HFD和CUMS胁迫下抑郁症的发生和发展。

长期HFD所产生的“脂质过氧化应激”可通过改变生物膜磷脂、酶以及膜受体而引起细胞结构和功能的改变，增加抑郁症的易感性。膜脂质不仅是维持膜结构完整性所必需的，还与应激反应（如炎症应答、细胞凋亡和神经发生等）有关[61]。与抑郁症发病机制相关的膜脂质种类包括甘油磷脂、胆固醇和鞘脂，其中甘油磷脂类物质包PC、PE、磷脂酰甘油、磷脂酸、乙醇胺缩醛磷脂等。磷脂占大脑干重的60%，是神经与突触结构的重要组成成分，对多巴胺、5-HT、谷氨酸等信号转导起关键作用。磷脂不饱和脂肪酸组分异常则为抑郁症与代谢综合征共病提供了合理的解释。

细胞内磷脂酶A2（cytosolic phospholipase A2，cPLA2）是膜磷脂代谢的关键酶。作为多不饱和脂肪酸代谢和前列腺素E2合成的关键酶，*cPLA2*和*COX-2*基因的遗传变异可降低二十碳五烯酸（eicosapentaenoic acid，EPA）和二十二碳六烯酸（docosahexaenoic acid，DHA）的含量，增加抑郁症发生的风险[62]。除诱导机体细胞因子含量增加外，CUMS也增加了谷氨酸盐含量。谷氨酸受体活化通过G蛋白机制激活cPLA2，诱导磷脂代谢产生大量的花生四烯酸。如图2所示，TLR4活化通过激活cPLA2加速磷脂代谢，产生大量花生四烯酸、游离脂肪酸等，导致膜通道活化和血流动力学改变。因此，HFD和CUMS通过激活TLR4介导的炎症反应，诱发磷脂代谢紊乱，是抑郁症发生的机制之一。

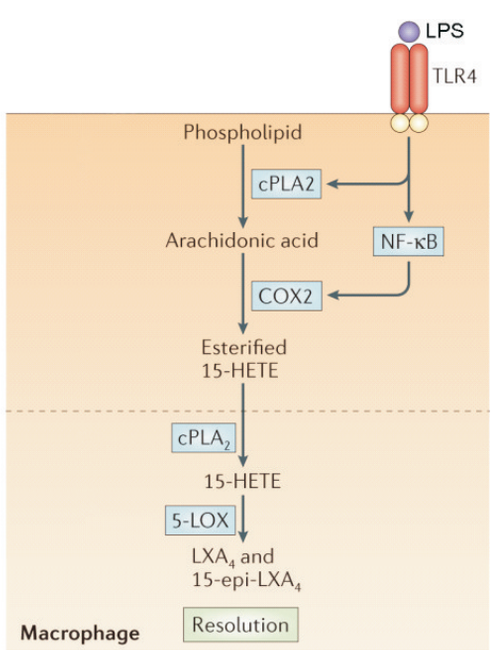

Figure 2. Mechanism of TLR4 regulating phospholipid metabolism.

图2 TLR4调控磷脂代谢的机制

4 结论

长期服用NE和5-HT再摄取抑制剂以及单胺氧化酶抑制剂可引起高血压；5-HT再摄取抑制剂可阻断血小板对5-HT的摄取，降低血小板聚集功能，与非甾体抗炎药物联用可增加出血风险。对抑郁症发病机制的不完全理解，是临床治疗效果欠佳的主要原因。

同时兼顾抑郁症发病机制的不同假说，探究治疗新靶标，有望为治疗抑郁症提供新策略。炎症反应、脂质代谢紊乱和抑郁症密切相关。HFD联合CUMS可模拟当代社会环境因素诱发抑郁症伴随炎症损伤和脂质代谢紊乱的现状。建立HFD和CUMS诱导的抑郁症动物模型，基于炎症反应介导的脂质代谢紊乱探究抑郁症的治疗方法，可为抑郁症的临床治疗提供参考。

[参 考 文 献]

[1] Park LT, Zarate CA Jr. Depression in the primary care setting[J]. New Engl J Med, 2019, 380(6):559-568.

[2] Hieronymus F, Lisinski A, Nilsson S, et al. Influence of baseline severity on the effects of SSRIs in depression: an item-based, patient-level post-hoc analysis [J]. Lancet Psychiatry, 2019, 6(9):745-752.

[3] Beijers L, Wardenaar KJ, van Loo HM, et al. Data-driven biological subtypes of depression: systematic review of biological approaches to depression subtyping[J]. Mol Psychiatry, 2019, 24(6):888-900.

[4] Schildkraut JJ, Schanberg SM, Breese GR, et al. Norepinephrine metabolism and drugs used in the affective disorders: a possible mechanism of action[J]. Am J Psychiatry, 1967, 124(5):600-608.

[5] Bourne H, Bunney W Jr, Colburn R, et al. Noradrenaline, 5-hydroxytryptamine, and 5-hydroxyindoleacetic acid in hindbrains of suicidal patients[J]. Lancet, 1968, 292(7572):805-808.

[6] Abdallah CG, Averill CL, Salas R, et al. Prefrontal connectivity and glutamate transmission: relevance to depression pathophysiology and ketamine treatment[J]. Biol Psychiatry Cogn Neurosci Neuroimaging, 2017, 2(7):566-574.

[7] Ananth MR, DeLorenzo C, Yang J, et al. Decreased pretreatment amygdalae serotonin transporter binding in unipolar depression remitters: a prospective PET study[J]. J Nucl Med, 2018, 59(4):665-670.

[8] Moriguchi S, Takano H, Kimura Y, et al. Occupancy of norepinephrine transporter by duloxetine in human brains measured by positron emission tomography with (*S*, *S*)-[^{18}F] FMeNER-D_2 [J]. Int J Neuropsychopharmacol, 2017, 20(12):957-962.

[9] Wang L, Zhou C, Zhu D, et al. Serotonin-1A receptor alterations in depression: a meta-analysis of molecular imaging studies[J]. BMC Psychiatry, 2016, 16:319.

[10] 彭云丽. 慢性应激诱发抑郁行为的炎性机制研究[D]. 上海：中国人民解放军海军军医大学, 2013:80-85.
Peng L. Inflammatory mechanism underlying depressive behaviors induced by chronic stress [D]. Shanghai: Second Miliary Medical University, 2013:80-85.

[11] 王嫩媞. 高脂食物诱导肥胖小鼠抑郁焦虑表型评价及机制初探索[D]. 上海：上海交通大学, 2016:46-50.
Wang W. Evaluation and mechanism of depression and anxiety in obese mice induced by hig fat diet[D]. Shanghai: Sahnghai Jiao Tong University, 2016:46-50.

[12] Keller J, Gomez R, Williams G, et al. HPA axis in major depression: cortisol, clinical symptomatology and genetic variation predict cognition[J]. Mol Psychiatry, 2017, 22(4):527-536.

[13] Miller AH, Raison CL. Cytokines, p38 MAP kinase and the pathophysiology of depression[J]. Neuropsychopharmacology, 2006, 31(10):2089-2090.

[14] Nemeroff CB. Recent findings in the pathophysiology of depression[J]. Focus, 2008, 6(1):3-14.

[15] Liu Z, Liu W, Yao L, et al. Negative life events and corticotropin-releasing-hormone receptor 1 gene in recurrent major depressive disorder[J]. Sci Rep, 2013, 3:1548.

[16] Parekh A, Smeeth D, Milner Y, et al. The role of lipid biomarkers in major depression[J]. Healthcare (Basel), 2017, 5(1):5.

[17] 郑啸, 王广基, 郝海平. 抑郁症中的免疫代谢调控异常与药物干预研究进展[J]. 药学学报, 2017, 52(1):19-25.
Zheng X, Wang G, Hao H. Update on immune and metabolic dysregulation in major depressive disorder and the implications for drug intervention[J]. Acta Pharm Sin, 2017, 52(1):19-25.

[18] Dong X, Wang D, Lu Y, et al. Antidepressant effects of Kai-Xin-San in fluoxetine-resistant depression rats [J]. Braz J Med Biol Res, 2017, 50(10):e6161.

[19] Liu X, Li J, Zheng P, et al. Plasma lipidomics reveals potential lipid markers of major depressive disorder[J]. Anal Bioanal Chem, 2016, 408(23):6497-6507.

[20] 周云丰, 陶雪, 王丽莎, 等. 嗅球切除动物模型的特点和应用研究进展[J]. 药学学报, 2019, 54(7):1157-1165.
Zhou Y, Tao X, Wang L, et al. Progress in characteristics and application of olfactory bulbectomy animal model [J]. Acta Pharm Sin, 2019, 54(7):1157-1165.

[21] Laugerette F, Furet JP, Debard C, et al. Oil composition of high-fat diet affects metabolic inflammation differently in connection with endotoxin receptors in mice[J]. Am J

Physiol Endocrinol Metab, 2012, 302(3):E374-E386.

[22] Papp M, Willner P, Muscat R. An animal model of anhedonia: attenuation of sucrose consumption and place preference conditioning by chronic unpredictable mild stress[J]. Psychopharmacology (Berl), 1991, 104(2): 255-259.

[23] 赵丹, 王少贤, 梁文杰, 等. 慢性应激模型大鼠体重、摄食变化和粪便代谢物的相关性研究[J]. 中国病理生理杂志, 2019, 35(7):1302-1309.
Zhao D, Wanf S, Liang W, et al. Correlation between fecal metabolites and body weight/food intake in ratsafter chronic immobilization stress[J]. Chin J Pathophysiol, 2019, 35(7):1302-1309.

[24] 王宁. TLR4/NF-κB信号通路在抑郁模型大鼠高脂血症产生中的作用研究[D]. 唐山: 华北理工大学, 2019: 44-48.
Wang N. The role of TLR4/NF-κB signaling pathway in the production of hyperlipidemia in depression model rats [D]. Tangshan: North China University of Science and Technology, 2019:44-48.

[25] 高晓玲. 抑郁对胆固醇逆转运的影响及相关的分子机制[D]. 广州: 广州中医药大学, 2014:50-59.
Gao X. Depression effects on reverse cholesterol transport and related molecularmechanisms [D]. Guangzhou: Guangzhou University of Chinese Medicine, 2014:50-59.

[26] 孙红爽, 乜春城, 李鹏霖, 等. 高脂饲料结合慢性应激致大鼠非酒精性脂肪肝的药物治疗[J]. 中国老年学杂志, 2020, 40(1):177-181.
Sun H, Nie C, Li P, et al. Drug treatment of nonalcoholic fatty liver caused by high-fat diet combined with chronic stress[J]. Chin J Gerontol, 2020, 40(1):177-181.

[27] Kuo LE, Czarnecka M, Kitlinska JB, et al. Chronic stress, combined with a high-fat/high-sugar diet, shifts sympathetic signaling toward neuropeptide Y and leads to obesity and the metabolic syndrome[J]. Ann N Y Acad Sci, 2008, 1148:232-237.

[28] Wang SL, Gao XL, Li PT, et al. Chronic unpredictable mild stress combined with a high-fat diets aggravates atherosclerosis in rats[J]. Lipids Health Dis, 2014, 13:77.

[29] Bruder-Nascimento T, Campos DHS, Alves C, et al. Effects of chronic stress and high-fat diet on metabolic and nutritional parameters in Wistar rats[J]. Arq Bras Endocrinol Metabol, 2013, 57(8):642-649.

[30] Simas BB, Nunes EA, Crestani CC, et al. Cardiovascular and metabolic consequences of the association between chronic stress and high-fat diet in rats[J]. Stress, 2018, 21(3):247-256.

[31] 金星, 刘剑刚, 史大卓. 慢性应激抑郁对心肌梗死大鼠血管活性物质及炎症因子的影响[J]. 中国病理生理杂志, 2010, 26(1):70-74.
Jin X, Liu J, Shi D. Influence of chronic stress on vasoactive substances and inflammatory factor in rat model with acute myocardial infarction by factorial analysis[J]. Chin J Pathophysiol, 2010, 26(1):70-74.

[32] Troubat R, Barone P, Leman S, et al. Neuroinflammation and depression: a review[J]. Eur J Neurosci, 2021, 53(1):151-171.

[33] Madison A, Kiecolt-Glaser JK. Stress, depression, diet, and the gut microbiota: human-bacteria interactions at the core of psychoneuroimmunology and nutrition[J]. Curr Opin Behav Sci, 2019, 28:105-110.

[34] Pistell PJ, Morrison CD, Gupta S, et al. Cognitive impairment following high fat diet consumption is associated with brain inflammation[J]. J Neuroimmunol, 2010, 219 (1/2):25-32.

[45] Dalvi PS, Chalmers JA, Luo V, et al. High fat induces acute and chronic inflammation in the hypothalamus: effect of high-fat diet, palmitate and TNF-α on appetite-regulating NPY neurons[J]. Int J Obes (Lond), 2017, 41 (1):149-158.

[36] Gulhane M, Murray L, Lourie R, et al. High fat diets induce colonic epithelial cell stress and inflammation that is reversed by IL-22[J]. Sci Rep, 2016, 6:28990.

[37] De Sousa Rodrigues ME, Bekhbat M, Houser MC, et al. Chronic psychological stress and high-fat high-fructose diet disrupt metabolic and inflammatory gene networks in the brain, liver, and gut and promote behavioral deficits in mice[J]. Brain Behav Immun, 2017, 59:158-172.

[38] Zhang Y, Gu F, Chen J, et al. Chronic antidepressant administration alleviates frontal and hippocampal BDNF deficits in CUMS rat[J]. Brain Res, 2010, 1366:141-148.

[39] Réus GZ, Generoso JS, Rodrigues ALS, et al. Chapter 10. Intracellular signaling pathways implicated in the pathophysiology of depression[M]//Quevedo J, Carvalho AF, Zarate CA. Neurobiology of depression: road to novel therapeutics. Waltham: Academic Press, 2019:97-109.

[40] 储江. 慢性应激诱导的抑郁大鼠空间学习记忆能力障碍及机制[D]. 武汉: 华中科技大学, 2015:30-34.
Chu J. Spatial learning and memory deficit in chronic stress-induced depressive rats and the mechanism[D]. Wuhan: Huazhong University of Science and Technology, 2015:30-34.

[41] Alzoubi KH, Abdul-Razzak KK, Khabour OF, et al. Adverse effect of combination of chronic psychosocial stress and high fat diet on hippocampus-dependent memory in rats[J]. Behav Brain Res, 2009, 204(1):117-123.

[42] Baran BE, Campbell AM, Kleen JK, et al. Combination of high fat diet and chronic stress retracts hippocampal dendrites[J]. Neuroreport, 2005, 16(1):39-43.

[43] Arcego DM, Toniazzo AP, Krolow R, et al. Impact of high-fat diet and early stress on depressive-like behavior and hippocampal plasticity in adult male rats[J]. Mol Neurobiol, 2018, 55(4):2740-2753.

[44] Tsai SF, Wu HT, Chen PC, et al. Stress aggravates high-fat-diet-induced insulin resistance via a mechanism that involves the amygdala and is associated with changes in neuroplasticity[J]. Neuroendocrinology, 2018, 107(2): 147-157.

[45] Schachter J, Martel J, Lin CS, et al. Effects of obesity on depression: a role for inflammation and the gut microbiota [J]. Brain Behav Immun, 2018, 69:1-8.

[46] Hassan AM, Mancano G, Kashofer K, et al. High-fat diet induces depression-like behaviour in mice associated with changes in microbiome, neuropeptide Y, and brain metabolome[J]. Nutr Neurosci, 2019, 22(12):877-893.

[47] 李楠楠. 口服益生菌对慢性轻度应激致小鼠类焦虑、抑郁行为的干预作用及肠-炎症-脑轴影响的研究[D]. 沈阳: 中国医科大学, 2019:45-48.
Li N. Oral probiotics on anxiety- and depressive-like behaviors induced by chronic mild stress in mice and the effects of gutmicrobiota-inflammation-brain axis [D]. Shenyang: China Medical University, 2019:45-48.

[48] Bridgewater LC, Zhang C, Wu Y, et al. Gender-based differences in host behavior and gut microbiota composition in response to high fat diet and stress in a mouse model[J]. Sci Rep, 2017, 7:10776.

[49] 祖先鹏. 抑郁症患者代谢组与肠道菌群结构特征分析及Bacopaside I抗抑郁作用的机制研究[D]. 上海: 中国人民解放军海军军医大学, 2018:55-60.
Zu X. Characterization of metabolome and intestinal flora indepressive patients and mechanism study on theantidepressive effects of Bacopaside I[D]. Shanghai: Second Miliary Medical University, 2018:55-60.

[50] 杨磊. 首发抑郁症患者肠道菌群与细胞因子的关联性研究[D]. 郑州: 郑州大学, 2018:38-43.
Yang L. An association study on the intestinal microflora and cytokines in first-episode depressive disorders [D]. Zhengzhou: Zhengzhou University, 2018:38-43.

[51] Cheng Y, Pardo M, de Souza Armini R, et al. Stress-induced neuroinflammation is mediated by GSK3-dependent TLR4 signaling that promotes susceptibility to depression-like behavior[J]. Brain Behav Immun, 2016, 53:207-222.

[52] Garate I, Garcia-Bueno B, Madrigal JL, et al. Stress-induced neuroinflammation: role of the Toll-like receptor-4 pathway[J]. Biol Psychiatry, 2013, 73(1):32-43.

[53] Lopresti AL. Chapter 15. Mitochondrial dysfunction and oxidative stress: relevance to the pathophysiology and treatment of depression[M]//Quevedo J, Carvalho AF, Zarate CA. Neurobiology of depression: road to novel therapeutics. Waltham: Academic Press, 2019:159-168.

[54] Velloso LA, Folli F, Saad MJ. TLR4 at the crossroads of nutrients, gut microbiota, and metabolic inflammation [J]. Endocr Rev, 2015, 36(3):245-271.

[55] Yiu JH, Dorweiler B, Woo CW. Interaction between gut microbiota and toll-like receptor: from immunity to metabolism[J]. J Mol Med (Berl), 2017, 95(1):13-20.

[56] Setiawan E, Wilson AA, Mizrahi R, et al. Role of translocator protein density, a marker of neuroinflammation, in the brain during major depressive episodes[J]. JAMA Psychiatry, 2015, 72(3):268-275.

[57] Maes M, Yirmyia R, Noraberg J, et al. The inflammatory & neurodegenerative (I&ND) hypothesis of depression: leads for future research and new drug developments in depression[J]. Metab Brain Dis, 2009, 24(1):27-53.

[58] Schwarcz R, Bruno JP, Muchowski PJ, et al. Kynurenines in the mammalian brain: when physiology meets pathology[J]. Nat Rev Neurosci, 2012, 13(7):465-477.

[59] Hu ZP, Fang XL, Fang N, et al. Melatonin ameliorates vascular endothelial dysfunction, inflammation, and atherosclerosis by suppressing the TLR 4/NF-κB system in high-fat-fed rabbits[J]. J Pineal Res, 2013, 55(4): 388-398.

[60] Hotamisligil GS. Inflammation, metaflammation and immunometabolic disorders[J]. Nature, 2017, 542(7640): 177-185.

[61] Holthuis JC, Menon AK. Lipid landscapes and pipelines in membrane homeostasis[J]. Nature, 2014, 510(7503): 48-57.

[62] Su KP, Huang SY, Peng CY, et al. Phospholipase A2 and cyclooxygenase 2 genes influence the risk of interferon-α-induced depression by regulating polyunsaturated fatty acids levels[J]. Biol Psychiatry, 2010, 67(6): 550-557.

（**责任编辑**：宋延君，罗　森）

中国现代应用药学
Chinese Journal of Modern Applied Pharmacy
ISSN 1007-7693,CN 33-1210/R

《中国现代应用药学》网络首发论文

题目：硫酸化修饰对玄参多糖抗炎活性的影响
作者：高丽娜，周利润，李曼曼，李姿锐，贾玲玉，王建安
收稿日期：2021-01-14
网络首发日期：2021-06-15
引用格式：高丽娜，周利润，李曼曼，李姿锐，贾玲玉，王建安．硫酸化修饰对玄参多糖抗炎活性的影响[J/OL]．中国现代应用药学.
https://kns.cnki.net/kcms/detail/33.1210.R.20210615.1429.002.html

网络首发时间：2021-06-15 17:40:07
网络首发地址：https://kns.cnki.net/kcms/detail/33.1210.R.20210615.1429.002.html

硫酸化修饰对玄参多糖抗炎活性的影响

高丽娜，周利润，李曼曼，李姿锐，贾玲玉，王建安*(济宁医学院药学院，山东 日照 276800)

摘要：目的 比较研究玄参多糖经硫酸化修饰前后其抗炎活性的变化及机制。**方法** ♂ICR 小鼠经腹腔注射脂多糖(lipopolysaccharide，LPS)建立急性炎症反应模型，分别给予玄参多糖和硫酸化玄参多糖进行药物干预，以阿司匹林作为阳性对照，运用 Real time RT-PCR 检测肝脏组织白介素-6(interleukin-6，IL-6)、白介素-1β(interleukin-1β，IL-1β)、单核细胞趋化蛋白-1(monocyte chemoattractant protein-1，MCP-1)和肿瘤坏死因子-α(tumor necrosis factor-α，TNF-α)的 mRNA 表达，运用 ELISA 检测血清中的 IL-6、IL-1β、MCP-1 和 TNF-α 的蛋白表达，运用 Western blotting 法检测肝脏组织中核因子 κB(nuclear factor-kappaB，NF-κB)、phospho-NF-κB 的表达水平。**结果** 硫酸化玄参多糖和玄参多糖均可显著抑制 LPS 诱导的 IL-6、IL-1β、MCP-1 和 TNF-α mRNA 和蛋白表达增加，玄参多糖经硫酸化修饰后，其抗炎活性显著增强，其作用机制可能与调控 NF-κB 信号转导通路活化有关。**结论** 硫酸化修饰可显著提高玄参多糖的抗炎活性，具有更好的应用前景，为玄参的开发应用提供了理论基础。

关键词：玄参；多糖；硫酸化多糖；细胞因子；NF-κB

Effects of Sulfation Modification on Anti-inflammatory Activity of Polysaccharides from Scrophulariae Radix

GAO Lina, ZHOU Lirun, LI Manman, LI Zirui, JIA Lingyu, WANG Jian'an*(*School of Pharmacy, Jining Medical University，Rizhao 276800, China*)

ABSTRACT: OBJECTIVE To comparative study on the changes and mechanisms of anti-inflammatory activity of polysaccharide from Scrophulariae Radix before and after sulfation modification. **METHODS** The systemic inflammatory model was established by intraperitoneal injection of lipopolysaccharide(LPS) in male ICR mice. Then polysaccharides from Scrophulariae Radix and sulphated polysaccharides from Scrophulariae Radix were used for drug intervention and aspirin was used as a positive control. Real-time reverse transcription polymerase chain reaction (RT-PCR) was used to detect the mRNA expression of interleukin-6(IL-6), IL-1β, monocyte chemoattractant protein-1(MCP-1) and tumor necrosis factor-α(TNF-α) in liver tissue. The protein expression of IL-6, IL-1β, MCP-1 and TNF-α in serum was detected by ELISA. The level of nuclear factor-kappaB(NF-κB) and phospho-NF-κB in liver tissue was detected by Western blotting. **RESULTS** The results show that both Scrophulariae Radix and Scrophulariae Radix significantly improved LPS-induced over-expression of IL-6 IL-1β, MCP-1 and TNF-α in both mRNA and protein levels. Compared to Scrophulariae Radix, Scrophulariae Radix exerted more significant anti-inflammatory activities and the mechanism may be associated with activation of NF-κB signaling pathway. **CONCLUSION** Sulfation modification of Scrophulariae Radix showed stronger anti-inflammatory efficacy and has better application prospects, which provides a theoretical basis for the development and application of Scrophulariae Radix.

KEYWORDS: Scrophulariae Radix; polysaccharide; sulfated polysaccharide; cytokines; NF-κB

玄参是玄参科 Scrophulariaceae 玄参属 Scrophularia 植物玄参 *Scrophularia ningpoensis* Hemsl.的干燥根，为滋阴降火之要药。现代研究发现玄参多糖在调控糖脂代谢、免疫功能、抗氧化、抗肿瘤、抗疲劳等方面具有潜在的应用价值[1-3]。玄参多糖由半乳糖和葡萄糖等单糖组成，为中性多糖。前期研究中，课题组对玄参多糖的提取工艺进行了优化，并初步考察了玄参多糖对的抗炎和抗氧化活性[4]，但关于玄参多糖结构修饰的研究仍未见报道。对多糖进行结构修饰是增强或产生新药理活性的重要手段[5-6]，多糖的硫酸化修饰在提高抗炎、抗肿瘤、抗病毒、抗氧化、抗凝血活性等方面具有显著作用[7-9]。本实验采用氯磺酸-吡啶法制备硫酸化玄参多糖，建立脂多糖(lipopolysaccharide，LPS)诱导的小鼠急性炎症反应模型，对比研究玄参多糖经硫酸化修饰前后，其抗炎活性的变化，初步阐明硫酸化修饰对玄参多糖抗炎活性及其分子机制的影响。

基金项目：国家中医药管理局全国中药资源普查项目(GZY-KJS-2018-004)，2018 年中医药公共卫生服务补助专项“全国中药资源普查项目”(财社[2018]43 号)，济宁医学院教师科研扶持基金(JY2017KJ047)，济宁医学院 2018 年校级教育教学研究项目(18069)

作简者介：高丽娜，女，博士，副教授 Tel: (0633)2983695 E-mail: linagao228@126.com *通信作者：王建安，男，硕士，教授 Tel: (0633)2983695 E-mail: anansen@163.com

1 材料

1.1 仪器

7500 型全自动荧光定量 PCR 仪(美国 ABI 公司产品)；PCR-C1000 逆转录仪(美国 Bio-Rad 公司产品)；MK3 型酶标仪(美国 Thermo Fisher Scientific 公司产品)。

1.2 药品与试剂

由正规药材市场购买所得干燥玄参切片，经济宁医学院药学院中药教研室王建安教授鉴定为玄参科 *Scrophulariaceae* 玄参属 *Scrophularia* 植物玄参 *Scrophularia ningpoensis* Hemsl.根的切片。阿司匹林(Bayer 公司，批号：BJ38317；规格：每片 100 mg，30 片)。

BCA 蛋白浓度测定试剂盒(北京索莱宝科技有限公司，批号：20181213)；白介素-6(interleukin-6，IL-6)ELISA 试剂盒(Invitrogen 公司，88-7046-22)；单核细胞趋化蛋白-1(monocyte chemoattractant protein-1，MCP-1) ELISA 试剂盒(Invitrogen 公司，BMS6005)；肿瘤坏死因子-α(tumor necrosis factor-α，TNF-α) ELISA 试剂盒(Peprotech 公司，900-k54)；白介素-1β(interleukin-1β，IL-1β) ELISA 试剂盒(Peprotech 公司，BGK10749)；Improm-II逆转录试剂盒(Promega 公司，A3800)；UNIQ-10 column Trizol 总 RNA 提取试剂盒(生工生物工程股份有限公司，B511321)；细胞裂解试剂盒(生工生物工程股份有限公司，D612005)；β-actin 小鼠源一抗(Cell signaling technology 公司，3700)；NF-κBp65 兔源一抗(Cell signaling technology 公司，8242)；Phospho-NF-κBp65 兔源一抗(Ser536，Cell signaling technology 公司，3033)兔源一抗、抗兔二抗(Cell signaling technology 公司，7074)、抗小鼠二抗(Cell signaling technology 公司，7076)；LPS(Sigma-Aldrich 公司，L2630)；SYBR Green JumpStart TaqReadyMix 试剂盒(Sigma-Aldrich 公司，KCQS01)。

1.3 动物

♂SPF 级 ICR 小鼠，40 只体质量 13~14 g 购自济南朋悦实验动物繁育有限公司，动物生产许可证号 SCXK(鲁)20190003，饲养环境：饲养温度为(24±2)℃的室内，常规饲料，自由饮水进食，适应性饲养 1 周后用于实验。

2 方法

2.1 玄参多糖及硫酸化玄参多糖制备

取玄参根切片，烘干后打粉，过 10 目筛，取 200 g 干燥后的玄参粉末，加约 6 L 水浸泡，微沸煎煮 2 h，煎煮液过滤，药渣再煎煮 1 次，合并滤液。将过滤后的提取液减压浓缩至一定体积，加 4 倍量无水乙醇混匀，静置过夜，弃去上清；沉淀加适量水溶解，过大孔树脂柱(DM-130)脱除色素，洗脱液减压浓缩，Sevage 法脱除蛋白[10]；将脱除色素和蛋白的玄参多糖提取液浓缩，冷冻干燥，得玄参多糖粉末。采用氯磺酸-吡啶法制得硫酸化玄参多糖，经冷冻干燥得硫酸化玄参多糖粉末[11]。本实验所制硫酸化玄参多糖的得率为 2.01%，取代度为 1.22。

2.2 动物分组与处理

将 40 只♂ICR 小鼠随机分为 5 组(每组 8 只)：正常对照组、LPS 组(1 mg·kg^{-1})、阿司匹林组(200 mg·kg^{-1})、玄参多糖组(200 mg·kg^{-1})；硫酸化玄参多糖组(200 mg·kg^{-1})。为与阿司匹林组作用效果进行比较，本实验所用玄参多糖和硫酸化玄参多糖浓度均为 200 mg·kg^{-1}，不同组小鼠分别灌胃给予相应剂量的玄参多糖、硫酸化玄参多糖或阿司匹林 4 天(每天 1 次)，正常对照组和 LPS 组则给予同等剂量的生理盐水。末次灌胃给药 30 min 后，腹腔注射 LPS，诱导急性炎症反应。小鼠经腹腔注射 LPS 90 min 后，眼内眦取血，分离血清，于–20 ℃冰箱保存，备用；迅速分离小鼠肝脏组织并精确称量和记录，置于–80 ℃冰箱保存，备用。

2.3 小鼠肝脏组织中细胞因子的mRNA表达检测

取肝小鼠肝脏组织充分裂解后，按照 UNIQ-10 Column Trizol 试剂盒进行操作，提取组织中的总 RNA[12]。使用逆转录试剂盒将总 RNA 逆转录合成 cDNA。加入随机引物 5 μL，样品 5 μL，并在冰上混匀，在 50℃下延伸 15 min，然后在 80 ℃下放置 5 min 使其高温变性，加入引物进行 real time RT-PCR 反应，采用 $2^{-\Delta\Delta C_T}$法进行数据统计。β-actin 为看家基因，β-actin、IL-6、IL-1β、MCP-1 和 TNF-α 的引物序列见表 1。

2.4 小鼠血清中细胞因子的蛋白含量检测

取小鼠血清，按试剂盒说明书操作，测定各组

表 1 Real-time RT-PCR 引物序列

Tab. 1 Real-time RT-PCR oligonucleotide primers

基因	引物	序列(5′–3′)	PCR 产物(bp)
β-actin	Forward	TGTTACCAACTGGGACGACA	165
(NM_007393.3)	Reverse	GGGGTGTTGAAGGTCTCAAA	
IL-6	Forward	TCCAGTTGCCTTCTTGGGAC	140
(NM_031168.1)	Reverse	GTGTAATTAAGCCTCCGACTTG	
TNF-α	Forward	TAGCCAGGAGGGAGAACAGA	127

(NM_013693.2)	Reverse	TTTTCTGGAGGGAGATGTGG	
MCP-1	Forward	CCCAATGAGTAGGCTGGAGA	125
(NM_0113333.3)	Reverse	TCTGGACCCATTCCTTCTTG	
IL-1β	Forward	GACCTTCCAGGATGAGGACA	183
(NM_008361.3)	Reverse	AGCTCATATGGGTCCGACAG	

血清中 IL-6、IL-1β、MCP-1 和 TNF-α 的蛋白含量。用于测定 IL-6 和 IL-1β 的血清样本分别按 1∶150 倍稀释进行检测，MCP-1 和 TNF-α 的血清样本分别按 1∶100 倍稀释进行检测。

2.5 Western blotting 分析

取小鼠肝脏组织，按照 m∶v=1∶9，加入相应体积的 RIPA 裂解液，超声破碎提取总蛋白，以 BCA 法进行蛋白定量。采用 SDS-PAGE 恒压电泳(100 V，90~120 min)分离蛋白，湿转法将蛋白质转移到聚偏氟乙烯(PVDF)膜上(300 mA，60 min)，用含有 5%脱脂奶粉的 PBTS 室温封闭 2 h，加入一抗(NF-κBp65 和 Phospho-NF-κBp65 稀释度为 1:1000 或 β-actin 稀释度为 1∶10000)于 4 ℃摇床孵育过夜。以 PBST(0.5% Tween-20)洗膜后，用辣根过氧化物酶标记的二抗(稀释度均为 1∶10000)室温孵育 1.5 h，PBST 润洗 5 次后，采用 ECL 发光试剂盒进行化学发光检测，采用 Image J 软件进行半定量分析，并进行磷酸化程度分析。

2.6 统计学分析

各组间实验数据采用单因素方差分析，数据分析结果以 $\bar{x} \pm s$ 表示，两组间比较采用 t 检验，$P < 0.05$ 表示有统计学意义。

3 结果

3.1 玄参多糖和硫酸化玄参多糖抑制 LPS 诱导肝脏组织中炎性因子的 mRNA 表达

与正常对照组相比，LPS 组 IL-6、IL-1β、MCP-1 和 TNF-α mRNA 的表达明显升高(P<0.01)。与 LPS 组相比，阿司匹林、玄参多糖、硫酸化玄参多糖组小鼠肝脏组织中 IL-6、IL-1β、MCP-1 和 TNF-α mRNA 的表达显著降低(P<0.01)，且硫酸化玄参多糖较阿司匹林和玄参多糖的作用效果更为显著(P<0.01)。提示玄参多糖经硫酸化修饰后，其对 LPS 诱导的炎性因子 mRNA 表达的抑制作用更强。结果见表 2。

表 2 玄参多糖和硫酸化玄参多糖对 LPS 诱导小鼠肝脏组织炎性因子 mRNA 表达的影响

Tab. 2 Effects of sulfated and non-sulfated polysaccharide from Scrophulariae Radix on LPS-induced mRNA expression of proinflammatory cytokines in mice liver tissues

组别	TNF-α	IL-6	IL-1β	MCP-1
正常对照	1.01±0.01	1.05±0.02	1.03±0.02	1.01±0.03
LPS 组	10.69±1.37[1)]	9.57±1.04[1)]	6.82±1.32[1)]	9.86±0.65[1)]
阿司匹林/200 mg·kg^{-1}	5.42±0.55[2)3)]	3.79±0.56[2)3)]	3.74±0.76[2)3)]	6.67±0.48[2)3)]
玄参多糖/200 mg·kg^{-1}	5.22±0.14[2)3)]	5.17±0.70[2)3)]	3.42±0.27[2)3)]	4.93±0.26[2)3)]
硫酸化玄参多糖/200 mg·kg^{-1}	3.99±0.41[2)]	3.05±0.28[2)]	2.16±0.22[2)]	3.60±0.32[2)]

注：和与正常对照组比较，[1)]P<0.01；与 LPS 组比较，[2)]P<0.01；与硫酸化玄参多糖组比较，[3)]P<0.01。

Note: Compared with normal control group, [1)]P<0.01; compared with LPS group, [2)]P<0.01; compared with sulfated polysaccharides from Scrophulariae Radix group, [3)]P<0.01.

3.2 玄参多糖和硫酸化玄参多糖抑制 LPS 诱导血清中炎性因子的蛋白表达增加

与正常对照组相比，LPS 可显著诱导 IL-6、IL-1β、MCP-1 和 TNF-α 的蛋白表达升高(P<0.01)。与 LPS 组比较，阿司匹林、玄参多糖、硫酸化玄参多糖组小鼠血清中 IL-6、IL-1β、MCP-1 和 TNF-α 的表达显著降低(P<0.01)。与玄参多糖组或阿司匹林组比较，硫酸化玄参多糖对小鼠血清中 IL-6、IL-1β 和 MCP-1 表达的抑制作用更为显著(P<0.01)。因此，在 LPS 诱导的急性炎症反应初期，硫酸化修饰显著提高了玄参多糖的抗炎活性。结果见表 3。

3.3 玄参多糖和硫酸化玄参多糖降低肝脏组织中 NF-κB p65 和 phospho-NF-κB p65 水平

与正常对照组比较，LPS 组小鼠肝脏组织中 NF-κB p65 和 phospho-NF-κB p65 的表达水平显著提高(P<0.01)。阿司匹林、玄参多糖和硫酸化玄参多糖干预组小鼠肝脏组织中 NF-κB p65 和 phospho-NF-κB p65 蛋白含量较 LPS 组显著降低(P<0.01)。以 phospho-NF-κB p65 与 NF-κB p65 灰度值比值考察 NF-κB p65 磷酸化程度变化，结果参多糖和硫酸化玄参多糖可能通过抑制 NF-κB 信号通路激活减少细胞因子释放，发挥抗炎作用的。与玄参多糖组(0.81±0.06)比较，硫酸化玄参多糖

(0.78±0.04)对 NF-κB p65 磷酸化的抑制作用更强，但无统计学差异。结果见图 1 和表 4。

表 3 玄参多糖和硫酸化玄参多糖对 LPS 诱导小鼠血清中促炎因子蛋白表达的影响

Tab. 3 Effects of sulfated and non-sulfated polysaccharide from Scrophulariae Radix on LPS-induced protein expression of proinflammatory cytokines in mice serum

组别	TNF-α	IL-6	IL-1β	MCP-1
正常对照	4.75±0.65	24.05±2.51	71.03±1.69	20.30±1.23
LPS 组	430.45±50.07[1)]	13 632.82±309.03[1)]	13 739.12±230.32[1)]	2 222.05±298.43[1)]
阿司匹林/200 mg·kg^{-1}	362.33±43.71[2)3)]	5 939.86±131.21[2)3)]	583.30±33.23[2)3)]	493.04±32.54[2)3)]
玄参多糖/200 mg·kg^{-1}	26.55±10.69[2)]	5 892.93±125.53[2)3)]	546.19±25.61[2)3)]	483.12±34.20[2)3)]
硫酸化玄参多糖/200 mg·kg^{-1}	31.91±8.11[2)]	5 059.59±182.43[2)]	314.86±25.90[2)]	173.71±22.20[2)]

注：与正常对照组比较，[1)]P<0.01；与 LPS 组比较，[2)]P<0.01；与硫酸化玄参多糖组比较，[3)]P<0.01。

Note: Compared with normal control group, [1)]P<0.01; compared with LPS group, [2)]P<0.01; compared with sulfated polysaccharides from Scrophulariae Radix group, [3)]P<0.01.

表 4 NF-κB p65 和 phospho-NF-κB p65 Western blotting 结果进行灰度值分析(相对于 β-actin)

Tab. 4 Gray value of Western blot bands of NF-κB p65 and phospho-NF-κB(relative to β-actin)

组别	NF-κB p65	phospho-NF-κB p65	phospho-NF-κB p65/NF-κB p65
正常对照	0.15±0.0030	0.077±0.011	0.52±0.0066
LPS 组	0.59±0.0032[1)]	1.15±0.019[1)]	1.95±0.022[1)]
阿司匹林/200 mg·kg^{-1}	0.34±0.0039[2)]	0.54±0.017[2)]	1.58±0.032[2)]
玄参多糖/200 mg·kg^{-1}	0.43±0.0079[2)]	0.64±0.020[2)]	1.51±0.020[2)]
硫酸化玄参多糖/200 mg·kg^{-1}	0.37±0.00035[2)]	0.58±0.021[2)]	1.50±0.054[2)]

注：与正常对照组比较，[1)]P<0.01；与 LPS 组比较，[2)]P<0.01。

Note: Compared with normal control group, [1)]P<0.01; compared with LPS group, [2)]P<0.01.

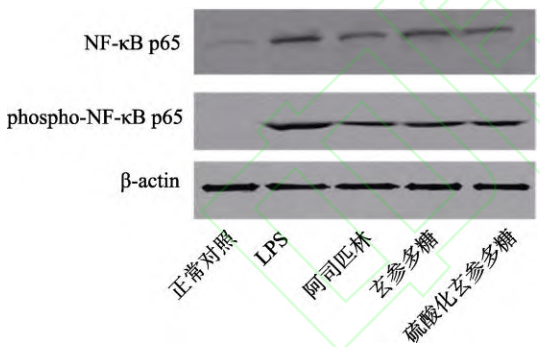

图 1 玄参多糖和硫酸化玄参多糖对 LPS 诱导小鼠肝脏组织中 NF-κB p65、phospho-NF-κB p65 表达水平的影响

Fig. 1 Effects of sulfated and non-sulfated polysaccharide from Scrophulariae Radix on LPS-induced NF-κB p65 and phospho-NF-κB p65 levels in mice liver tissues

4 讨论

玄参多糖为玄参的主要成分之一，具有抗氧化、抗疲劳、调节糖脂代谢等作用[1-3]。对多糖主链、支链等结构进行修饰，可改变其生物活性。多糖结构修饰方法主要包括乙酰化、硫酸化、羧甲基化等[13-15]。硫酸化修饰是指在多糖的羟基结构引入硫酸基团，使其立体构象发生变化，进而提高或产生新的药理活性。玄参多糖的硫酸化修饰未见报道，本文首次研究硫酸化修饰对玄参多糖抗炎活性的影响。

LPS 是典型的炎症反应诱导剂，炎性状态下细胞会释放多种促炎因子，细胞因子 IL-6、TNF-α、IL-2、IL-1β 和趋化因子(如 MCP-1)等可激活 NF-κB 诱发炎症级联反应，同时，NF-κB 通过复杂的分子网络调控多种炎性基因的表达[16]。本文主要基于 LPS 诱导的急性炎性损伤模型，评价玄参多糖修饰前后对 IL-6、IL-1β、MCP-1 和 TNF-α mRNA 和蛋白表达的影响，可初步了解硫酸化玄参多糖对急性期炎症反应的调控作用。结果显示玄参多糖经硫酸化修饰后对 LPS 诱导的急性期 TNF-α、IL-6、IL-1β 和 MCP-1 的 mRNA 和蛋白表达的抑制作用更为显著，其作用机制与调控 NF-κB 信号通路激活有关。

在本研究设定的实验条件下，玄参多糖经硫酸化修饰后，其抗炎活性显著增强。但在分子机制方面，硫酸化修饰前后玄参多糖对 NF-κB p65 的磷酸化程度未见统计学差异，这可能与药物的实验浓度以及作用时间有关。此外，玄参多糖硫酸化修饰程度与其抗炎活性的相关性有待进一步研究，例如，考察不同硫酸化程度对其抗炎活性的影响，探讨不同炎性损伤模型(急性、亚急性、慢性)中硫酸化修饰对多糖抗炎活性的影响，为进

一步揭示玄参多糖结构与生物活性之间的关系提供理论依据。

综上所述，玄参多糖经硫酸化修饰后可显著抑制 LPS 诱导的急性期炎性因子的表达水平升高，其作用机制可能与 NF-κB 信号通路活化有关。为进一步阐明硫酸化玄参多糖的抗炎作用机制，需明确其发挥作用的结构单元以及结构修饰产生的构效关系，为指导玄参的临床应用提供理论依据。

REFERENCES

[1] LI Z H, ZHANG N, DONG W R, et al. Effect of polysaccharides of Radix scrophulariae on immune functions in mice under normal physiological and hypoimmunical state [J]. China Pharm(中国药房), 2017, 28(10): 1316-1319.

[2] ZHAO H W, ZHANG N, LI Z H, et al. The effect of polysaccharides from Radix scrophulariae on type 2 diabetes rats[J]. Inf Tradit Chin Med(中医药信息), 2017, 34(5): 8-12.

[3] ZHENG Y Y, WANG J, JIANG J P, et al. Effects of polysaccharides from Scrophulariae Radix on glucolipid metabolism and hepatic insulin signaling pathway in type 2 diabetic rats[J]. Chin Tradit Herb Drugs(中草药), 2020, 51(6): 1586-1592.

[4] WANG J N, HUANG L F, REN Q, et al. Polysaccharides of Scrophularia ningpoensis hemsl. : Extraction, antioxidant, and anti-inflammatory evaluation[J]. Evid Based Complement Alternat Med, 2020, 2020: 8899762. Doi: 10.1155/2020/8899762.

[5] SONG J X, REN T, WANG H, et al. Sulfated modification and DPPH free radical scavenging ability of polysaccharide from Rhodiola sachalinensis[J]. Chin Tradit Herbal Drugs(中草药), 2017(24): 5125-5129.

[6] ZHANG K, ZHANG Y, WANG L H, et al. Study on sulfated modification and anti-psoriasis activity of polysaccharide from Dictamnus dasycarpus[J]. China Pharm(中国药房), 2019, 30(8): 1049-1056.

[7] HUANG L X, SHEN M Y, MORRIS G A, et al. Sulfated polysaccharides: Immunomodulation and signaling mechanisms[J]. Trends Food Sci Technol, 2019(92): 1-11.

[8] WANG Z J, XIE J H, SHEN M Y, et al. Sulfated modification of polysaccharides: Synthesis, characterization and bioactivities[J]. Trends Food Sci Technol, 2018(74): 147-157.

[9] HUO Y F, WANG H L, WEI E H, et al. Two new compounds from the roots of Scrophularia ningpoensis and their anti-inflammatory activities[J]. J Asian Nat Prod Res, 2019, 21(11): 1083-1089.

[10] DONG H, BAO Y Q, HAN P H, et al. Optimization of sulfated modification conditions of polysaccharide from White Ginseng [J]. J Jilin Med Univ(吉林医药学院学报), 2018, 39(6): 430-432.

[11] CHEN L, HUANG G L. Antioxidant activities of sulfated pumpkin polysaccharides[J]. Int J Biol Macromol, 2019(126): 743-746.

[12] WANG Q S, GAO L N, ZHU X N, et al. Co-delivery of glycyrrhizin and doxorubicin by alginate nanogel particles attenuates the activation of macrophage and enhances the therapeutic efficacy for hepatocellular carcinoma[J]. Theranostics, 2019, 9(21): 6239-6255.

[13] XU Y, WU Y J, SUN P L, et al. Chemically modified polysaccharides: Synthesis, characterization, structure activity relationships of action[J]. Int J Biol Macromol, 2019(132): 970-977.

[14] XIE L M, SHEN M Y, HONG Y Z, et al. Chemical modifications of polysaccharides and their anti-tumor activities [J]. Carbohydr Polym, 2020(229): 115436. Doi: 10.1016/j.carbpol.2019.115436.

[15] YANG Y X, CHEN J L, LEI L, et al. Acetylation of polysaccharide from Morchella angusticeps peck enhances its immune activation and anti-inflammatory activities in macrophage RAW264. 7 cells[J]. Food Chem Toxicol, 2019(125): 38-45.

[16] ZHANG Q, LENARDO M J, BALTIMORE D. 30 years of NF-κB: A blossoming of relevance to human pathobiology[J]. Cell, 2017, 168(1/2): 37-57.

收稿日期：2021-01-14

(本文责编：陈怡心)

ISSN 1001-1528
CN 31-1368/R

■ 中国精品科技期刊 ■ 中国中文核心期刊 ■ 中国科技核心期刊
■ 中国科学引文数据库来源期刊 ■ 《中国学术期刊影响因子年报》统计源期刊
■ 中国生物学文献(CBA)源期刊 ■ 《中文科技期刊数据库》全文收录
■ 《中文科技资料目录-医药卫生》收录源期刊 ■ RCCSE核心期刊 ■ T2级优秀中医药科技期刊

CHINESE TRADITIONAL PATENT MEDICINE

2021年8月 第43卷 第8期

Vol.43 No.8 2021

中成药

ZHONGCHENGYAO

ISSN 1001-1528
9 771001 152210 08>

主 办
国家食品药品监督管理局信息中心中成药信息站
上 海 中 药 行 业 协 会

杂志官方微信

中成药
ZHONGCHENGYAO

2021 年第 43 卷第 8 期
月刊
1978 年 8 月创刊

主管单位
上海市卫生健康委员会
主办单位
国家食品药品监督管理局
信息中心中成药信息站
上海中药行业协会
出版单位
《中成药》编辑部
印刷单位
上海东港安全印刷有限公司
国内发行
上海市报刊发行局
海外总发行
中国国际图书贸易集团有限公司
出版日期
2021 年 8 月 20 日
主编
陈建生
执行主编
[illegible]
发行范围
公开发行
国内定价
每期 40.00 元
全年 480.00 元
国内统一连续出版物号
CN 31-1368/R
国际标准连续出版物号
ISSN 1001-1528

目 次

阿胶酶解物 HPLC 指纹图谱建立

付英杰[1]， 李新健[2]， 贾玉民[3]， 陈 智[4]， 任 强[1]， 于定荣[2*]， 陈 娅[1]
（1. 济宁医学院药学院，山东 日照 276826；2. 中国中医科学院中药研究所，北京 100700；3. 东阿阿胶股份有限公司，国家胶类中药工程技术研究中心，山东 东阿 252201；4. 山东中医药大学药学院，山东 济南 250355）

摘要：目的 建立阿胶酶解物 HPLC 指纹图谱。**方法** 阿胶酶解物的分析采用 Gemini NX C_{18}（250 mm×4.6 mm，5 μm）；流动相 0.2 mol/L 无水硫酸钠-乙腈-水，梯度洗脱；体积流量 1 mL/min；柱温 25 ℃；检测波长 280 nm，并进行相似度、聚类分析及主成分分析。**结果** 胰蛋白酶酶解物指纹图谱显示 3 厂家样品存在 5 个共有峰；糜蛋白酶酶解物指纹图谱显示了 3 厂家样品的高一致性，出现 13 个共有峰；各样品相似度均大于 0.9。同仁堂及多数东阿阿胶的类别距离<5，可与相对分散的福牌阿胶进行区分；同仁堂阿胶类别距离<5，但 3 厂家类别不易区分。同仁堂与东阿阿胶相对集中，而福牌阿胶较分散；在散点图 A1～A2、A2～A4 可区分出东阿阿胶、A1～A3、A3～A4 中可区分出福牌阿胶，A2～A3 可以区分 3 厂家阿胶、A1～A4 可以区分 3 厂家与其他品牌阿胶。**结论** 该方法稳定可靠，可用于阿胶的质量控制。

关键词： 阿胶；酶解物；指纹图谱；聚类分析；主成分分析
中图分类号： R282.5 **文献标志码：** A **文章编号：** 1001-1528(2021)08-2120-06
doi：10.3969/j.issn.1001-1528.2021.08.026

Establishment of HPLC fingerprints for enzymatic hydrolysates of *Colla Corii Asini*

FU Ying-jie[1], LI Xin-jian[2], JIA Yu-min[3], CHEN Zhi[4], REN Qiang[1], YU Ding-rong[2*], CHEN Ya[1]
(*1. College of Pharmacy, Jining Medical University, Rizhao 276826, China*; *2. China Academy of Chinese Medical Sciences, Beijing 100700, China*; *3. Dong'e Ejiao Co., Ltd., Dong'e 252201, China*; *4. Shandong University of TCM, Jinan 250355, China*)

KEY WORDS: *Colla Corii Asini*（E'jiao）; enzymatic hydrolysate; fingerprint; cluster analysis; principal component analysis

阿胶 *Colla Corii Asini* 始载于《神农本草经》，列为上品[1]。2015 年版《中国药典》规定阿胶是由马科动物驴 *Equus asinus* L. 的干燥皮或鲜皮经煎煮、浓缩制成的固体胶，具有补血滋阴、润燥、止血的功效，多用于治疗眩晕心悸、肌痿无力、心烦不眠、虚风内动、肺燥咳嗽、痨咳咯血、吐血尿血、便血崩漏等[2-4]。阿胶含有大量的胶原蛋白、多肽、氨基酸和丰富的微量元素，阿胶的蛋白类含量约 60%～80%[5-8]，但其有效成分尚不完全明确。阿胶有补血[9]、抗氧化[10]、抗疲劳[11]、耐氧化耐寒冷、抗休克、增强记忆力、改善皮肤、促骨愈合、抑瘤增效，在一定程度上还能拮抗血液的肝素化，起到止血等作用[12-14]。

目前，阿胶的质量评价仍然主要依靠传统的生药学鉴别等方法，其经验依赖性强、准确性较低[15]。2015 年版《中国药典》将阿胶用胰酶

收稿日期： 2020-08-11
基金项目： 国家自然科学基金青年基金项目（81703703）；国家自然科学基金应急管理项目（81541089）；中医药公共卫生服务补助项全国中药资源普查项目（财社〔2018〕43）
作者简介： 付英杰(1983—)，男，博士，副教授，硕士生导师，研究方向为中药新药与炮制原理。Tel：15965001526，E-mail：pulpil163.com
***通信作者：** 于定荣（1975—），男，博士，副研究员，硕士生导师，研究方向为中药炮制、中药化学、中药制剂以及质量标准。Tel：13717521473，E-mail：yudingrong0826@sina.com